PRESENTATION OF A NEW HIGH-FREQUENCY

COMMUNICATION SYSTEM PERFORMANCE

PREDICTION TECHNIQUE

by
Thomas Fiscus Gatts, Jr.

Thesis submitted to the Faculty of the Graduate School
of the University of Maryland in partial fulfillment
of the requirements for the degree of
Master of Science
1965

APPROVAL SHEET

Title of Thesis: PRESENTATION OF A NEW HIGH-FREQUENCY COMMUNICATION SYSTEM PERFORMANCE PREDICTION TECHNIQUE

Name of Candidate: Thomas Fiscus Gatts, Jr.
Master of Science, 1965

Thesis and Abstract Approved: Henry R. Reed
Henry R. Reed
Professor
Electrical Engineering

Date Approved: May 10, 1965

ABSTRACT

Title of Thesis: PRESENTATION OF A NEW HIGH-FREQUENCY COMMUNICATION SYSTEM PERFORMANCE PREDICTION TECHNIQUE

Thomas Fiscus Gatts, Jr., Master of Science, 1965

Thesis directed by: Professor Henry R. Reed

The prediction technique developed by the National Bureau of Standards has been used extensively by high-frequency communicators. An adaption of this technique is used to demonstrate the type of results obtained when applied to the Buffalo, N. Y. to Boston, Mass. (B/B) link for January and July 1965. A new prediction technique is presented which will allow the HF communicator to predict system performance between the maximum useable frequency (MUF) and the lowest useable frequency (LUF) and which is flexible enough to allow system parameter changes to be made and the effect on the overall system determined. The new technique is demonstrated by applying it to the B/B link for January and July 1965 and displaying the results in the form of relative gain contours, which show the

effect on communication capability of reducing the LUF by increasing system gain and the increase in process gain that may be achieved for the purpose of raising the data rate or decreasing transmission error rate. Some of the many applications of the results of this new technique are presented. The results are used: (1) to facilitate the selection of necessary operating frequencies to provide communication throughout a 24-hour period, (2) to estimate the severity and length of occurrence of multipath, (3) to investigate possible frequency adaption, and (4) to investigate possible power adaption.

ACKNOWLEDGEMENTS

It is a great pleasure to acknowledge with gratitude the invaluable guidance and assistance provided me in preparing this thesis by my Supervising Professor, Dr. Henry R. Reed, Professor of Electrical Engineering, University of Maryland.

I also wish to thank Mr. P. J. Kintner, my former co-worker at Sylvania Electronic Products, Inc., Amherst Laboratories, Buffalo, New York, who offered many helpful comments and criticisms.

To my typist, Mrs. Thomas F. Gatts, Jr., I wish to extend my appreciation for her patience and encouragement.

TABLE OF CONTENTS

Section	Page
ACKNOWLEDGEMENTS	ii
I. APPLICATION OF PRESENT TECHNIQUES	1
A. Introduction	1
B. Geometrical Factors	3
1. Determination of the Antenna Direction and the Great Circle Distance	3
2. Determination of the Vertical Radiation Angle	3
C. Propagation Delay Time	5
D. Prediction of E- and F-layer MUF	5
E. Predicted Median System Loss	8
F. Predicted Atmospheric Noise	12
G. Predicted S/N at FOT	13
II. PRESENTATION OF NEW TECHNIQUE	15
A. Introduction	15
B. Reference System Definition	16
C. Relative Gain	18
D. LUF Relative Gain Contours	22
III. APPLICATIONS OF RELATIVE GAIN CONTOURS	25
A. Frequency Allocation Analysis	25
B. Multipath Calculation	28
C. Communication System Adaption	30
1. General Aspects and Scope	30
2. Frequency Adaption	31
3. Power Adaption	35

TABLE OF CONTENTS

Section Page

SELECTED BIBLIOGRAPHY.................................. 87

LIST OF TABLES

Table Page

1. Summary of Prediction Calculations - One-Hop January 1965 83

2. Summary of Prediction Calculations - Two-Hop January 1965 84

3. Summary of Prediction Calculations - One-Hop July 1965 85

4. Summary of Prediction Calculations - Two-Hop July 1965 86

LIST OF FIGURES

Figure		Page
1.1 a	Geometric Representation of Buffalo to Boston Link (Spherical Earth).............	37
1.1 b	Geometric Representation of Buffalo to Boston Link (Flat Earth)..................	37
1.2	Radiation Angle vs. Layer Height...........	38
1.3	Propagation Delay Time......................	39
1.4	F_2-Layer Height for January and July 1965..................................	40
1.5	Difference in Delay Time Between One-Hop and Two-Hop Propagation..................	41
1.6	MUF Predictions for January 1965 One-Hop..................................	42
1.7	MUF Predictions for January 1965 Two-Hop..................................	43
1.8	MUF Predictions for July 1965 One-Hop..................................	44
1.9	MUF Predictions for July 1965 Two-Hop..................................	45
2.1	S/N at FOT with Respect to the Reference System (January 1965)......................	46
2.2	Total Absorption vs. Frequency, January 1965..............................	47
2.3	Total Absorption vs. Frequency, July 1965.................................	48
2.4	Atmospheric Noise vs. Frequency, 0000 to 1000 GMT January 1965.............	49
2.5	Atmospheric Noise vs. Frequency, 1200 to 2200 GMT July 1965................	50
2.6	Atmospheric Noise vs. Frequency, 0000 to 1000 GMT July 1965................	51

LIST OF FIGURES

Figure		Page
2.7	Atmospheric Noise vs. Frequency, 1200 to 2200 GMT, July 1965..................	52
2.8	Relative Gain vs. LUF, 0000 to 1000 GMT, January 1965...............	53
2.9	Relative Gain vs. LUF, 1200 to 2200 GMT, January 1965...............	54
2.10	Relative Gain vs. LUF, 0000 to 1000 GMT, July 1965..................	55
2.11	Relative Gain vs. LUF, 1200 to 2200 GMT, July 1965..................	56
2.12	Relative Gain Contours, One-Hop, January 1965................................	57
2.13	Relative Gain Contours, Two-Hop, January 1965................................	58
2.14	Relative Gain Contours, One-Hop, July 1965....................................	59
2.15	Relative Gain Contours, Two-Hop, July 1965....................................	60
3.1	Communication Use Time Analysis, One-Hop, January 1965, Ten Frequencies................	61
3.2	Communication Use Time vs. System Gain, Ten Frequencies, January 1965...............	62
3.3	Communication Use Time vs. System Gain, Ten Frequencies, July 1965...................	63
3.4	Communication Use Time vs. System Gain, Six Frequencies, January 1965...............	64
3.5	Communication Use Time vs. System Gain, Six Frequencies, July 1965...................	65
3.6	Multipath Prediction Curves, 0000 to 1000 GMT, January 1965...............	66
3.7	Multipath Prediction Curves, 1200 to 2200 GMT, January 1965...............	67

LIST OF FIGURES

Figure		Page
3.8	Multipath Prediction Curves, 0000 to 1000 GMT, July 1965	68
3.9	Multipath Prediction Curves, 1200 to 2200 GMT, July 1965	69
3.10	Predicted Multipath Occurrence, January and July 1965	70
3.11	Constant Performance Contours - Frequency Varied, January 1965	71
3.12	Constant Performance Contours - Frequency Varied, January 1965	72
3.13	Constant Performance Contours - Frequency Varied, July 1965	73
3.14	Constant Performance Contours - Frequency Varied, July 1965	74
3.15	Constant Performance Contours - Gain Varied, January 1965, One-Hop	75
3.16	Constant Performance Contours - Gain Varied, January 1965, Two-Hop	76
3.17	Constant Performance Contours - Gain Varied, July 1965, One-Hop	77
3.18	Constant Performance Contours - Gain Varied, July 1965, Two-Hop	78
3.19	Analysis for Optimum Transmission, January 1965	79
3.20	Analysis for Optimum Transmission, July 1965	80
3.21	Constant Frequency Contours for Optimum Transmission, January 1965	81
3.22	Constant Frequency Contours for Optimum Transmission, July 1965	82

SECTION I

APPLICATION OF PRESENT TECHNIQUES

INTRODUCTION

Several techniques[1,2,8,9,10] have been developed for high-frequency communicators to use in predicting the various modes of propagation and associated signal levels to be expected for a given communication system operating on a specified link. Although differing in detail, the various techniques generally involve a prediction of the signal-to-noise ratio to be expected at the receiver as a function of distance, time-of-day, season, degree of solar activity and operating frequency. The technique developed by the National Bureau of Standards[2,3], has been used extensively by high-frequency communicators and an adaption of this technique will be used in this thesis to demonstrate the type of results obtained when the technique is applied to a specific communication system. The prediction techniques referred to above are limited in their usefulness to a high-frequency communicator because: (1) They only provide information about the upper and lower limits of operation (the variation within these limits can be quite large) and (2) It is difficult to make changes in the system parameters and see the resultant changes in predicted operational characteristics since the entire prediction technique would have to be repeated for each separate parameter change.

This thesis will present a new prediction technique which will allow the high-frequency communicator to predict communication system performance between the upper and lower limits and, at the same time, be flexible enough to allow system parameter changes to be made and the effect on the overall communication system to be determined. The new technique will be demonstrated by applying it to a specific communication system and displaying the results in a comprehensive and easy-to-use form. Some of the many applications for this new technique will be presented, also, to demonstrate its usefulness and flexibility.

All of the prediction techniques mentioned above can be applied to any high-frequency circuit but, for purposes of demonstration, the communication circuit to be used in this thesis will be between Buffalo, N. Y. and Boston, Mass. This relatively short high-frequency communication circuit is chosen because only two primary modes of communication are possible. Since the purpose of this thesis is to present a new prediction technique and to demonstrate its application, it is felt that longer distance circuits which have many possible communication modes would only serve to complicate, needlessly, the presentation.

The purpose of this section is to outline the procedures and show the results of using the National Bureau of Standards prediction techniques on the Buffalo, N. Y. to

Boston, Mass. (B/B) communication link to determine operational performance characteristics.

GEOMETRICAL FACTORS

Determination of the Antenna Direction and Great Circle Distance. Figure 1.1 a is a geometric representation of the Buffalo-to-Boston high-frequency communication link where B is Buffalo and A is Boston. In order to determine the proper orientation for the antennas the angles x and y must be calculated. To determine the distance between A and B along a great circle route, S must be determined. A is located at longitude 71° 16' West and latitude 42° 24' North. B is located at longitude 78° 44' West and latitude 42° 57' North. Using spherical geometry $x = 81^\circ\ 45'$ West, $y = 93^\circ\ 11'$ East and S is 612.93 km. Therefore, the antenna at Buffalo should be orientated 93° 11' East and the antenna at Boston should be orientated 81° 45' West in order to place them on the same great circle radio path. The National Bureau of Standards prediction techniques do not attempt to predict off-great-circle transmission.[1,2,3]

Determination of the Vertical Radiation Angle. The next step in analyzing the Buffalo-to-Boston HF communication link is to determine the proper vertical radiation angle necessary for the transmitted wave to reach the receiver. Since the height of the ionospheric layer that supports HF propagation varies from 80 km. to 420 km.,[1,2,3] a plot of vertical radiation angle (ϕ) vs. ionospheric layer height is needed.

A geometric representation of the Buffalo-to-Boston HF link is shown in Fig. 1.1 b where

S = arc length AB

C = chord length AB

ρ = radius of arc AB

h' = height of ionospheric layer

From the figure

$S = 2\rho\theta$

$\theta = \sin^{-1} C/2\rho$

For

B = Buffalo, N. Y.

A = Boston, Mass.

S = 381 mi. = 612.93 km.

ρ = radius of the earth = 6371 km.

Then

$$\theta = \frac{s}{2\rho} = \frac{612.93}{2(6371)} = 0.04810 \text{ rad.} = 2^\circ\ 45'\ 22''$$

$$C = 2\rho \sin\theta = 2(6371) \sin \frac{612.93}{2(6371)} = 612.64 \text{ km.}$$

Therefore, the error is small when assuming a flat earth for this link. Using this assumption, the calculations for the vertical radiation angle (ϕ) are as follows:

Since angle OCA = 90° when assuming a flat earth

$$\phi_1 \doteq \tan^{-1} \frac{h'}{AC} = \tan^{-1} \frac{h'}{306.5} \quad \text{for one-hop propagation}$$

$$\phi_2 \doteq \tan^{-1} \frac{h'}{153.2} \quad \text{for two-hop propagation}$$

$$\phi_3 \doteq \tan^{-1} \frac{h'}{102.2} \quad \text{for three-hop propagation}$$

ϕ_1, ϕ_2, and ϕ_3 are plotted as functions of h' in Fig. 1.2.

Propagation Delay Time. Figure 1.3 shows the time required for a transmission over a given path (one-, two-, three- or four-hop) to reach the receiver, given an ionospheric layer height. This figure is for the Buffalo-to-Boston link distance of 613 km.

A plot of predicted F_2-layer height variation with the time of day for January and July 1965[4] is given in Fig. 1.4. The E-layer height can be assumed constant at 110 km. for prediction calculations. By using Figs. 1.3 and 1.4, Fig. 1.5 was generated to show the typical difference in delay time (multipath delay) between one-hop and two-hop propagation to be expected for January and July 1965.

The predicted one-hop and two-hop maximum multipath delay for July 1965 via the F_2-layer will be 2.2 milliseconds, while the minimum will be 1.3 milliseconds. The predicted multipath delay for January 1965 via the F_2-layer will be a maximum of 1.5 milliseconds and a minimum of 1.1 milliseconds for one-hop and two-hop propagation. The predicted multipath delay for one-hop and two-hop propagation via the E-layer will be 0.4 milliseconds for January and July 1965.

PREDICTION OF E- AND F-LAYER MUF

All ionospheric regions affect the maximum frequency which will be returned to earth in a given distance but, for practical purposes, only the F_2 and E regions will be considered for this link.

The E region is relatively stable. Its normal variations can be predicted on the basis of solar activity and the angle of the sun. Most F_2-layer predictions use two basic parameters to express F-layer critical frequencies:[1,2,3] (1) The maximum frequency which will be returned if the signals are transmitted at the sharpest possible angle to the ionosphere; i.e., at vertical incidence when the transmission distance is zero. (2) The maximum frequency which will be returned at the most oblique angle to the ionosphere; i.e., when the transmission distance is maximum for a single ionospheric reflection. The maximum distance is about 4,000 km.

Normally an estimate of frequencies having ionospheric support 50 percent of the time and those having ionospheric support 90 percent of the time are used for HF communication system analysis. These frequencies are called the MUF (Maximum Useable Frequency) and the FOT (Optimum Traffic Frequency), respectively. The optimum frequency (FOT) for F_2-layer propagation is normally taken to be 0.85 of the F_2-MUF, although this figure may be considerably in error.

Although current techniques do not permit reliable estimates of the contribution of sporadic variations of the E-layer in the estimation of loss in high-frequency circuits, these variations often contribute to the MUF and are usually included in the MUF computations.[1,2,3]

The general computation procedure involves the assumption that ionospheric layers are concentric to the earth and that ionospheric conditions on short paths (4,000 km. or less) are approximated by conditions at the path midpoint.

The F_2-layer of the ionosphere is quite variable; the greatest deviations from "normal" usually occurring during ionospheric storms. Predictions of MUF are made for the monthly median values, which are equalled or exceeded 50% of the days during the month, at a specified time of day. MUF predictions are based on the sunspot number (which is a measure of solar activity), angle of the sun (sun's zenith angle), layer height, and the location of the transmitter and receiver.[5] The running average sunspot number (SSN) as used throughout this thesis is 10 since the year 1965 will be a low sunspot year.[6] The predicted MUF's for January and July, assuming a running average SSN of 10 are shown in Figs. 1.6, 1.7, 1.8 and 1.9.

It has been shown[1] that the maximum frequency useable over routes of various lengths is proportional to the secant of the angle of incidence at the ionized layers. This relationship has been incorporated into a nomogram, "Nomograms Showing the Relationship Between Layer Heights, Radiation Angles, Wave Frequencies, and the MUF's at Standard Distances,"[1] which can be used to show whether or not a layer will support a radio wave at various radiation angles. The monthly predictions issued by the Central Radio Propagation

Laboratory[4] for the F_2 4000 MUF and E 2000 MUF are used with this nomogram to determine the greatest angles for E-layer and F_2-layer transmission. In order for an F_2-layer transmission mode to be possible during the daylight hours, the waves at that radiation angle must be able to penetrate the E-layer. The above nomogram was used to determine these E-layer penetration frequencies (E-layer cut-off) and the results are plotted, Figs. 1.6, 1.7, 1.8 and 1.9.

PREDICTED MEDIAN SYSTEM LOSS

System loss is defined as the ratio of the radio frequency power available at the receiving antenna terminals relative to the input power at the transmitting antenna terminals.[11] Several techniques[1,2,8,9,10] for predicting the various modes of propagation and associated signal levels have been developed. Although differing in detail, the various techniques generally involve an estimation of the power attenuation as a function of distance, time of day, season, degree of solar activity and operating frequency. The method developed by P. O. Laitinen and G. W. Haydon has been used extensively and an adaptation of this method is the basis of the prediction technique discussed in this section.

System loss in high-frequency communication circuits may be defined as follows:

$$L_s = L_{rp} + L_i + L_g - G_p + L_{(p)}$$

L_S = System Loss (decibels)

L_{rp} = Free space transmission loss based on the length of the path being considered (decibels)

L_i = Losses due to ionospheric absorption (decibels)

L_g = Losses due to ground absorption of the reflected transmission (decibels)

G_p = Path antenna gain (the sum of transmitting antenna gain relative to an isotropic antenna in the direction of propagation and that of the receiving antenna in the direction of propagation) (decibels)

$L_{(p)}$ = Loss associated with day-to-day variations in ionospheric and circuit parameters (statistically determined and dependent upon circuit location, day or night, path length and percent of days being considered)[1] (decibels)

In high-frequency communication circuits, several propagation paths often are possible; a single reflection from the F region (1F); a single reflection from the E region (1E); multiple reflection from the E and F regions (2F, 3F, 2E, 3E, etc.). The probable paths are dependent upon the geometry of the circuit, involving layer heights and great circle distances and the relative ionization in the various regions. The primary transmission modes and their respective radiation angles for the Buffalo-to-Boston link can be determined using techniques outlined in Section I B. The results are tabulated for one-hop propagation, January 1965 (Table 1); two-hop propagation, January 1965 (Table 2); one-hop propagation, July 1965 (Table 3); and two-hop propagation, July 1965 (Table 4).

The free space transmission loss (L_{rp}) is a function of the great circle distance, radiation angle and operating frequency. The resultant predicted L_{rp} for the primary transmission modes and their corresponding MUF's of FOT's are found using nomograms.[1] The results are tabulated in Tables 1, 2, 3 and 4.

The predicted absorption loss is the combination of two losses: one, the average loss due to ionospheric absorption (L_i); two, the average loss due to ground absorption of the reflected transmission (L_g). The ionospheric absorption loss (L_i) is a function of the absorption index, radiation angle, gyro-frequency plus operating frequency and the number of hops. The ground absorption loss (L_g) is a function of the type of ground where the reflection occurs ("poor earth" is used in this thesis, however, measurements should be made to determine the actual relative permittivity and conductivity at the reflection points), radiation angle and the operating frequency. The resultant predicted absorption loss for the primary transmission modes and their corresponding MUF's or FOT's are found using nomograms.[1] The results are tabulated in Tables 1,2,3 and 4.

The difference, L_p, between the quasi-minimum system loss (lowest hourly median loss expected within the month) and the monthly median of the hourly median is estimated from a probability distribution of hourly median system loss.[1] For the B/B link (a temperate latitude circuit) this difference, L_p, averages about 9 db for 50 percent reliability.

To determine the antenna gain (G_p) one must have the radiation patterns for both the transmitting and receiving antennas. The radiation patterns should show the relationship between the operating frequency and the vertical radiation angle as a function of the antenna gain (above the gain of an isotropic antenna in free space). The radiation patterns should be determined experimentally in order to be of the greatest value, since the surrounding terrain at the antenna site affects the radiation patterns to a very large extent. Knowing the operating frequency and the required vertical radiation angle (determined in Section I B), one can determine the antenna gain from the antenna radiation patterns. The detailed data required for determining the antenna gains for various types of antennas is beyond the scope of this thesis; therefore, the transmitting and receiving antennas each are assumed to have a uniform gain of 5 db, above an isotropic antenna, for all required vertical radiation angles and operating frequencies.

The predicted median system loss (L_s) is now calculated according to the definition

$$L_s = L_{rp} + L_i + L_g - G_p + L_{(p)}$$

The results are tabulated in Tables 1,2,3 and 4.

PREDICTED ATMOSPHERIC NOISE

In the high-frequency band there exists a background of radio noise that is primarily atmospheric in nature, but galactic and man-made noise also may be important.[1] Galactic noise only is important when the operating frequency is above the critical frequency of the F_2-layer in the vicinity of the receiver. Preferably, man-made noise should be measured at the receiving location. Therefore, the radio noise considered in this section will be confined to atmospheric noise.

The data used in estimating the distributions of atmospheric noise power, contained in CCIR Revised Report 65,[6] were obtained mainly from sixteen stations located throughout the world. These stations, with one exception, use standardized recording equipment, the ARN-2 Radio Noise Recorder, and are operated by a number of organizations in an international cooperative program. The CCIR Revised Report 65[6] will be used to estimate the atmospheric noise power.

First, an estimate of the 1 mc/sec noise db above KTB is obtained using the "Noise Distribution Chart" (CCIR Revised Report 65)[1,6] for the proper month and time block, based on local time. Next, the appropriate "Atmospheric Radio Noise Chart"[1,6] is selected and entered with the 1 mc/sec noise level obtained above and the operating frequency, from which is obtained the predicted atmospheric noise, 1 cps bandwidth. The predicted atmospheric noise is tabulated in Tables 1,2,3 and 4.

PREDICTED S/N AT FOT

The total available signal power, relative to noise, in a one-cycle bandwidth is useful in estimating communication circuit performance. This ratio (S/N) in decibels is obtained by subtracting the noise power, in decibels, from the available signal power at the receiver, in decibels. The available signal power at the receiver, in decibels, equals the power available at the transmitter antenna terminals, in decibels, minus the median system loss, in decibels. In this thesis, a transmitter of 500 watts output power is assumed available. The signal power available at the transmitter antenna would be 27 db for a 500 watt transmitter. The available signal-to-noise ratio now is calculated using the atmospheric noise power and median system loss calculated in the previous subsections and the results are tabulated in Tables 1,2,3 and 4.

The results of this section would be adequate for a communicator to predict the signal-to-noise ratio to be expected if he were able always to operate at the FOT or MUF. Unfortunately the communicator generally does not have the frequency allocations necessary to follow the "best" frequencies throughout the day and night. Besides, it must be assumed that many other communicators are trying

ing to use the same path and hence not all will be able to use the "best" frequency. Therefore, the communicator should be provided with information about other possible frequencies and the resultant S/N to be expected when using his communication system. The next section will present a technique that provides the communicator with such information.

SECTION II

PRESENTATION OF NEW TECHNIQUE

INTRODUCTION

Present techniques for the prediction of performance of high-frequency communication circuits (an example was presented in Section I) are limited in their usefulness to the communicator. A communication system will not be able to operate always at the FOT or MUF because of the limited number of frequencies which can be allocated to any one communication system and because of interference caused by other communication systems attempting to use the same frequency. Therefore, the communicator must have information available on useable frequencies and performance characteristics below the MUF.

The high-frequency communicator needs a prediction technique that presents the results in a comprehensive manner and which is easy to use. Also, it would be desirable for the prediction technique to be flexible enough that system parameter changes could be entered and the effects on the overall communication system could be determined. This section will present a prediction technique that will allow the high-frequency communicator to determine system performance below the MUF and, at the same time, be flexible enough to meet the needs mentioned above.

REFERENCE SYSTEM DEFINITION

As the operating frequency is decreased, the available signal power normally decreases and the noise power increases, resulting in a decreasing available signal-to-noise ratio. As the available signal-to-noise ratio decreases, the circuit reliability is lowered. The frequency, at which any further decrease would yield an unacceptable reliability, is the lowest useful high frequency for the circuit (LUF).

The value of the lowest useful frequency, LUF, is determined in part by natural conditions existing in the ionosphere and in part by the characteristics of the link communication equipment. Nothing can be done to improve the natural state of the ionosphere, but available methods of improvement can be applied to improve system component characteristics. Some of the parameters that might be changed which would affect the gain of the system are: frequency, modulation technique, transmitter power, bandwidth, required error rate, required reliability, variation in receiver and transmitter antenna gain (due to variation in required launch angle) and data rate.

The basic problem is to determine the extent to which a communication system's useable frequency (LUF) is lowered for various decreases in required system gain, but to do this first it is necessary to define a system to be used as a reference. After the reference system is chosen, a required signal-to-noise ratio must be selected and the lowest useable frequencies calculated.

For the communication link selected for demonstration, B/B, the reference system chosen is: modulation - CW on-off, bandwidth - 3 kc., error rate - 10^{-3} errors/sec, transmitter power - 500 watts, receiver antenna gain - 5 db at all frequencies and vertical radiation angles, transmitter antenna gain - 5 db at all frequencies and vertical radiation angles, and level of reliability - 99 percent. This system is selected as a reference system because: (1) it is a possible system for operation on the B/B link, and (2) its S/N requirements are high, which gives a relatively high LUF. Based on the modulation, CW on-off, and the error rate, 10^{-3} errors/sec, the S/N, at the receiving antenna terminals, is chosen to be +34 db.

The results obtained in Section I and tabulated in Tables 1,2,3 and 4 were based on a bandwidth of 1 cps and a level of reliability of 50 percent. In order to apply those results to the operation of the reference system, it is necessary to convert the basis of the results from a bandwidth of 1 cps to 3 kc. and the level of reliability from 50 percent to 99 percent. To convert the base bandwidth to 3 kc, 35 db $\left[10 \log\left(\frac{3{,}000}{1}\right) \doteq 35 \text{ db}\right]$ must be subtracted from the S/N at FOT calculated in Section I. To convert the level of reliability to 99%, the "Daytime Reliability of Sky-Wave Circuit Below 60° Geomagnetic Latitude"[1] graph is used to determine that 14 db must be subtracted from the S/N at FOT calculated in Section I.

After the S/N at FOT, obtained in Section I, is converted to the reference system, a signal-to-noise ratio of 34 db would correspond to 0 db gain with respect to the required signal-to-noise ratio of the reference system. As an example of the above procedure, the signal-to-noise ratio in decibels at the FOT relative to the reference system vs. time of day, for one-hop propagation in January 1965, is shown in Fig. 3.1. Now that a reference system has been established, the next step is to determine the gains obtained when operating below the FOT or MUF and to reference these gains to the reference system gain.

RELATIVE GAIN

In Section I E the following definition of median system loss is given:

$$L_s = L_{rp} + L_i + L_g - G_p + L_{(p)} \qquad (2\text{-}1)$$

L_s = System loss (db)

L_{rp} = Free space transmission loss (db)

L_i = Ionospheric absorption loss (db)

L_g = Ground absorption loss (db)

G_p = Total antenna gain (db)

$L_{(p)}$ = Loss associated with day-to-day variations (db)

In Section I E ionospheric absorption loss and ground absorption loss were combined into one loss called the total absorption loss, L_A, and $L_{(p)}$ was determined for the B/B link to be about 9 db for 50 percent reliability. Then

Eq. (2-1) becomes

$$L_S = L_{rp} + L_A - G_p + 9 \text{ db} \tag{2-2}$$

In Section I G the total available signal power (S) relative to noise (N) in a 1 cps bandwidth is defined as

$$S/N = S - N \tag{2-3}$$

where

S/N = Signal-to-noise ratio in db

S = Signal power in db

N = Atmospheric noise power in db

In Section I G the available signal power at the receiver is defined as

$$S = P_t - L_S \tag{2-4}$$

where

S = Signal power in db

P_t = Transmitter power in db

L_S = System loss in db

Substituting Eqs. (2-2) and (2-4) into Eq. (2-3), Eq. (2-3) becomes

$$S/N = P_t - L_{rp} - L_A + G_p - 9 \text{ db} - N \tag{2-5}$$

For the reference system defined in Section II B

$P_t = 10 \log \left(\frac{500}{1}\right) = + 27$ db

$G_p = G_t + G_r = + 10$ db

To convert to a bandwidth of 3 kc: - 35 db

To convert to a reliability of 99%: - 14 db

Therefore, for the reference system, Eq. (2-5) becomes

$$S/N = - 21 - L_{rp} - L_A - N \quad \text{(db)} \tag{2-6}$$

but, since the required signal-to-noise ratio for the reference system is + 34 db, Eq. (2-6) becomes

$$S/N = -55 \text{ db} - L_{rp} - L_A - N \qquad (2\text{-}7)$$

where

S/N = Signal-to-noise ratio relative to a required S/N of + 34 db

The signal-to-noise ratio defined by Eq. (2-7), for the B/B communication link, will be called the relative system gain.

Example: one-hop, January 1965, 0000 GMT (See Table 1)

L_A = 0 db

L_{rp} = 103 db

N = -158 db

Using the above values in Eq. (2-7)

$$\begin{aligned} \text{Relative System Gain} &= -55 - L_{rp} - L_A - N \qquad (2\text{-}7) \\ &= -55 - 103 - 0 - (-158) \\ &= 0 \text{ db} \end{aligned}$$

By using Eq. (2-7) the relative system gain could be calculated as a function of the LUF for every two hours for January and July 1965 for the B/B communication link. However, to simplify the calculation and to gain an insight as to how the various parameters affect the relative system gain; the variations of both the predicted total absorption (L_A) and the predicted atmospheric noise (N) with operating frequency will be determined.

Absorption loss variation with frequency is calculated using the method described in Section I E for every two hours throughout the day for one-hop and two-hop propagation for January and July 1965 and the results are plotted in Figs. 2.2 and 2.3. Atmospheric noise variation with frequency is calculated using the methods described in Section I F for every two hours throughout the day for one-hop and two-hop propagation for January and July 1965 and the results are plotted in Figs. 2.4 through 2.7. The free space transmission loss (L_{rp}) variation with frequency can easily be determined using the "Nomogram of Transmission Loss Due to Ray-Path Distance"[1] so that no other simplification is necessary.

By using Eq. (2-7) and the above results it is now a relatively easy task to determine the relative system gain as a function of LUF for January and July 1965.

Example: one-hop, July 1965, 1600 GMT

For LUF = 8.02 mc/sec

$N = -173$ db (Fig. 2.7)

$L_A = 17.2$ db (Fig. 2.3)

$L_{rp} = 108$ db (Nomogram[1])

Substituting the above values in Eq. (2-7)

$$\text{Relative System Gain} = -55 - L_{rp} - L_A - N \qquad (2\text{-}7)$$

$$= -55 - 108 - 17.2 + 173$$

$$= -7.2 \text{ db}$$

For LUF = 7.0 mc/sec

$N = -172.5$ db (Fig. 2.7)

$L_A = 22.0$ db (Fig. 2.3)

$L_{rp} = 107$ db (Nomogram[1])

Substituting the above values in Eq. (2-7)

$$\text{Relative System Gain} = -55 - L_{rp} - L_A - N \qquad (2\text{-}7)$$
$$= -55 - 107 - 22 + 172.5$$
$$= -11.5 \text{ db}$$

For LUF = 6.0 mc/sec:

$N = -172.5$ db (Fig. 2.7)

$L_A = 28.5$ db (Fig. 2.3)

$L_{rp} = 106$ db (Nomogram[1])

Substituting the above values in Eq. (2-7)

$$\text{Relative System Gain} = -55 - 106 - 28.5 + 172.5$$
$$= -17.0 \text{ db}$$

For LUF = 5.0 mc/sec

$N = -173.0$ db (Fig. 2.7)

$L_A = 37.0$ db (Fig. 2.3)

$L_{rp} = 105$ db (Nomogram[1])

Substituting the above values in Eq. (2-7)

$$\text{Relative System Gain} = -55 - 105 - 37 + 173.0$$
$$= -24.0 \text{ db}$$

Using this information, the relative gain curve for one-hop, July 1965, 1600 GMT is plotted in Fig. 2.11. Similar calculations are made for every two hours for January and July 1965 and the results are plotted in Figs. 2.8 through 2.11.

LUF RELATIVE GAIN CONTOURS

In order to illustrate the effect of increasing or decreasing system gain on the overall operation of a communication link, LUF relative gain contours could be plotted. This plot should include the FOT, MUF and E-layer cut-off curves in order to determine the relative gain curve limits.

The B/B communication link will be used to demonstrate the LUF relative gain contours. After the FOT, MUF and E-layer cut-off curves are plotted, the relative gain contours are added. By using the relative gain vs. frequency (LUF) curves, Figs. 2.8 through 2.11, relative gain contours for every five decibels are plotted and the results are shown for one-hop and two-hop propagation for January and July 1965 in Figs. 2.12 through 2.15. These relative gain contours serve to show the effect on communication capability of reducing the LUF by increasing system gain. Conversely, they show also the increase in process gain that may be achieved at certain periods for the purpose of raising the data rate or decreasing transmission error rate.

Figures 3.12 through 3.15 can be used if the signal-to-noise requirements of a given system are related to the required signal-to-noise ratio for the reference system. For example, a system using frequency-shift-keying (FSK) for modulation, a bandwidth of 2 kc/sec, the same antennas and reliability requirements as the B/B reference system will operate at a 10^{-3} error rate with 5 db less required S/N than the reference system. The LUF for this FSK system is the 5 db contour shown in Figs. 2.12 through 2.15. Conversely, if the operation of the FSK system is maintained along the 0 db reference contour, 5 db excess gain or a S/N of 5 db more is available to reduce the error rate, increase the data rate or lower the transmitted power. Many more applications exist for the relative gain contours developed in this section and the most important of these applications will be presented in the next section.

SECTION III

APPLICATION OF RELATIVE GAIN CONTOURS

FREQUENCY ALLOCATION ANALYSIS

In order to operate any communication system it is necessary to have frequencies assigned by a central communication control center or the Federal Communication Commission. Therefore, it is necessary to make a frequency allocation request from the control center or the FCC stating what and how many frequencies are needed and to justify the request for those frequencies. The relative gain contours developed in Section II (for such a system as the above described B/B link) can be used to facilitate the selection of the frequencies to be requested and as a justification for the request.

The three requirements for a useable frequency are:

1. The frequency must be below the MUF.
2. The frequency must be above the E-layer cut-off.
3. The frequency must be above the LUF.

When at least one frequency satisfies the three requirements, communication is possible. If no single frequency satisfies each of the three requirements, communication with the system gain and required reliability is not possible.

By using the relative gain contours generated for a particular communication link, an analysis of useable communication time can be made. In order to demonstrate the procedure and the results of such an analysis, the relative gain contours generated in Section II for the B/B communication link will be used.

The communicator must determine first which frequency bands are available for his use and then select a representative frequency within each of these bands. The ten representative frequencies chosen for the B/B link are as follows: 7.75, 6.85, 5.90, 5.25, 4.85, 4.55, 3.80, 3.25, 2.70 and 2.15 mc/sec. These frequencies are entered on the relative gain contour for one-hop propagation January 1965 as shown in Fig. 3.1. By using the highest useable frequency available at any one time it is possible to determine the variation in relative system gain as one attempts to communicate throughout a 24-hour period. The results of this analysis can be conveniently displayed as shown in Fig. 3.2. Figure 3.2 shows that the communicator can expect to establish successful communication (in January 1965 via one-hop propagation), using the ten frequencies selected, for 12.1 hours with an overall system gain of 0 db (this is with respect to the reference system established in Section II B) which corresponds to a signal-to-noise ratio at the receiver terminals of 34 db. Figure 3.2 shows that communication could be established for an additional 4.0 hours but at a system gain of -5 db or a S/N of

29 db. In the remaining 7.9 hours of the day communication could be accomplished at a system gain of -10 db or a signal-to-noise ratio of 24 db. This analysis, using the relative gain contours and ten selected frequencies, enables the communicator to determine the amount of useable communication time available and the signal-to-noise ratio to be expected during this time. If the analysis demonstrated above is applied to the remaining relative gain contours developed in Section II, the results are as shown in Figs. 3.2 and 3.3.

Next, a trade-off study should be conducted using other representative frequencies to determine whether the same communication use time and system gain can be achieved with fewer frequencies. The six frequencies chosen for the trade-off study are as follows: 2.03, 2.70, 3.85, 4.85, 5.85 and 7.45 mc/sec. Using these six frequencies, the analysis demonstrated above is repeated and results are shown in Figs. 3.4 and 3.5. A comparison of Figs. 3.2 and 3.3 with Figs. 3.4 and 3.5 show that almost as much useable communication time is available with the six frequencies chosen for the trade-off study as with the ten frequencies. It can be shown that these six frequencies are the minimum number of frequencies necessary for communication without substantial loss in useable communication time. A request by the communicator for a frequency allocation of these six frequencies would be based on the above analysis.

MULTIPATH CALCULATIONS

In order to describe the severity of the multipath propagation encountered on the B/B high-frequency link it is necessary to define what is considered "mild multipath" and "severe multipath". If two signals appearing at the receiver at the same instant differ by 8 db or less in relative gain this will be called "severe multipath" condition. If the two signals differ by more than 8 db but less than 12 db in relative gain, such will be called "mild multipath" condition. For signals differing by more than 12 db the interference is considered to be negligible or a condition of no multipath is said to exist. By using the definitions given above a prediction as to the severity of the multipath to be encountered on the B/B link will be made.

By using the relative gain curves, it is possible to estimate the severity of the multipath between the one-hop and two-hop modes. This estimation is made using the definitions stated above. However, it must be noted that the definitions and hence the predictions are based on the assumption that the signals arrive at the receiver at the same instant. Arrival of the signals at the receiver at different times due to difference in time required to propagate over different paths is discussed in Section I C.

By using the relative gain curves (Figs. 2.8 through 2.11) and the definition of multipath severity given above, Figs. 3.6 through 3.9 can be developed to show the severity of multipath encountered, for each two hour period throughout the day, between the one-hop and two-hop propagation modes. It can be seen from the multipath curves, Figs. 3.6 through 3.9, that a no multipath condition, based on the definitions and conditions stated above, exists for frequencies near the MUF or FOT throughout the day. This implies that it is possible for a communicator to use this region of no multipath for an entire 24-hour period if he has the necessary assigned frequencies and system gains at his disposal. This frequency band of no predicted multipath (for the B/B link), on the average, lays between 0.93 x FOT and the FOT for January and 0.75 x FOT and the FOT for July.

The next step is to take into account the actual frequencies assigned to the communicator when determining the severity of the multipath present and the length of time the multipath is encountered. In order to demonstrate the procedure and the results of such an analysis, the relative gain contour showing the six assigned frequencies (Fig. 3.1) for the B/B communication link will be used together with the multipath prediction curves, Figs. 3.6 and 3.7. By using the same technique that was used to determine communication use time (Section III A), it is possible to determine from the multipath prediction curves (Figs. 3.6 and 3.7) the severity of multipath and the length of time it is present. The results of this analysis can be conveniently displayed as shown in Fig. 3.10. This technique is then applied for July 1965 and the results shown in Fig. 3.10.

Figure 3.10 shows a good deal less clear transmission time (no multipath) is available than is indicated by examining the multipath prediction curves, Figs. 3.6 and 3.7. Such is to be expected since Fig. 3.10 is based on specific assigned frequencies which limit the ability of the system to track the clear transmission band near the FOT.

It should be noted also from Fig. 3.10 that the occurrence of severe multipath conditions are confined to nighttime periods. This means that in order to experimentally evaluate an adaptive system under severe multipath conditions it would be necessary to conduct a large part of an experimental program at night. Up to nine hours (predicted) of severe multipath conditions will exist during the winter months, while as few as two hours of severe multipath conditions will exist during the winter.

COMMUNICATION SYSTEM ADAPTION

General Aspects and Scope. Previous sections have described the environmental conditions and media propagation phenomena that affect high-frequency communication transmissions. These have been in reference particularly to the B/B link but are considered here to be representative. Such factors as have been discussed may be referenced best as the geometrical factors in high-frequency system definition. When considered in combination with such basic operational factors as input message loading, allowable output error rate and available power, there results definite concepts as to the possible adjustable parameters of a high-frequency adaptive system. With the aid of the relative gain contours that have been developed such adjustable parameters and their inter-relationships will be discussed.

The major areas of high-frequency system adaption that can be considered are stated in the following list. These are presented in a somewhat relative order that reflects both degree of importance and difficulty of implementation.

1. Frequency (including allocation considerations).
2. Power (including intimate antenna relations).
3. Modulation (including deversity of frequency and time).
4. Data Rate.
5. Coding Structure.
6. Antenna Considerations (including strategic, spectrum adaption and diversity).

In the remainder of this section the relative gain contours will be used to investigate possible frequency adaption and power adaption.

Frequency Adaption. The relative gain contours as presented in Section II (Figs. 2.12 through 2.15) show at a glance the need for frequency adaption. To obtain a measure of the frequency translation requirements for a 24-hour adaptive system the slope of these gain contours for a dynamic range of approximately 25 db in steps of 5 db are plotted for the one-hop and two-hop transmissions for the months of January and July 1965. These curves which represent frequency translation requirements per hour to maintain a constant performance are presented in Figs. 3.11 through 3.14. The basic assumption here is that a constant signal-to-noise ratio at the receiver input under all fading and multipath conditions will produce constant performance. This is not true except for a perfectly unperturbed media, but such a presentation does perform the service of providing a first estimate of the dynamic frequency requirement.

It is obvious that much is to be gained by a communicator that could make the necessary adaption in frequency in order to maintain a constant overall system performance. The constant performance contours (Figs. 3.11 through 3.14) show that a communicator would have to have a very large selection of allocated frequencies and a communication system that had a large dynamic range. However, the degree of frequency adaption is severely limited by the constriction of the high-frequency spectrum and the necessary regulations as to allocation of fixed operational frequencies.

By using the relative gain contours generated for a particular communication link and the specific assigned frequencies for that link an analysis of frequency adaption can be made. In order to demonstrate the procedure and the results of such an analysis, the relative gain contours presented in Section II for the B/B communication link will be used.

The technique to be used in this analysis is essentially the same as that used in Sections III A and B. Select a relative gain contour and enter the six frequencies determined in Section III A. For each frequency it is possible to determine the variation in relative system gain as one attempts to communicate throughout a 24-hour period. The results of this analysis, which show the variation of relative gain for each frequency, are shown in Figs. 3.15 through 3.18.

By using this technique now it is possible to determine when frequency changes should be made in order to achieve maximum signal-to-noise ratios. In order to picture the operation of a system throughout a 24-hour period Figs. 3.19 and 3.20 are drawn using the technique described above. From Figs. 3.19 and 3.20 constant frequency contours are determined which show a primary and alternate frequency adaption plan (Figs. 3.21 and 3.22) for communication throughout a 24-hour period.

These 24-hour scenarios, Figs. 3.21 and 3.22, show the large number of frequency changes necessary to maintain maximum signal-to-noise ratios. The most frequent frequency changes occur at sunset and sunrise as was expected since this is when the ionosphere is undergoing its most rapid changes in ionization. Figures similar to these scenarios might provide another method of optimum frequency selection for allocation requests.

Frequency adaption may be used also to minimize multipath effects. The frequency adaption, as evidenced in the trial scenarios shown in Figs. 3.21 and 3.22, was developed on the basic assumption of obtaining maximum signal-to-noise ratios consistent with minimum multipath effects. However, in at least one case a decision was made to shift to the lower-loss operation at the higher frequency. This is at the time of the cut-off of the two-hop path at the higher frequency. Thus a minimum of multipath operation was the decision basis in this instance and not maximum power. Also, for the 4-hour period in January from 1500 to 1900, GMT, an approximate 4 db loss was accepted for operation at a lower frequency in order to avoid potentially mild multipath during the period. At the time indicated, two hours before noon and two hours after noon, EST, the two-hop path suffers considerably more absorption at the lower frequency. This provides an improved multipath situation at the lower frequency for continued high quality transmission. The 4 db penalty resulted in a net saving of 5 db for multipath margin allowance (9 db - 4 db) thus demonstrating that frequency adaption, by avoiding multipath, can provide a relative performance gain. It should be noted here that this particular situation and the consequent adaptive decision was forced by the lack of a sufficient number of allocated frequencies. In Fig. 3.19 the solid line adaptive frequency path could have moved to a higher frequency to follow the clear, no-multipath, frequency lane that exists near the F_2 - FOT if the spacing were 500 kc/sec, but with a frequency spacing of 1 mc/sec the alternate procedure was taken.

Further considerations that influence modulation and data rate adaption are apparent. When frequency adaption can provide isolation from severe multipath effects, modulation and data rates may be held constant, otherwise one of these parameters would be adjusted to aid transmissions at that time.

The performance contours also provide a measure of frequency adaption requirements for either constant performance at constant data rate, increased performance at the same data rate or increased data rate possibilities at constant performance.

<u>Power Adaption</u>. Generally, the application of high-frequency communications requires fixed power transmission, although some proposals and actual applications have been concerned with diurnal power changes. The basic need for improved performance in high-frequency communications and the long-haul requirements have influenced both design and operational practice to stress fixed maximum power usage.

Constant power operation is representative of millions of dollars worth of installed equipment. Therefore, the pattern for adaption definition that is obtained from the environmental model suggests that the consequent diurnal variation in available power at the receiver be used to provide increased data rates during favorable times of the 24-hour period.

Therefore, the premise taken here is that outside of specific application, a power-limited system is assumed and the excess power available at a given time is treated as a bonus to support increased data rate or increased performance, or both. Typical curves that indicate such gain availability were presented in the previous subsection, Figs. 3.15 through 3.18.

The diurnal power effect is more pronounced in January 1965 because of nearly continuous F_2-layer operation. The July maximum levels tend to remain constant during the 24-hour period at approximately the nighttime levels of the winter operation. This is because of the switch from F_2-layer to E-layer propagation during the summer day. It will be noted that the summer operation experiences a dynamic power range of 20 db during the day and 6 db during the night, as compared to the day and night 11 db dynamic range for winter operation. It is to be emphasized that these estimates were made from the optimum transmission curves of Figs. 3.21 and 3.22.

FIGURE 1.1

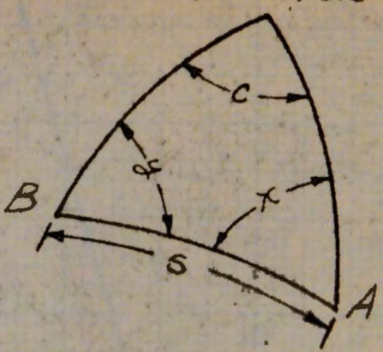

SPHERICAL EARTH

(a)

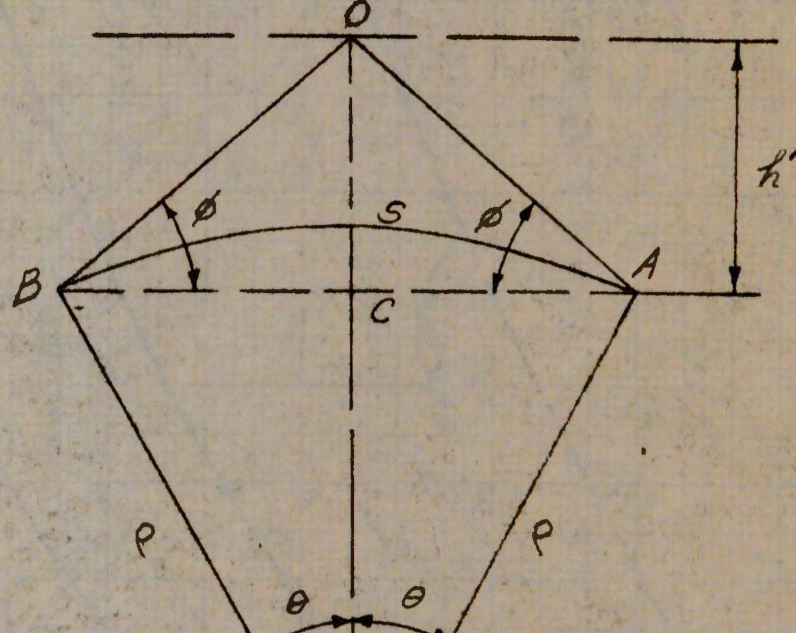

FLAT EARTH

(b)

GEOMETRIC REPRESENTATION OF B/B LINK

FIGURE 1.2

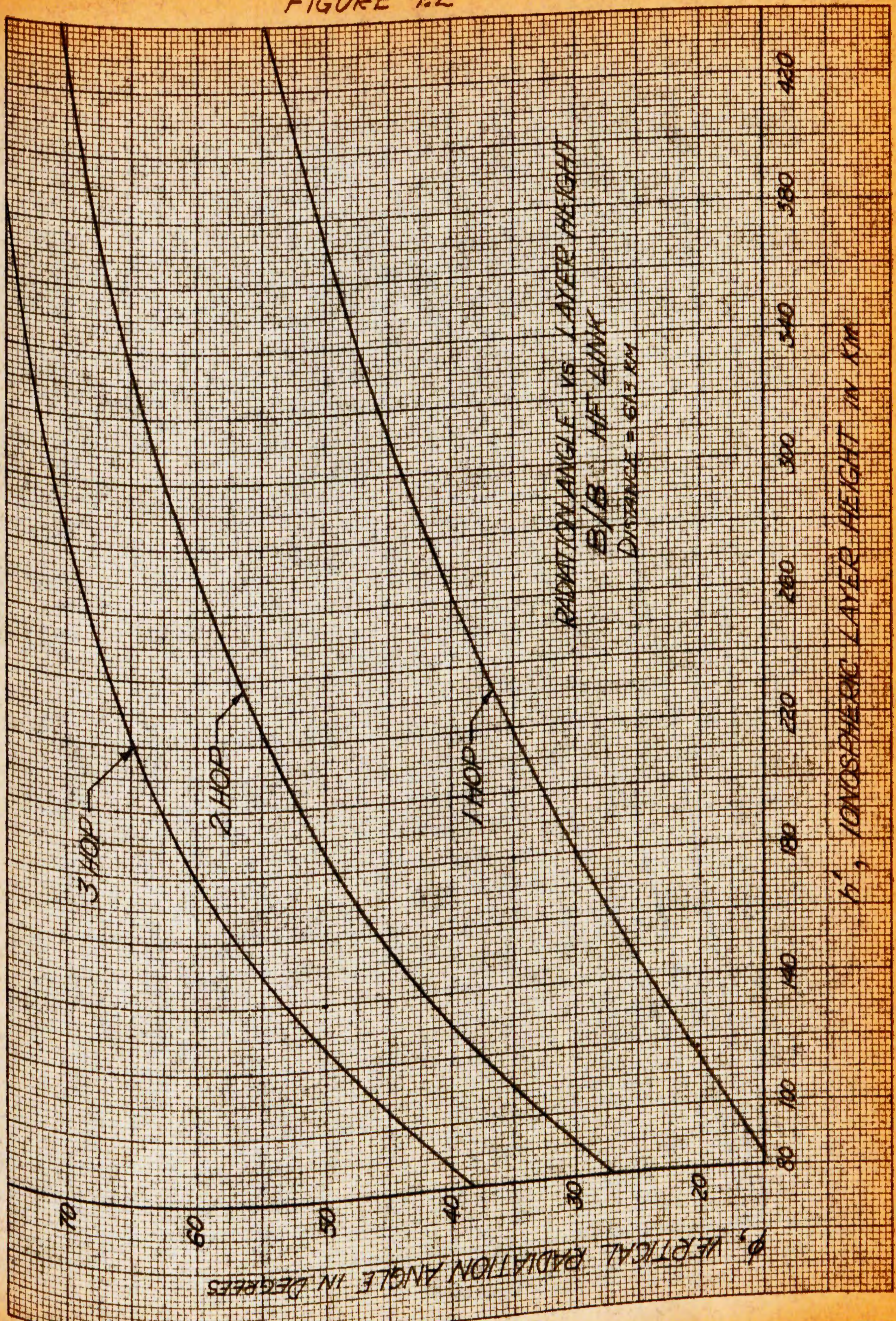
RADIATION ANGLE VS LAYER HEIGHT
B/B HF LINK
DISTANCE = 613 KM
3 HOP
2 HOP
1 HOP
h', IONOSPHERIC LAYER HEIGHT IN KM
φ, VERTICAL RADIATION ANGLE IN DEGREES
80
100
140
180
220
260
300
340
380
420
20
30
40
50
60
70

FIGURE 1.3

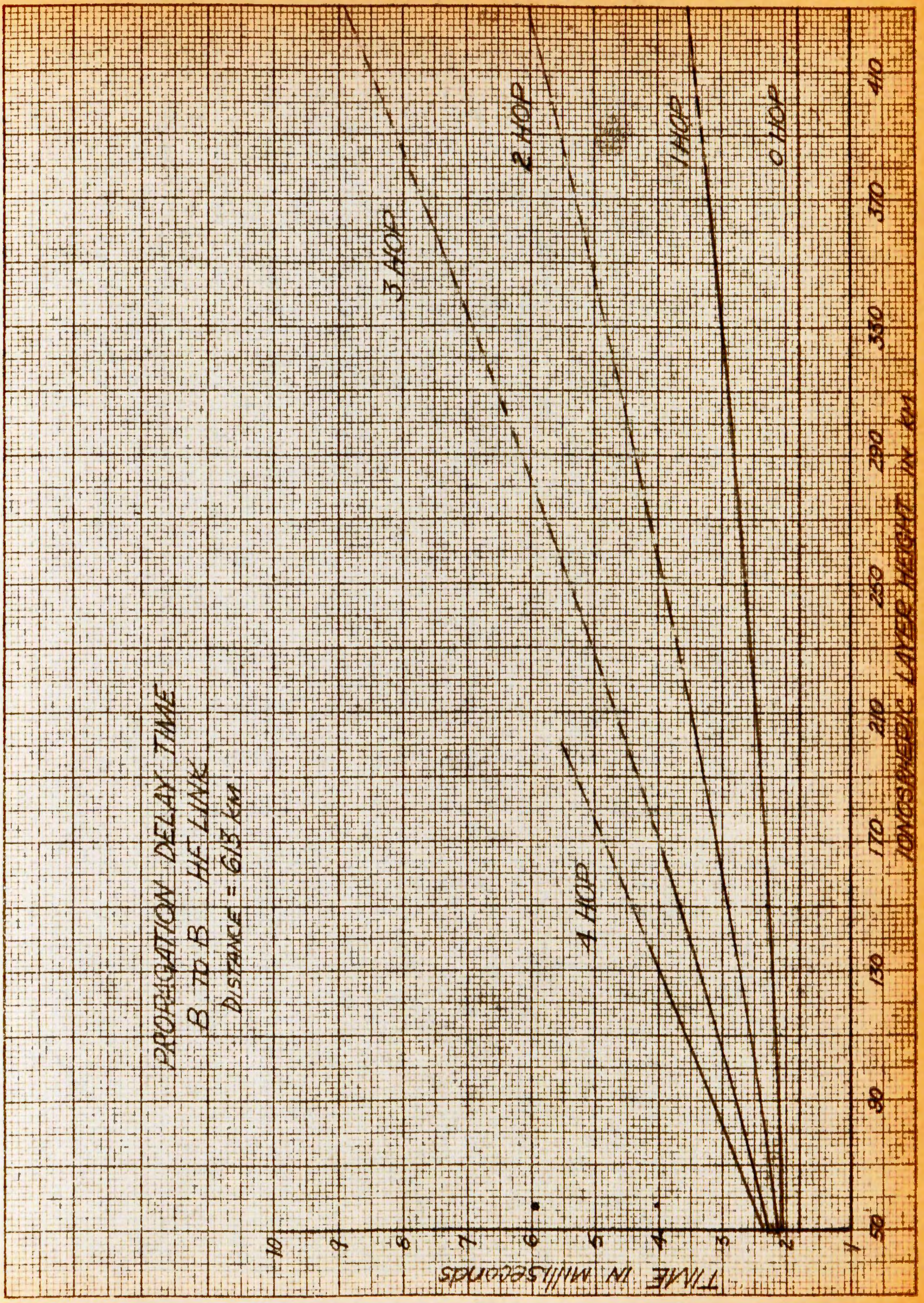
PROPAGATION DELAY TIME
B TO B HF LINK
DISTANCE = 613 KM
0 HOP
1 HOP
2 HOP
3 HOP
4 HOP
TIME IN MILLISECONDS
1
2
3
4
5
6
7
8
9
10
IONOSPHERIC LAYER HEIGHT IN KM
50
90
130
170
210
250
290
330
370
410

FIGURE 1.4

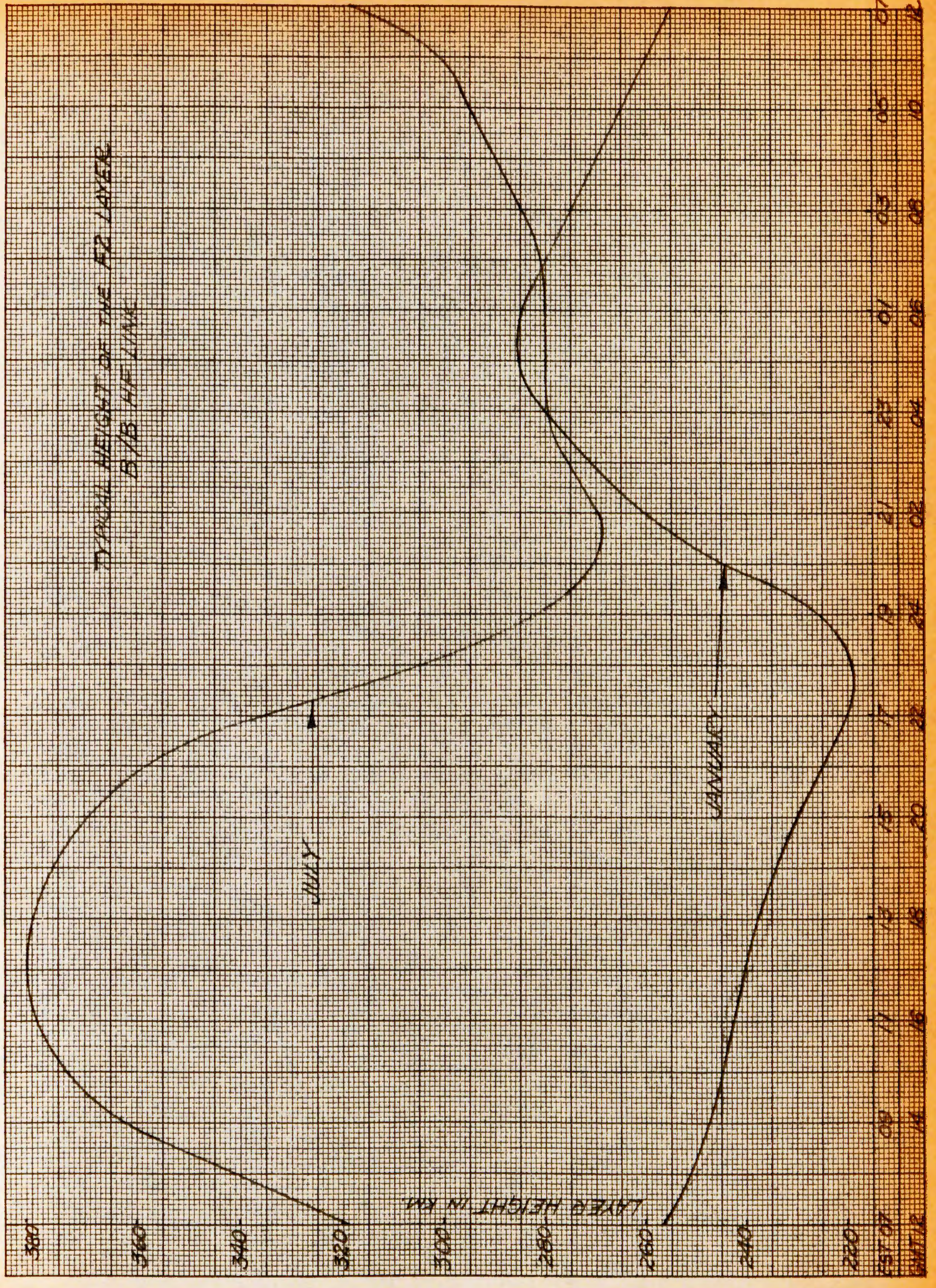

TYPICAL HEIGHT OF THE F2 LAYER
B/B HF LINE
JULY
JANUARY
LAYER HEIGHT IN KM
380
360
340
320
300
280
260
240
220
EST 07 09 11 13 15 17 19 21 23 01 03 05 07
GMT 12 14 16 18 20 22 24 02 04 06 08 10 12

FIGURE 1.5

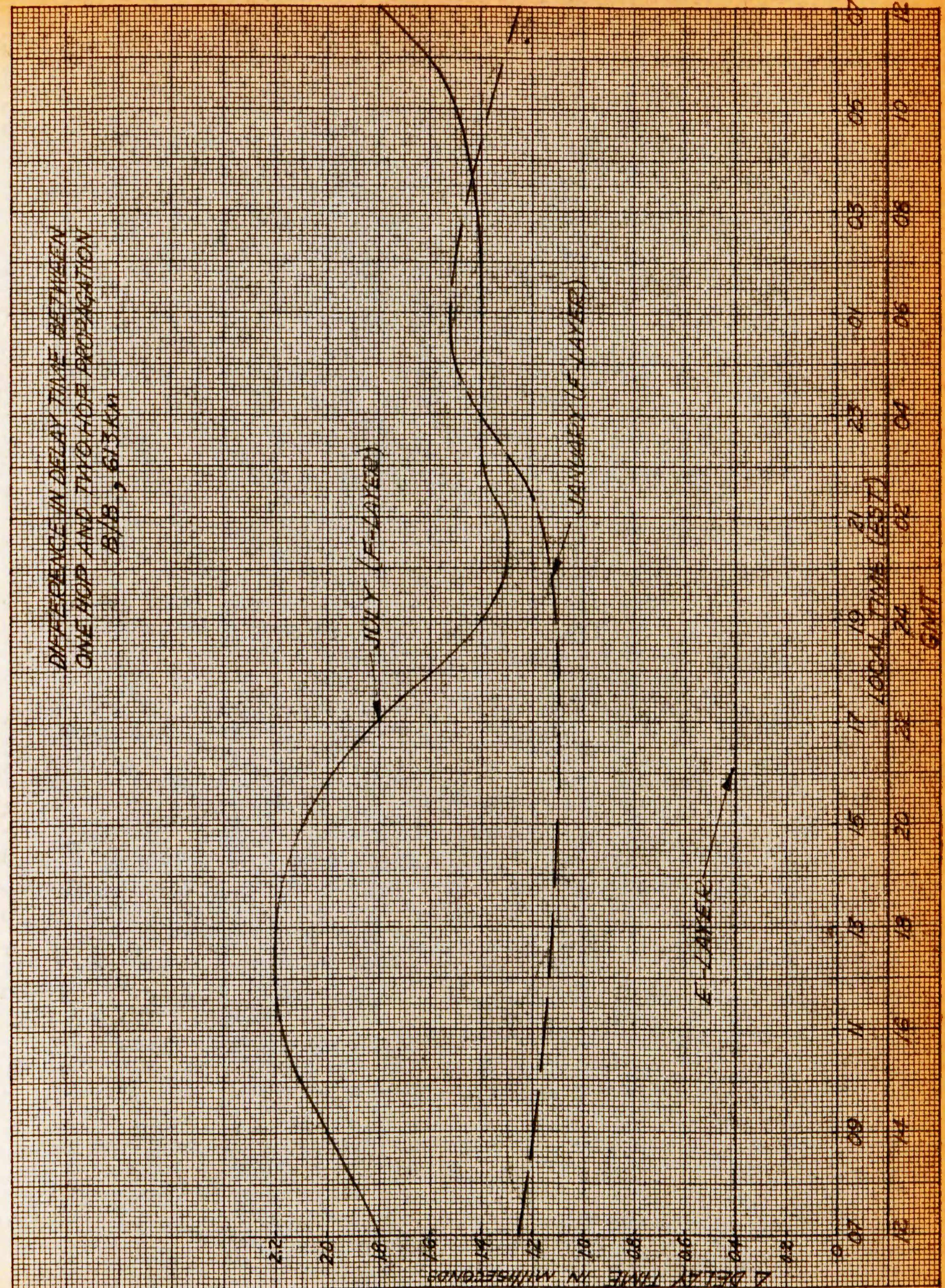

DIFFERENCE IN DELAY TIME BETWEEN
ONE HOP AND TWO HOP PROPAGATION
B/B, 613 Km
JULY (F-LAYER)
JANUARY (F-LAYER)
E-LAYER
Δ DELAY TIME IN MILLISECONDS
0
0.2
0.4
0.6
0.8
1.0
1.2
1.4
1.6
1.8
2.0
2.2
07 09 11 13 15 17 19 21 23 01 03 05 07
LOCAL TIME (EST)
12 14 16 18 20 22 24 02 04 06 08 10 12
GMT

FIGURE 1.6

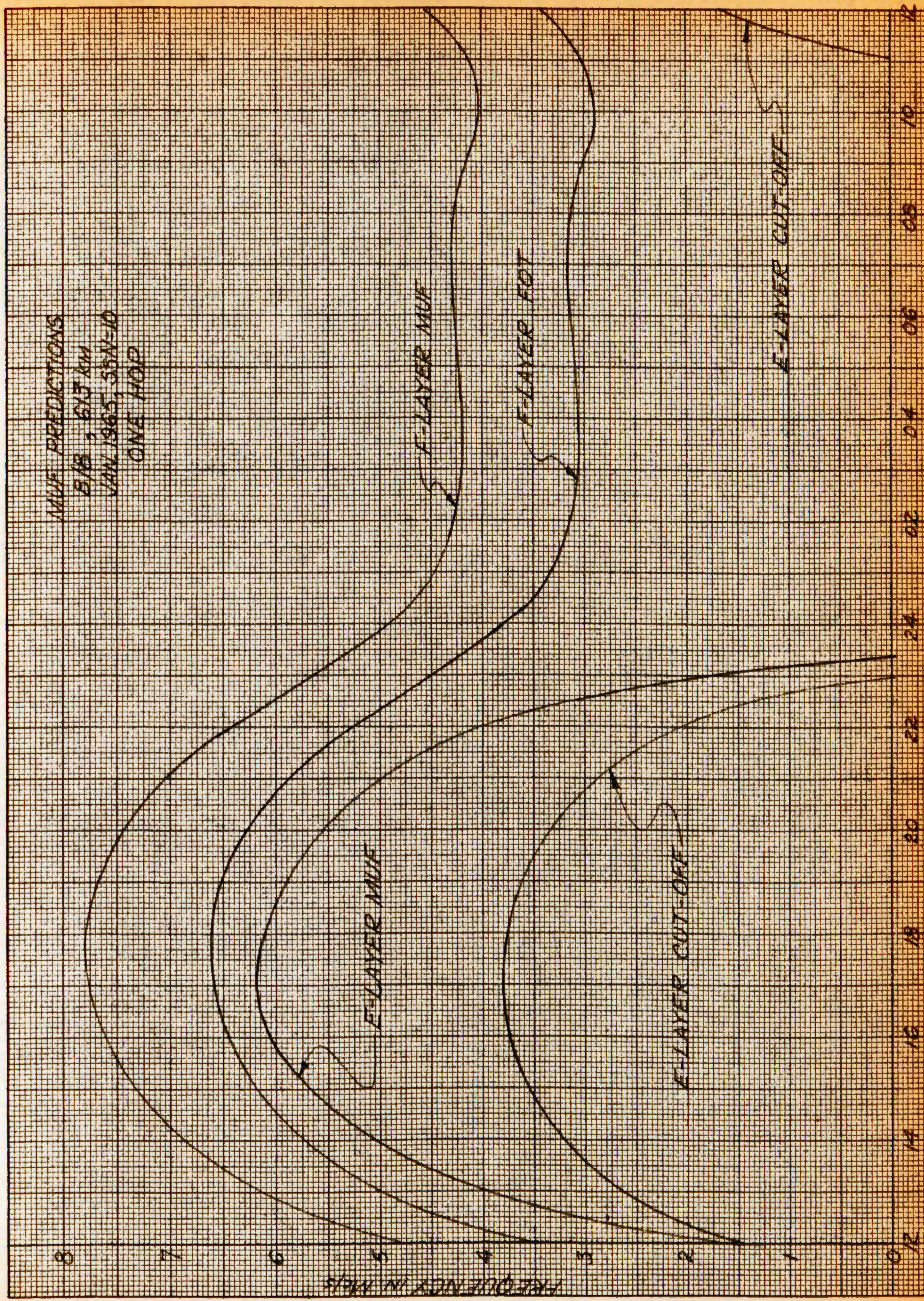
MUF PREDICTIONS
B/B - 613 km
JAN. 1965, SSN-10
ONE HOP
F-LAYER MUF
F-LAYER FOT
E-LAYER MUF
E-LAYER CUT-OFF
G.M.T.
FREQUENCY IN Mc/s

FIGURE 1.7

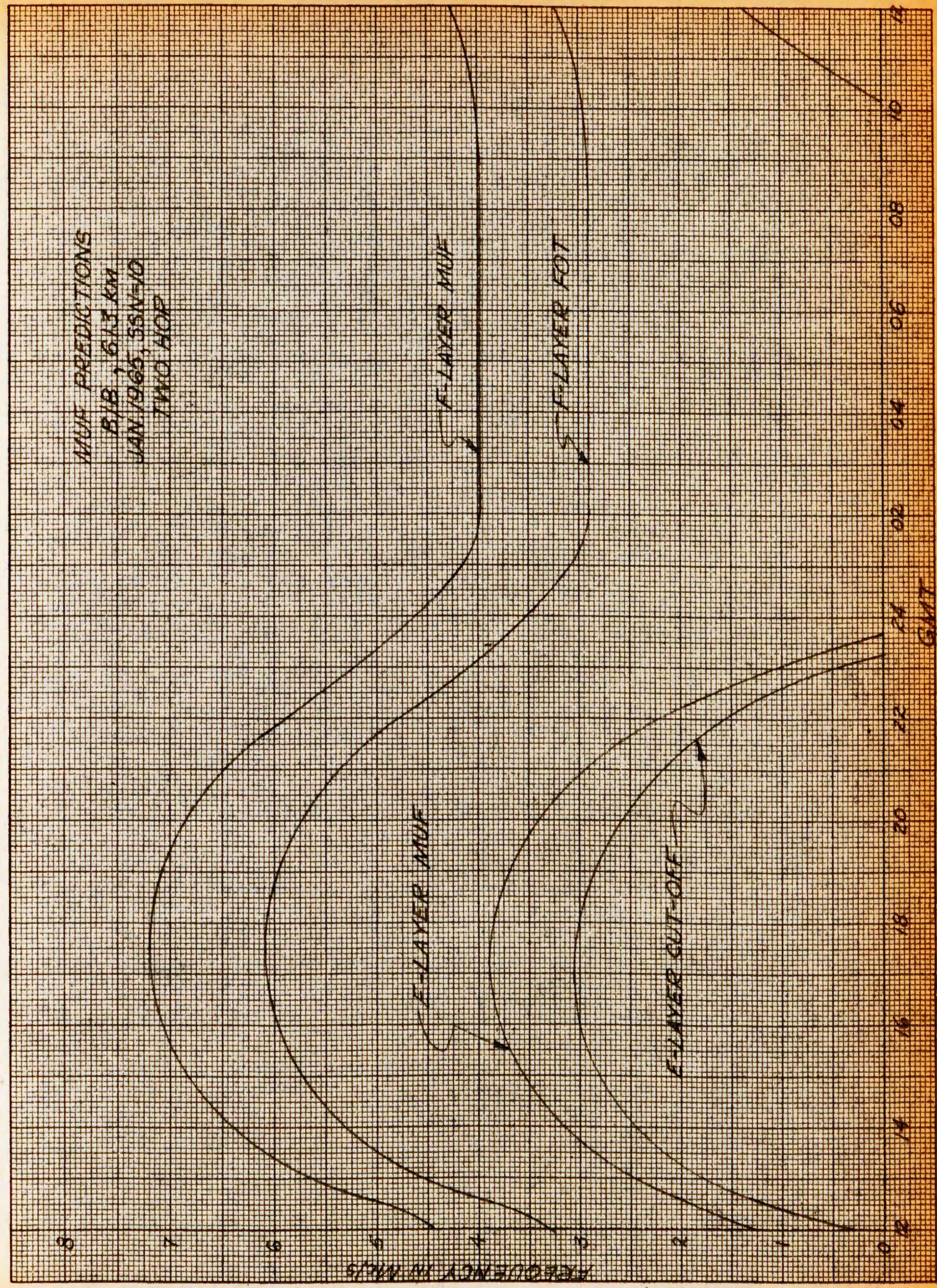

MUF PREDICTIONS
B.I.B., 613 KM
JAN 1965, SSN=10
TWO HOP
F-LAYER MUF
F-LAYER FOT
E-LAYER MUF
E-LAYER CUT-OFF
FREQUENCY IN MC/S
GMT
0
1
2
3
4
5
6
7
8
12
14
16
18
20
22
24
02
04
06
08
10
12

FIGURE 1.8

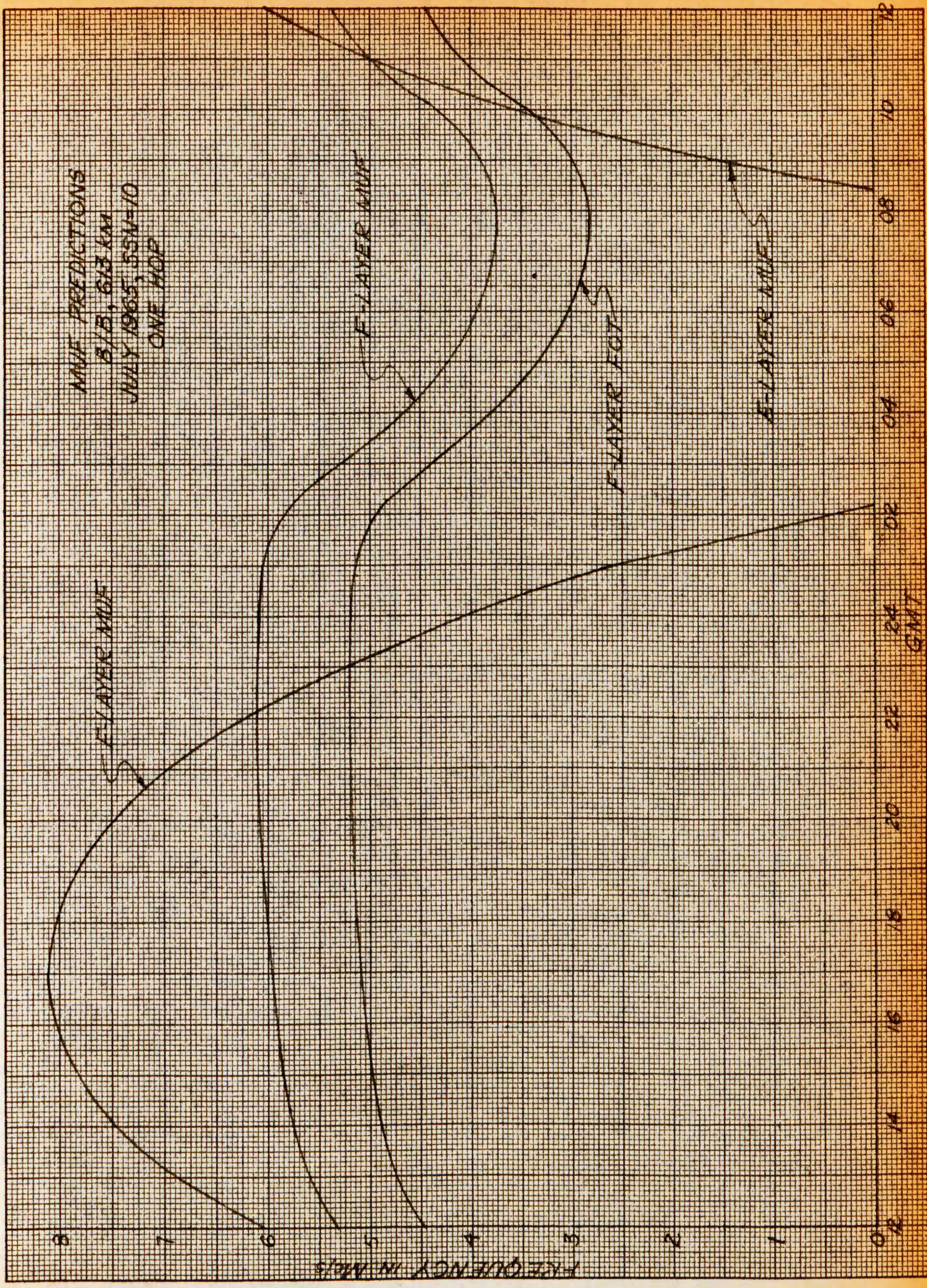

MUF PREDICTIONS
B/B, 613 KM
JULY 1965, SSN=10
ONE HOP
F-LAYER MUF
F-LAYER FOT
E-LAYER MUF
F1 LAYER MUF
FREQUENCY IN Mc/s
GMT
0
1
2
3
4
5
6
7
8
12
14
16
18
20
22
24
02
04
06
08
10
12

FIGURE 1.9

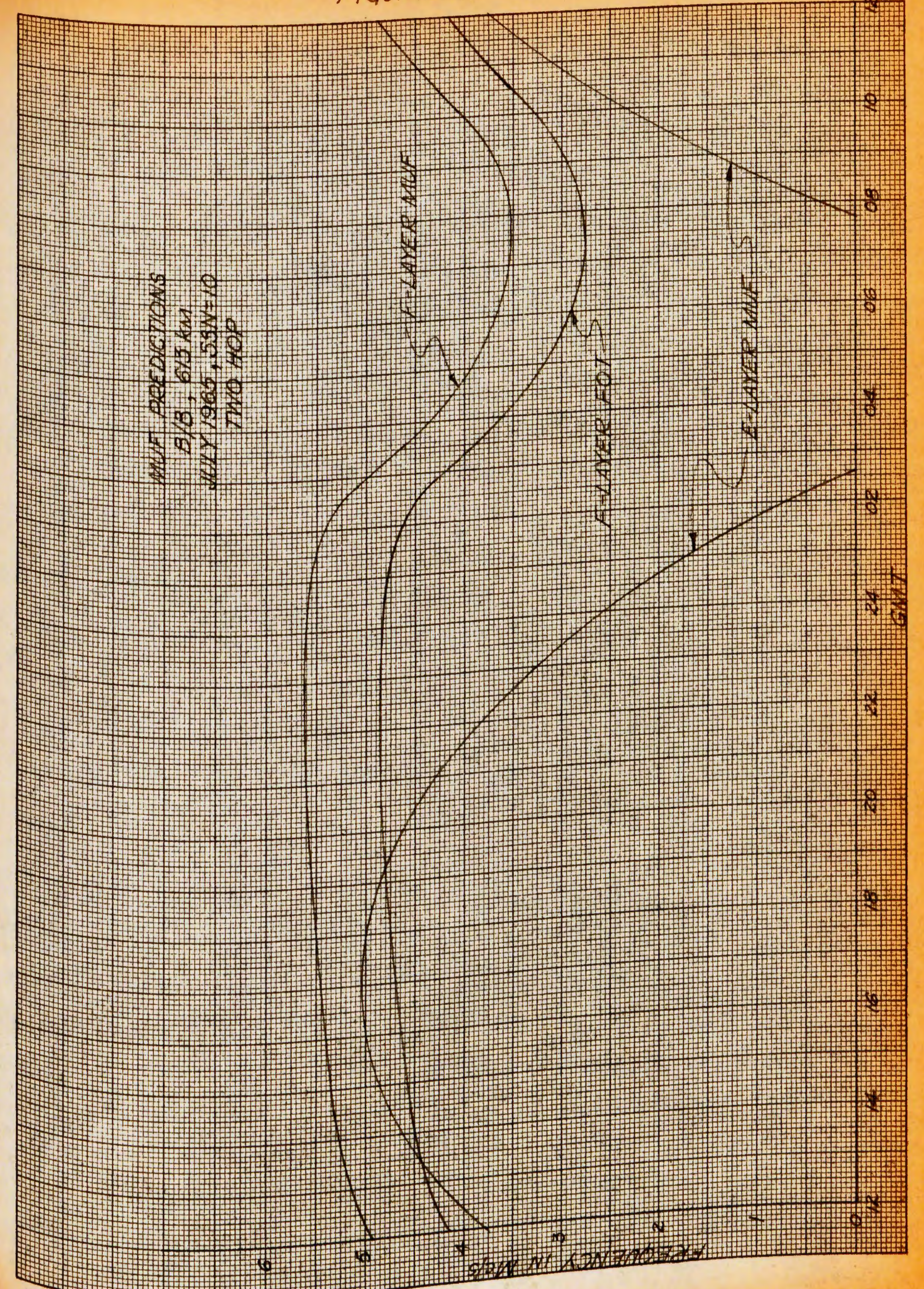
MUF PREDICTIONS
B/B, 613 KM
JULY 1965, SSN=10
TWO HOP
F-LAYER MUF
F-LAYER FOT
E-LAYER MUF
GMT
FREQUENCY IN MC/S
12
14
16
18
20
22
24
02
04
06
08
10
12
0
1
2
3
4
5
6

FIGURE 2.1

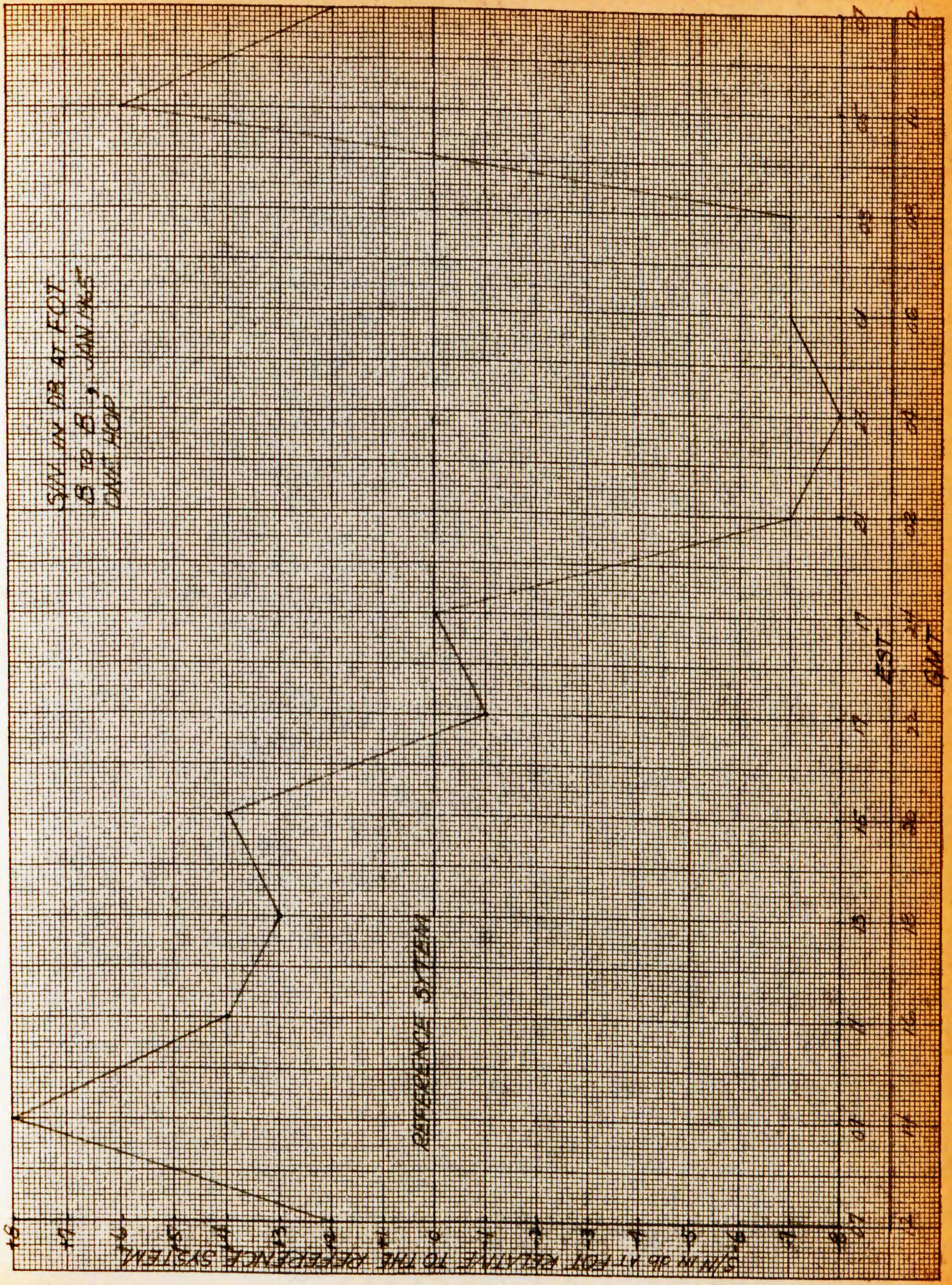
S/N IN DB AT FOT
ONE HOP
REFERENCE SYSTEM
EST
GMT
S/N IN db AT FOT RELATIVE TO THE REFERENCE SYSTEM

FIGURE 2.2

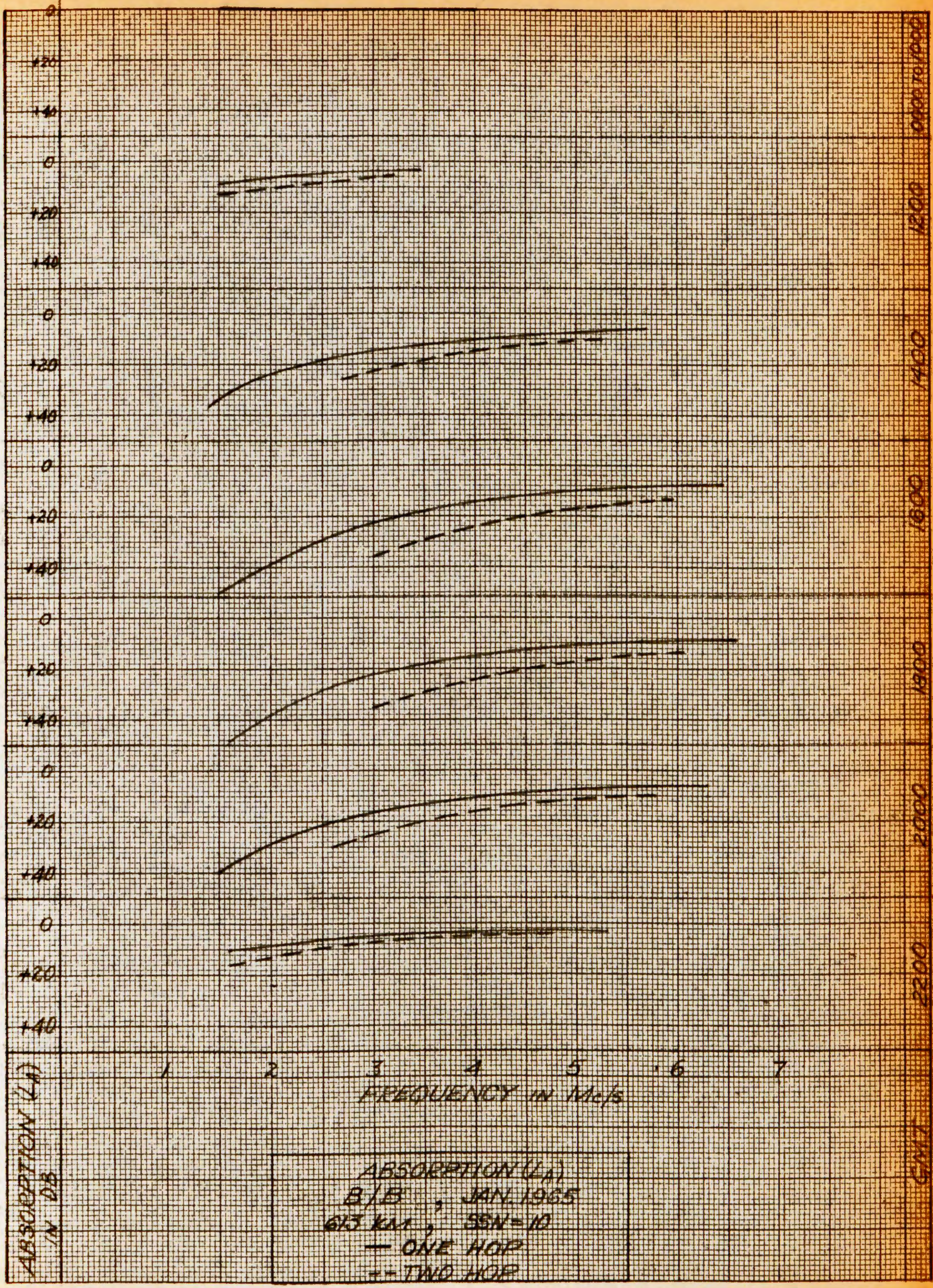

ABSORPTION (L_A) IN DB
FREQUENCY IN Mc/s
1 2 3 4 5 6 7
0 +20 +40
0000 TO 1000
1200
1400
1600
1800
2000
2200
GMT
ABSORPTION (L_A)
B/B, JAN. 1965
613 KM, SSN = 10
— ONE HOP
-- TWO HOP

FIGURE 2.3

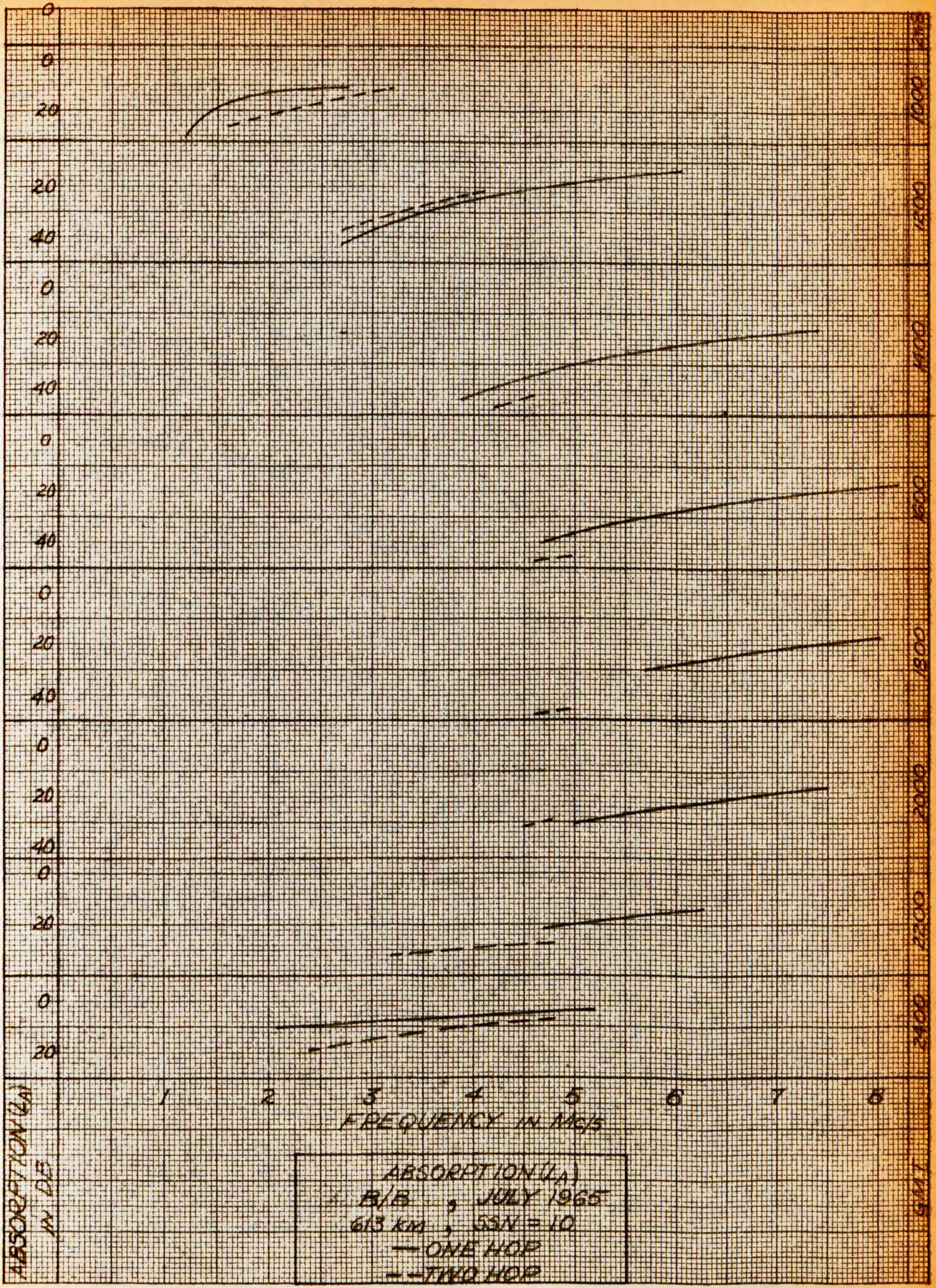
ABSORPTION (L_A) IN DB
FREQUENCY IN Mc/s
1 2 3 4 5 6 7 8
0 20 40
1000
1200
1400
1600
1800
2000
2200
2400
GMT
ABSORPTION (L_A)
B/B , JULY 1965
613 km , SSN = 10
— ONE HOP
- - TWO HOP

FIGURE 2.4

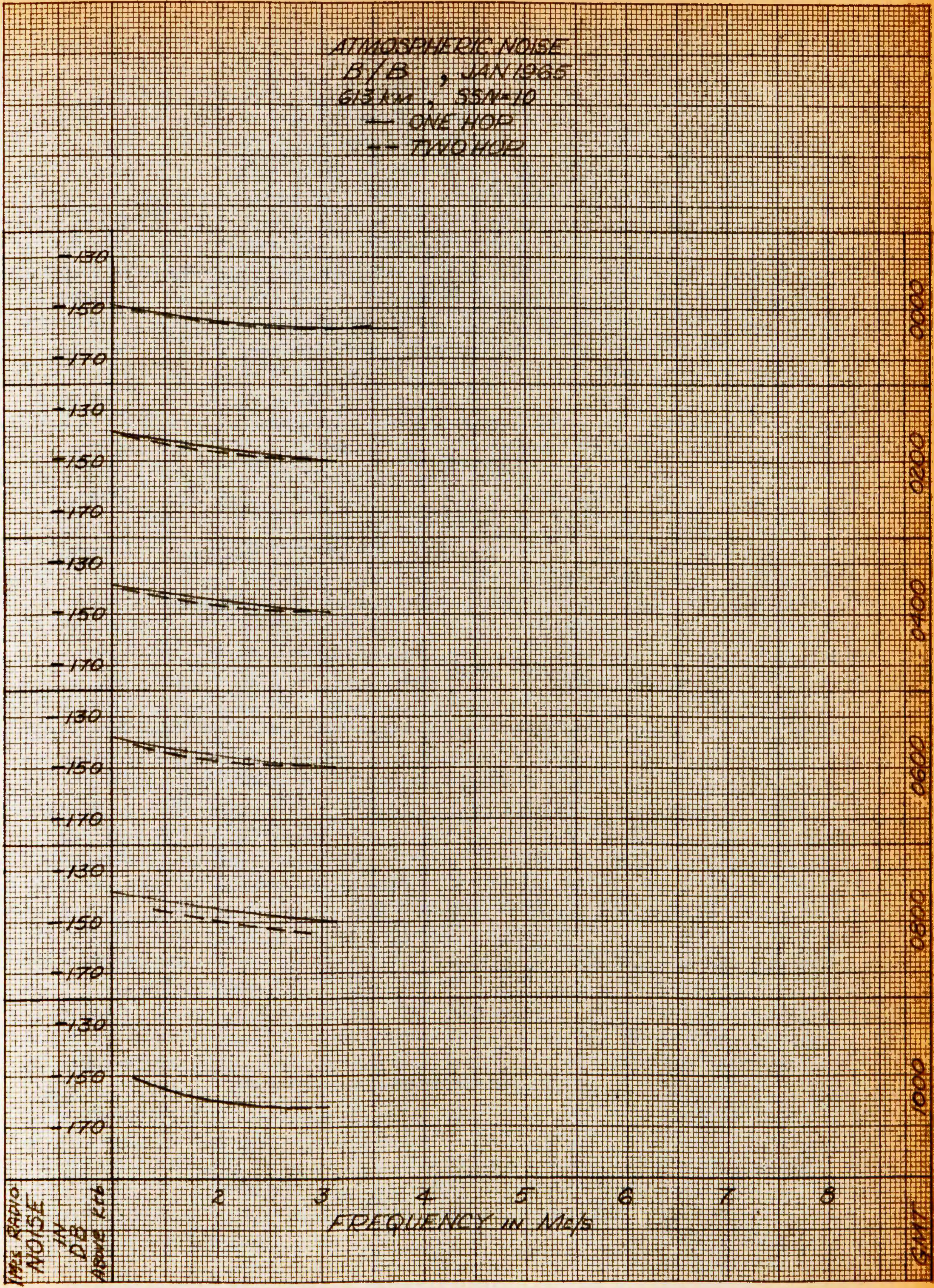
ATMOSPHERIC NOISE
B/B , JAN 1965
613 km , SSN=10
— ONE HOP
-- TWO HOP
-130
-150
-170
0000
0200
0400
0600
0800
1000
GMT
2
3
4
5
6
7
8
FREQUENCY in Mc/s
RADIO NOISE IN DB Above kTb

FIGURE 2.5

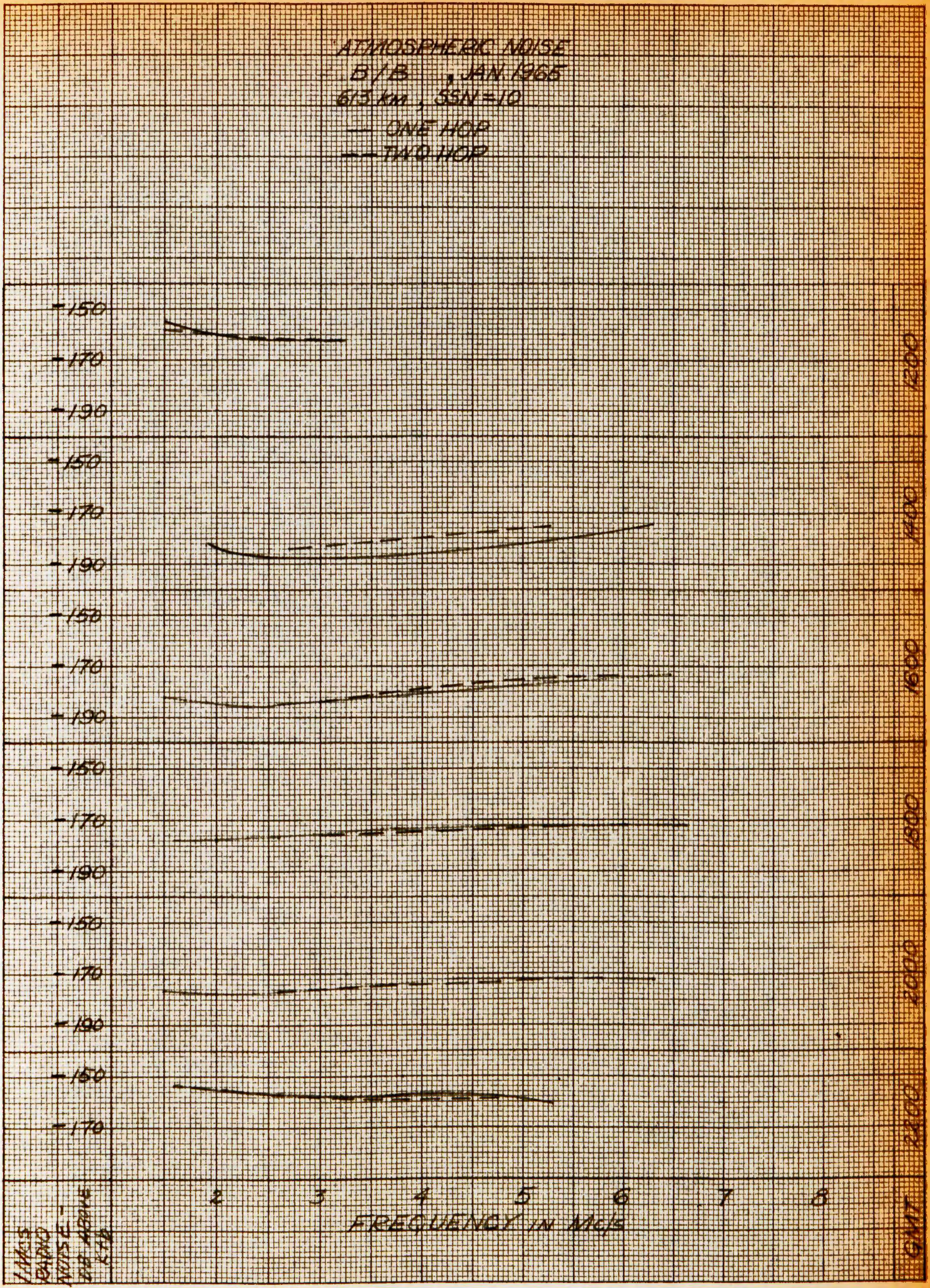
ATMOSPHERIC NOISE
B/B , JAN. 1965
613 km , SSN=10
— ONE HOP
– – TWO HOP
-150
-170
-190
-150
-170
-190
-150
-170
-190
-150
-170
-190
-150
-170
-190
-150
-170
1200
1400
1600
1800
2000
2400
2
3
4
5
6
7
8
FREQUENCY IN Mc/s
1 Mc/s RADIO NOISE – DB ABOVE 1 KT
GMT

FIGURE 2.6

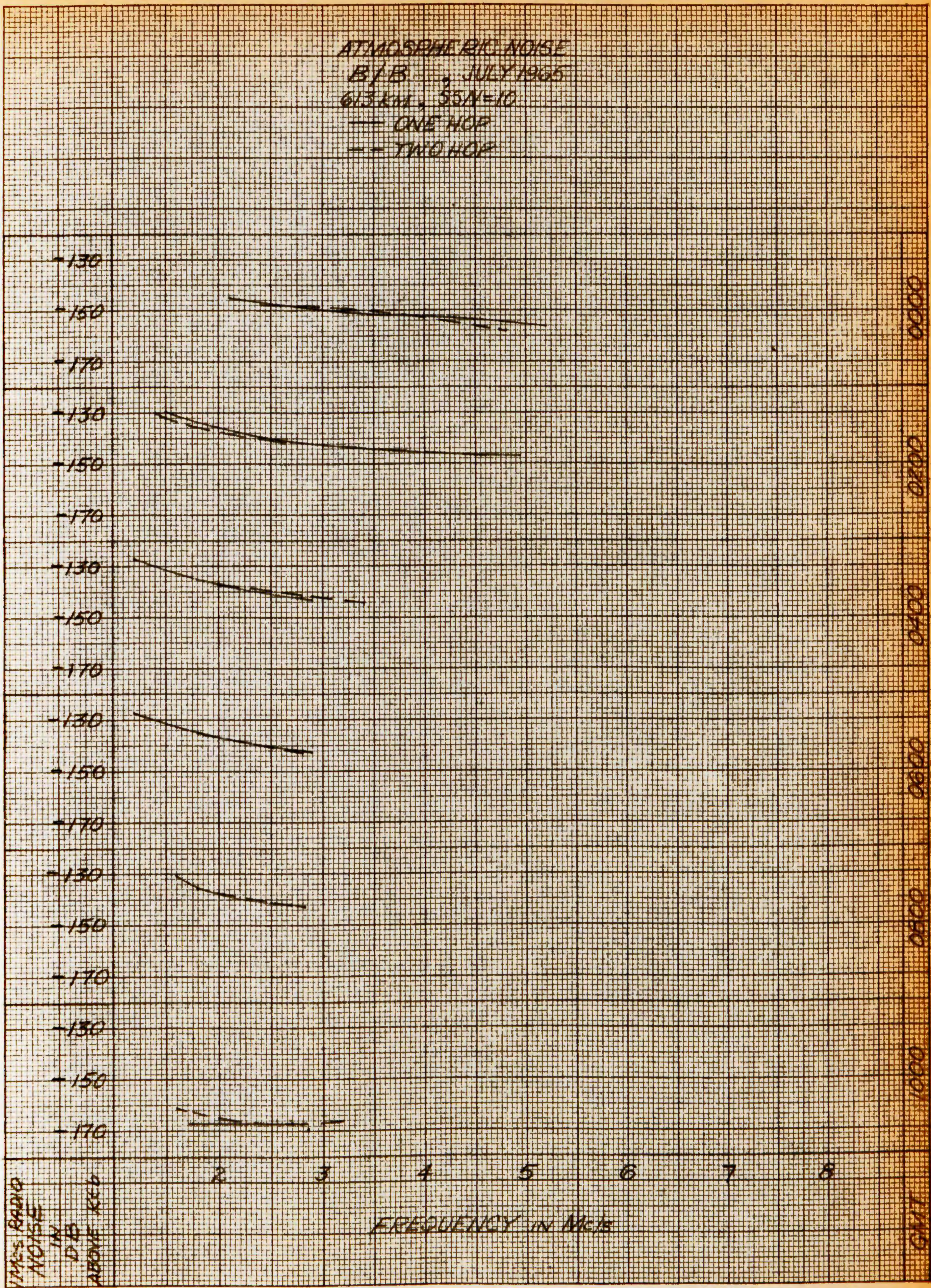
ATMOSPHERIC NOISE
B/B , JULY 1965
613 KM , SSN=10
— ONE HOP
-- TWO HOP
-130
-150
-170
0000
0200
0400
0600
0800
1000
GMT
2
3
4
5
6
7
8
FREQUENCY IN Mc/s
1Mc/s RADIO NOISE IN DB ABOVE KTb

FIGURE 2.7

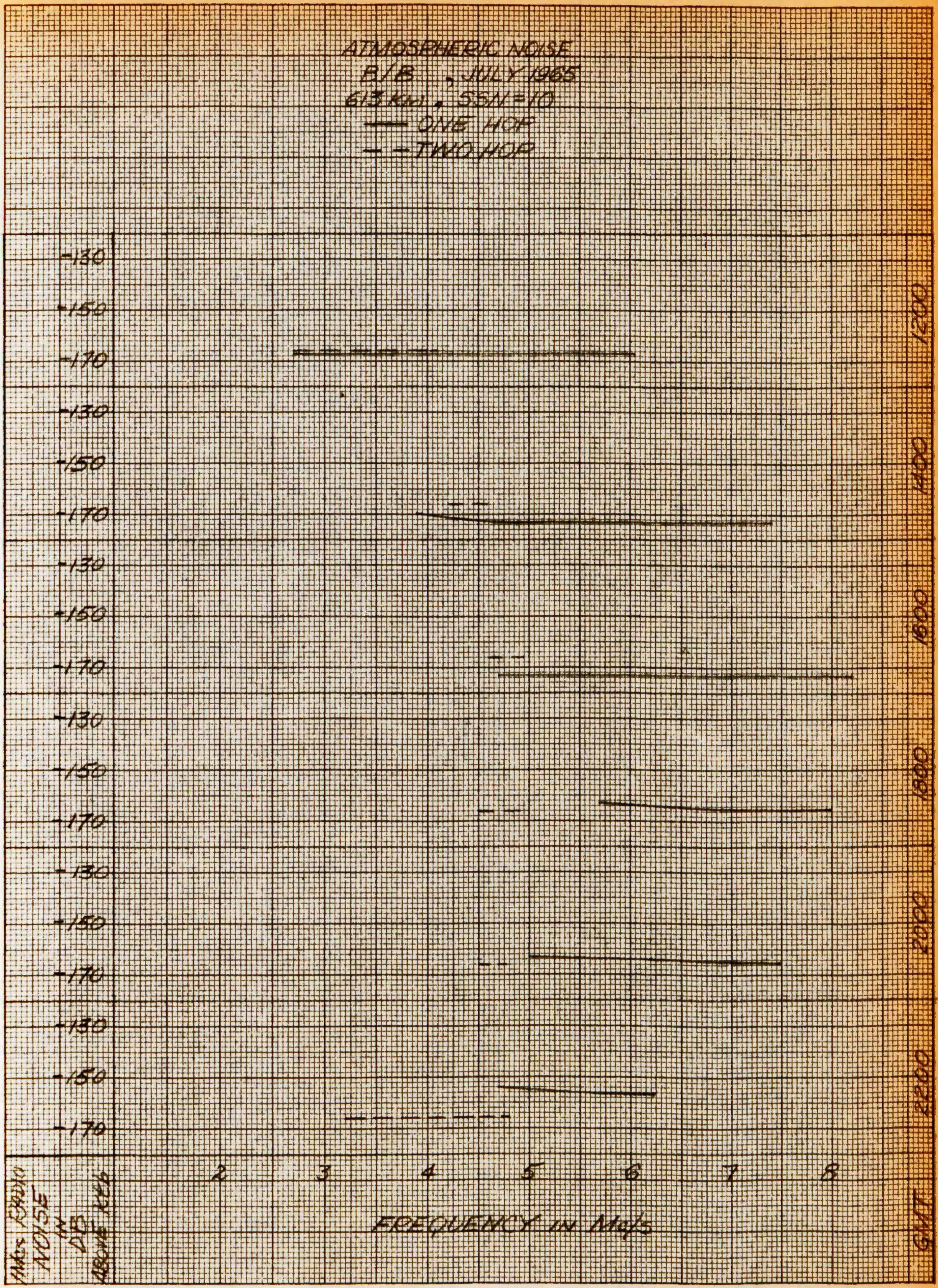
ATMOSPHERIC NOISE
B/B , JULY 1965
613 KM , SSN = 10
ONE HOP
TWO HOP
-130
-150
-170
1200
1400
1600
1800
2000
2200
GMT
2
3
4
5
6
7
8
FREQUENCY IN Mc/s
Atmos RADIO NOISE IN DB Above KTB

FIGURE 2.8

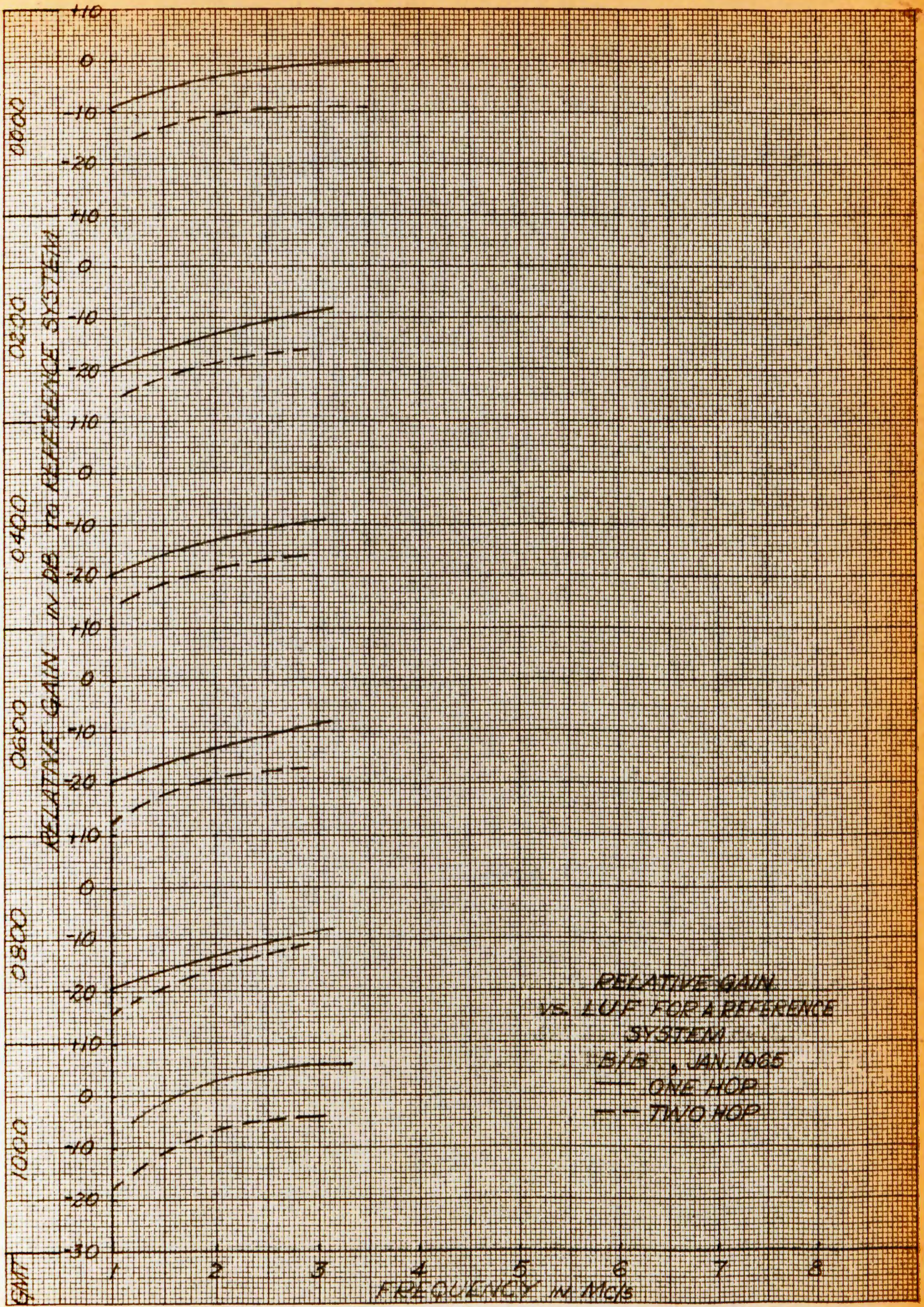
RELATIVE GAIN IN DB TO REFERENCE SYSTEM
0000
0200
0400
0600
0800
1000
GMT
+10
0
-10
-20
-30
1
2
3
4
5
6
7
8
FREQUENCY IN Mc/s
RELATIVE GAIN
VS. LUF FOR A REFERENCE
SYSTEM
B/R , JAN. 1965
ONE HOP
TWO HOP

FIGURE 2.9

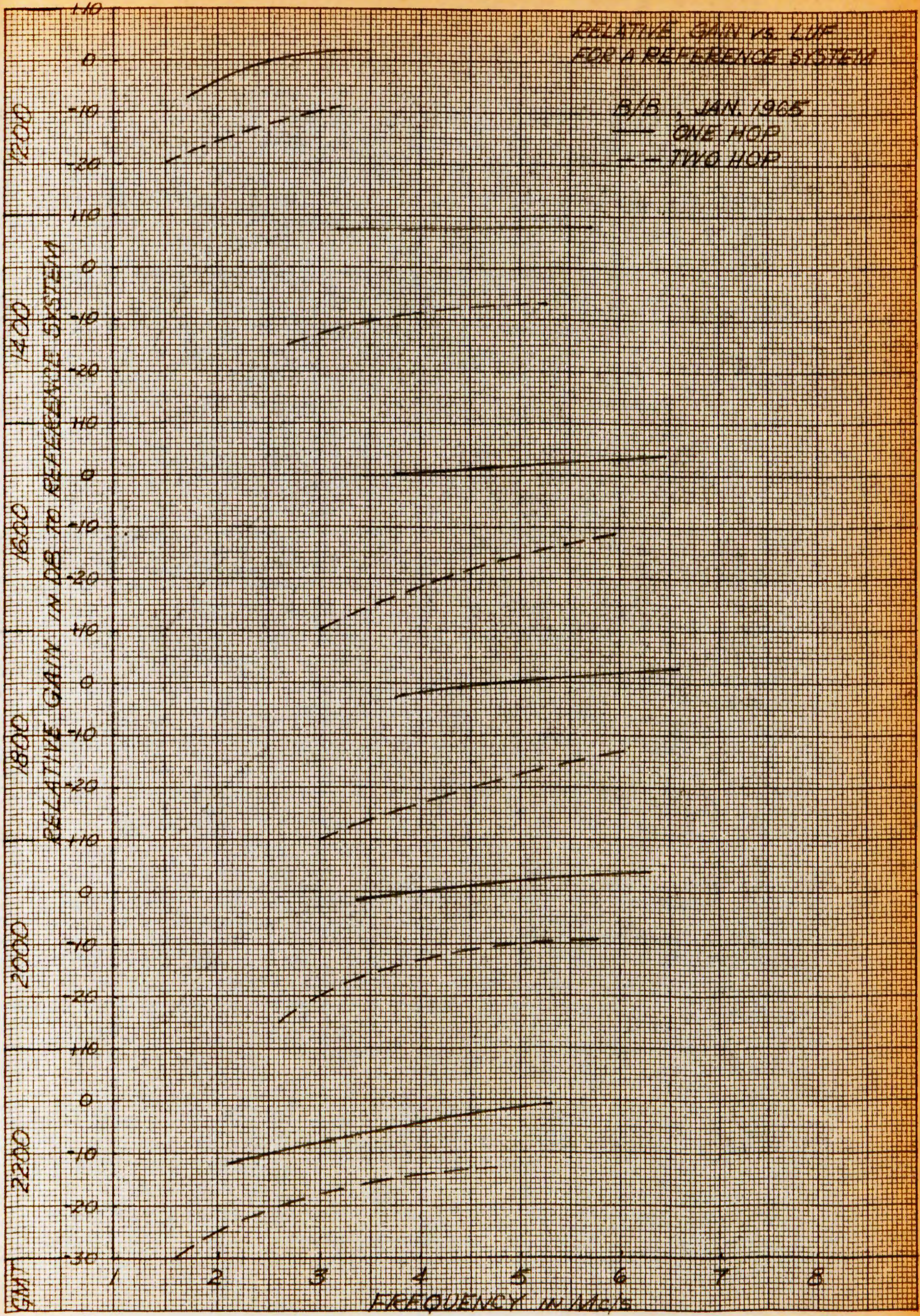
RELATIVE GAIN vs. LUF
FOR A REFERENCE SYSTEM
B/B , JAN. 1965
ONE HOP
TWO HOP
RELATIVE GAIN IN DB TO REFERENCE SYSTEM
FREQUENCY IN Mc/s
GMT
1200
1400
1600
1800
2000
2200
+10
0
-10
-20
-30
1
2
3
4
5
6
7
8

FIGURE 2.10

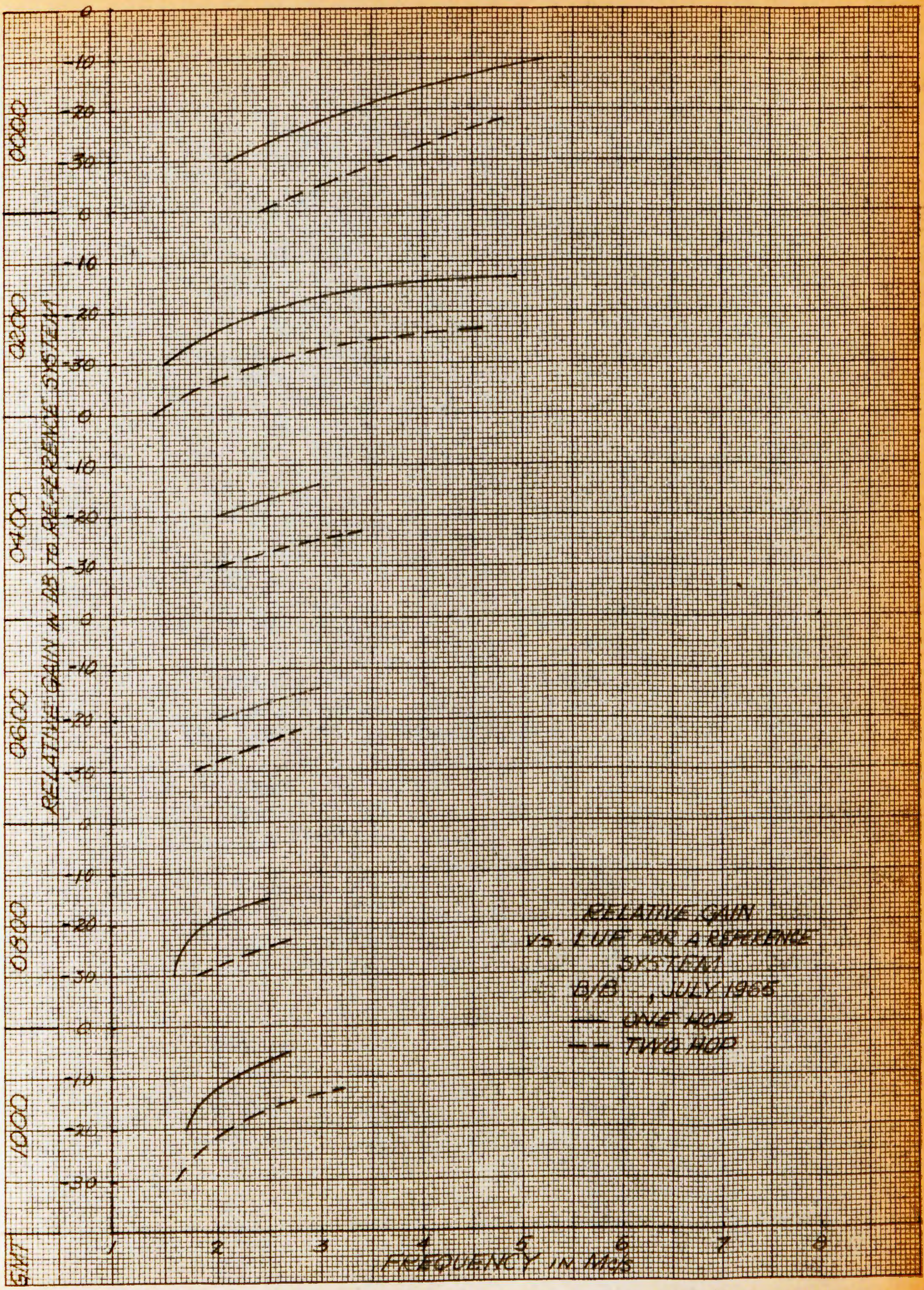

0000
0200
0400
0600
0800
1000
G.M.T.
RELATIVE GAIN IN DB TO REFERENCE SYSTEM
FREQUENCY IN Mc/s
RELATIVE GAIN
VS. L.U.F. FOR A REFERENCE SYSTEM
B/B , JULY 1965
ONE HOP
TWO HOP

FIGURE 2.11

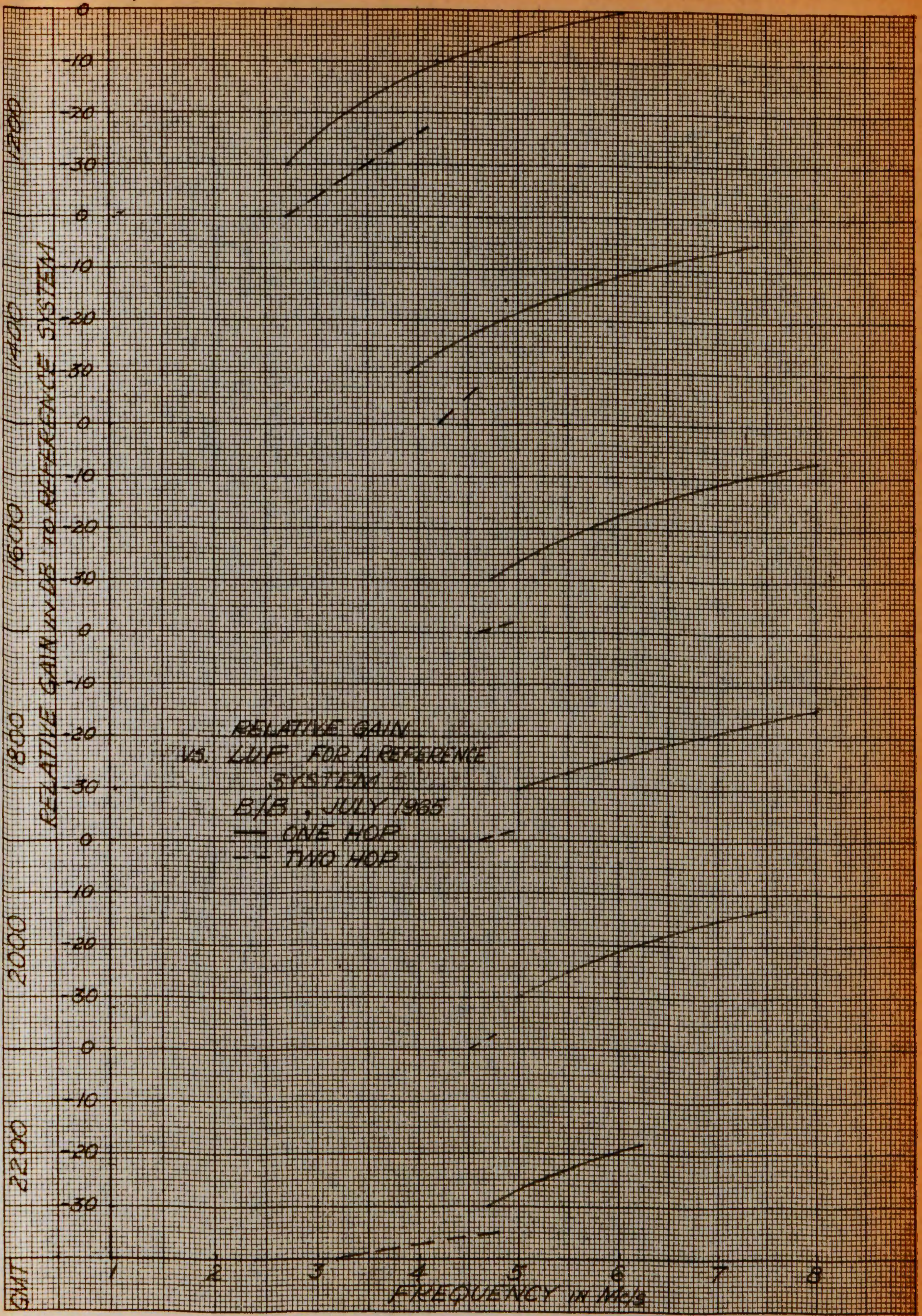
RELATIVE GAIN IN DB TO REFERENCE SYSTEM
GMT
1200
1400
1600
1800
2000
2200
0
-10
-20
-30
RELATIVE GAIN
VS. LUF FOR A REFERENCE
SYSTEM
B/B, JULY 1965
ONE HOP
TWO HOP
1
2
3
4
5
6
7
8
FREQUENCY IN Mc/s

FIGURE 2.12

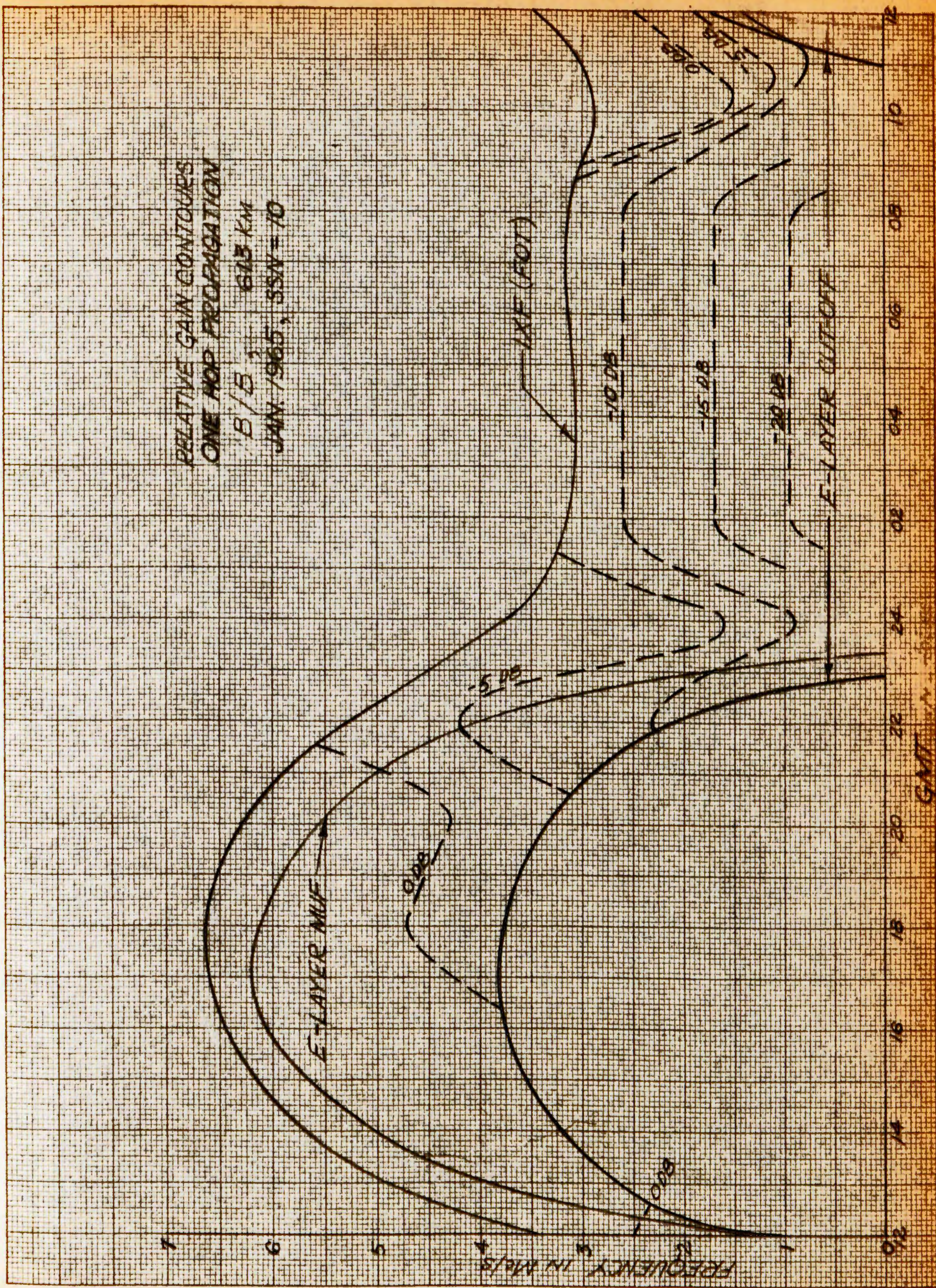
RELATIVE GAIN CONTOURS
ONE HOP PROPAGATION
B/B, 613 Km
JAN. 1965, SSN = 10
LXF (FOT)
E-LAYER MUF
E-LAYER CUTOFF
0 DB
-5 DB
-10 DB
-15 DB
-20 DB
FREQUENCY, IN Mc/s
GMT

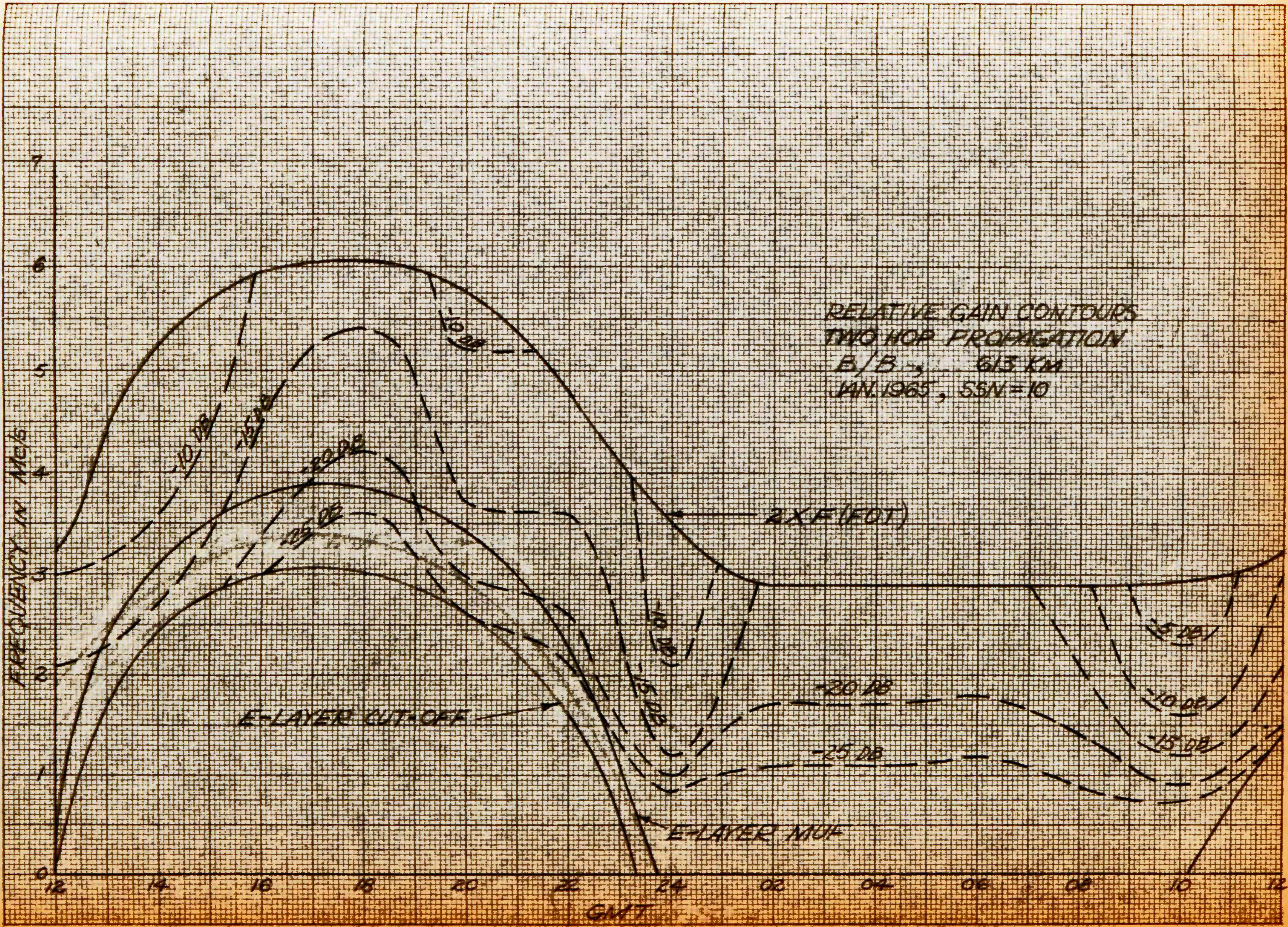
RELATIVE GAIN CONTOURS
TWO HOP PROPAGATION
B/B -, 613 KM
JAN. 1965, SSN = 10
FREQUENCY IN Mc/s
GMT
2 X F (EOT)
E-LAYER CUT-OFF
E-LAYER MUF
-10 DB
-15 DB
-20 DB
-25 DB
0
1
2
3
4
5
6
7
12
14
16
18
20
22
24
02
04
06
08
10
12

FIGURE 2.13

FIGURE 2.14

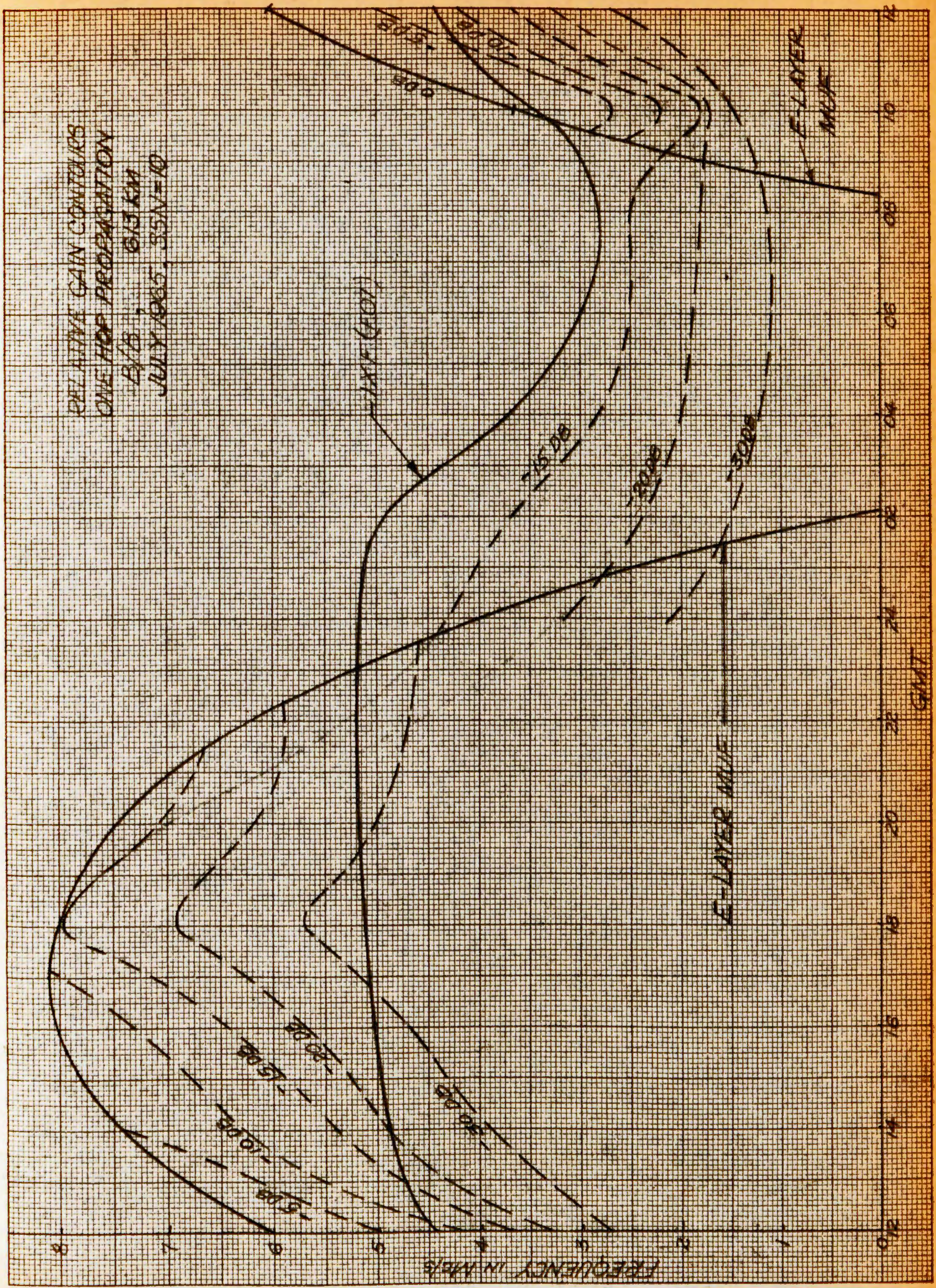
RELATIVE GAIN CONTOURS
ONE HOP PROPAGATION
JULY 1965, SSN=10
E-LAYER MUF
15 DB
20 DB
30 DB
GMT
FREQUENCY IN Mc/s

FIGURE 2.15

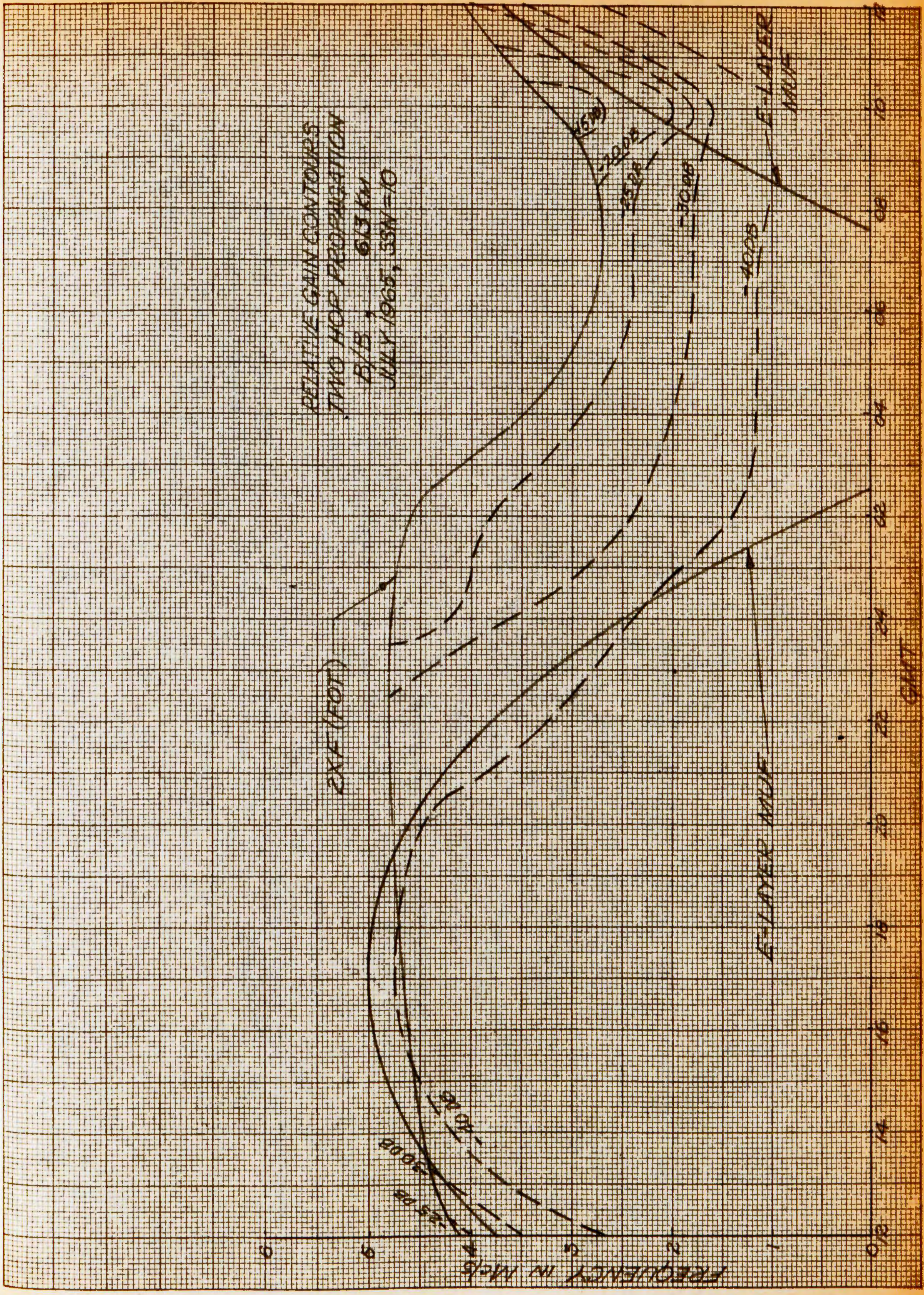
RELATIVE GAIN CONTOURS
TWO HOP PROPAGATION
B/B 613 Km
JULY 1965, SSN=10
2xF (POT)
E-LAYER MUF
E-LAYER MUF
-15dB
-20dB
-25dB
-30dB
-40dB
FREQUENCY IN Mc/s
GMT

FIGURE 3.1

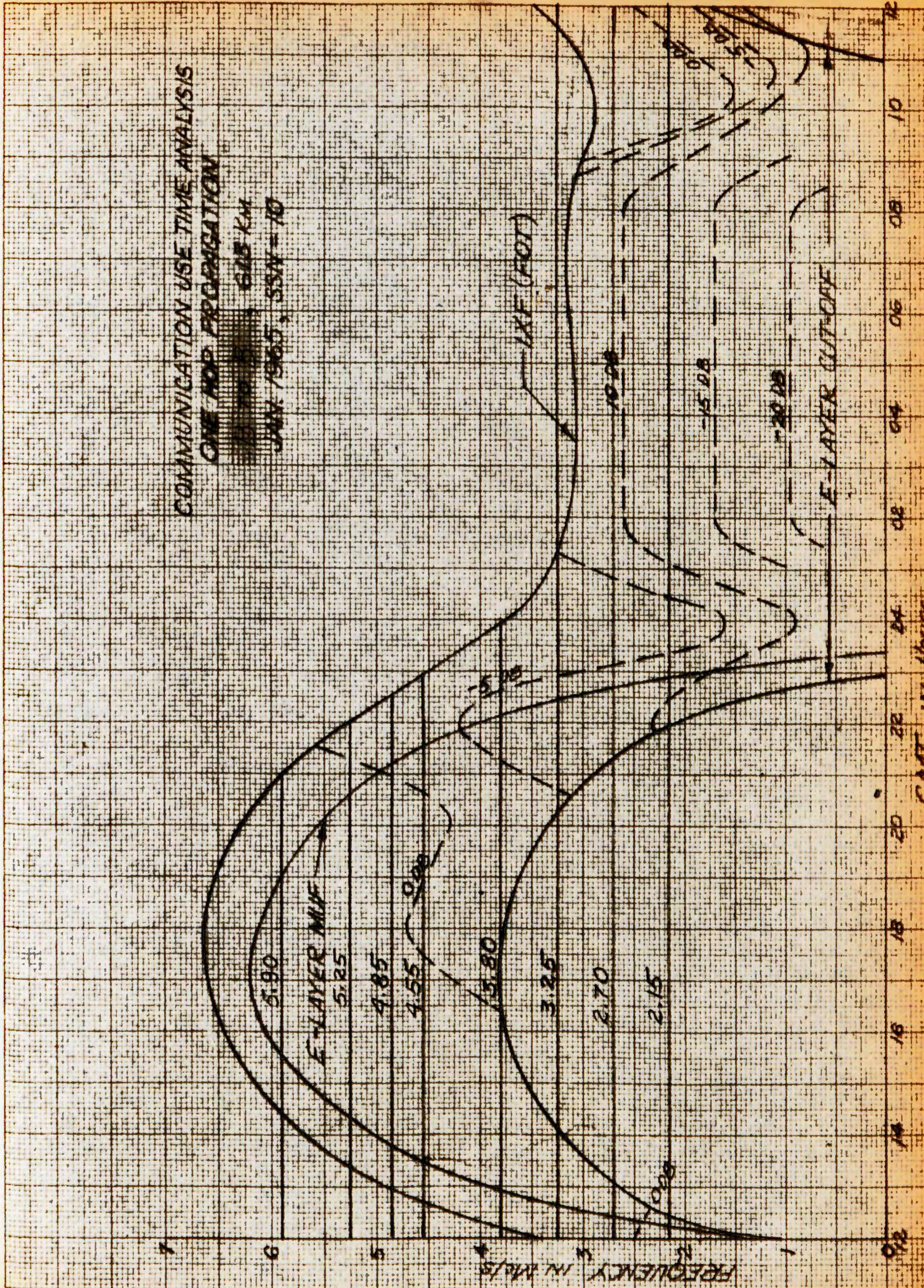
COMMUNICATION USE TIME ANALYSIS
ONE HOP PROPAGATION
JAN. 1965, SSN = 10
E-LAYER MUF
LUF (POT)
E-LAYER CUTOFF
5.90
5.25
4.85
4.55
3.80
3.26
2.70
2.15
-5 DB
0 DB
-10 DB
-15 DB
-20 DB
GMT IN HOURS
FREQUENCY IN MC/S

FIGURE 3.2

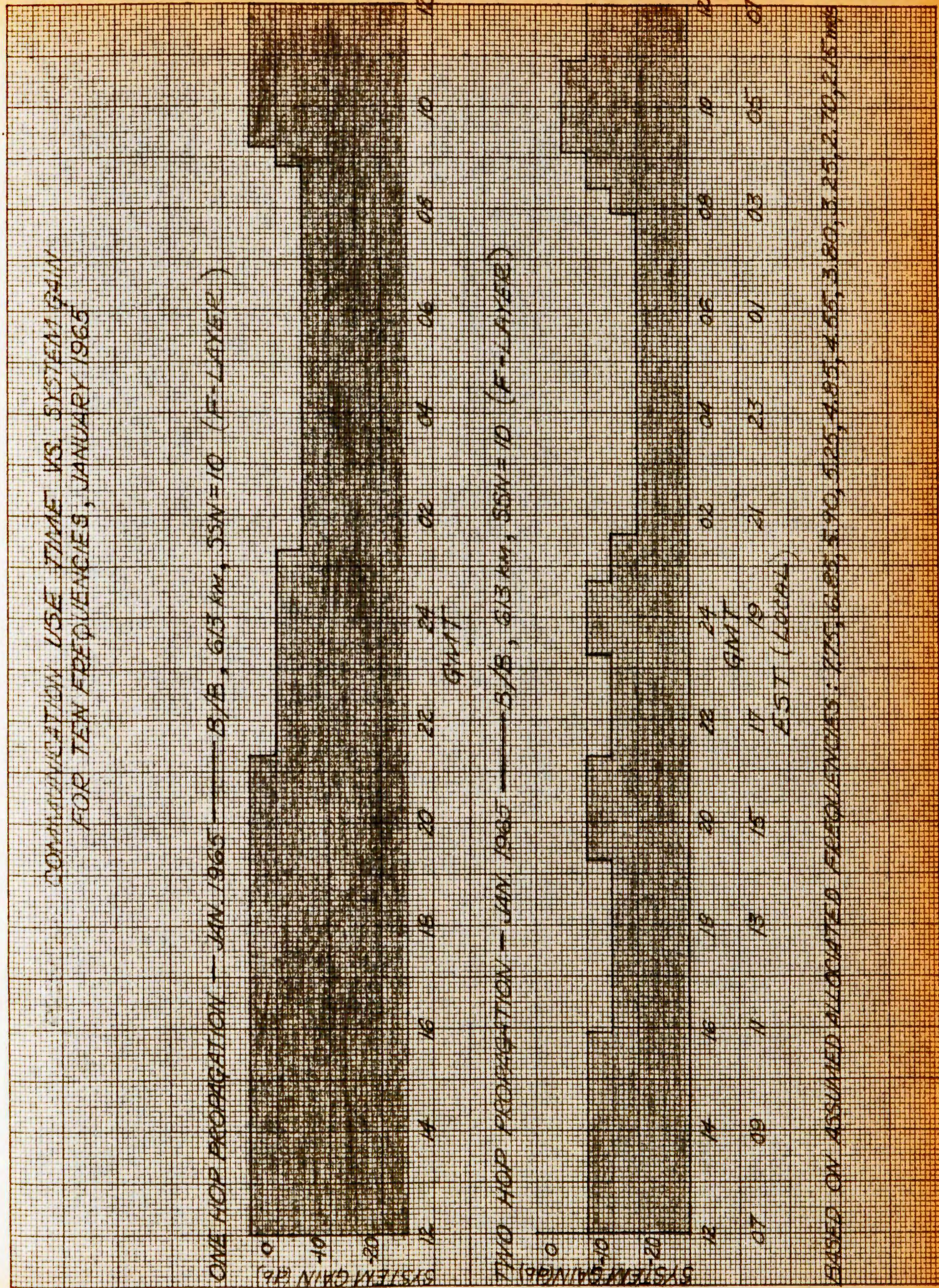
COMMUNICATION USE TIME VS. SYSTEM GAIN
FOR TEN FREQUENCIES, JANUARY 1965
ONE HOP PROPAGATION — JAN. 1965 —— B/B, 613 km, SSN=10 (F-LAYER)
SYSTEM GAIN (db)
0
-10
-20
12 14 16 18 20 22 24 02 04 06 08 10 12
GMT
TWO HOP PROPAGATION — JAN. 1965 —— B/B, 613 km, SSN=10 (F-LAYER)
SYSTEM GAIN (db)
0
-10
-20
12 14 16 18 20 22 24 02 04 06 08 10 12
GMT
07 09 11 13 15 17 19 21 23 01 03 05 07
EST (LOCAL)
BASED ON ASSUMED ALLOCATED FREQUENCIES: 7.75, 6.85, 5.90, 5.25, 4.85, 4.55, 3.80, 3.25, 2.70, 2.15 mc

FIGURE 3.3

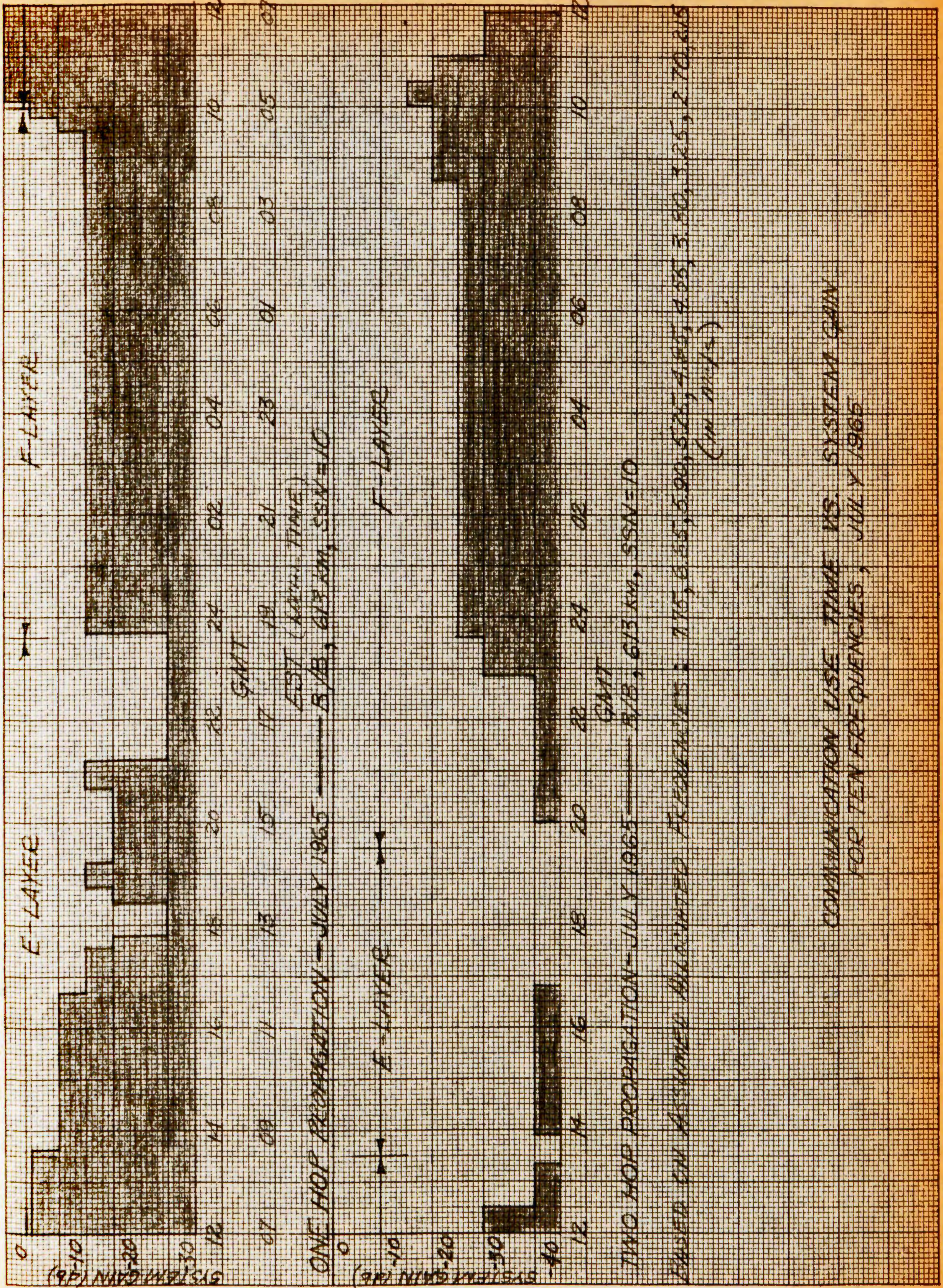

COMMUNICATION USE TIME VS. SYSTEM GAIN
FOR TEN FREQUENCIES, JULY 1966

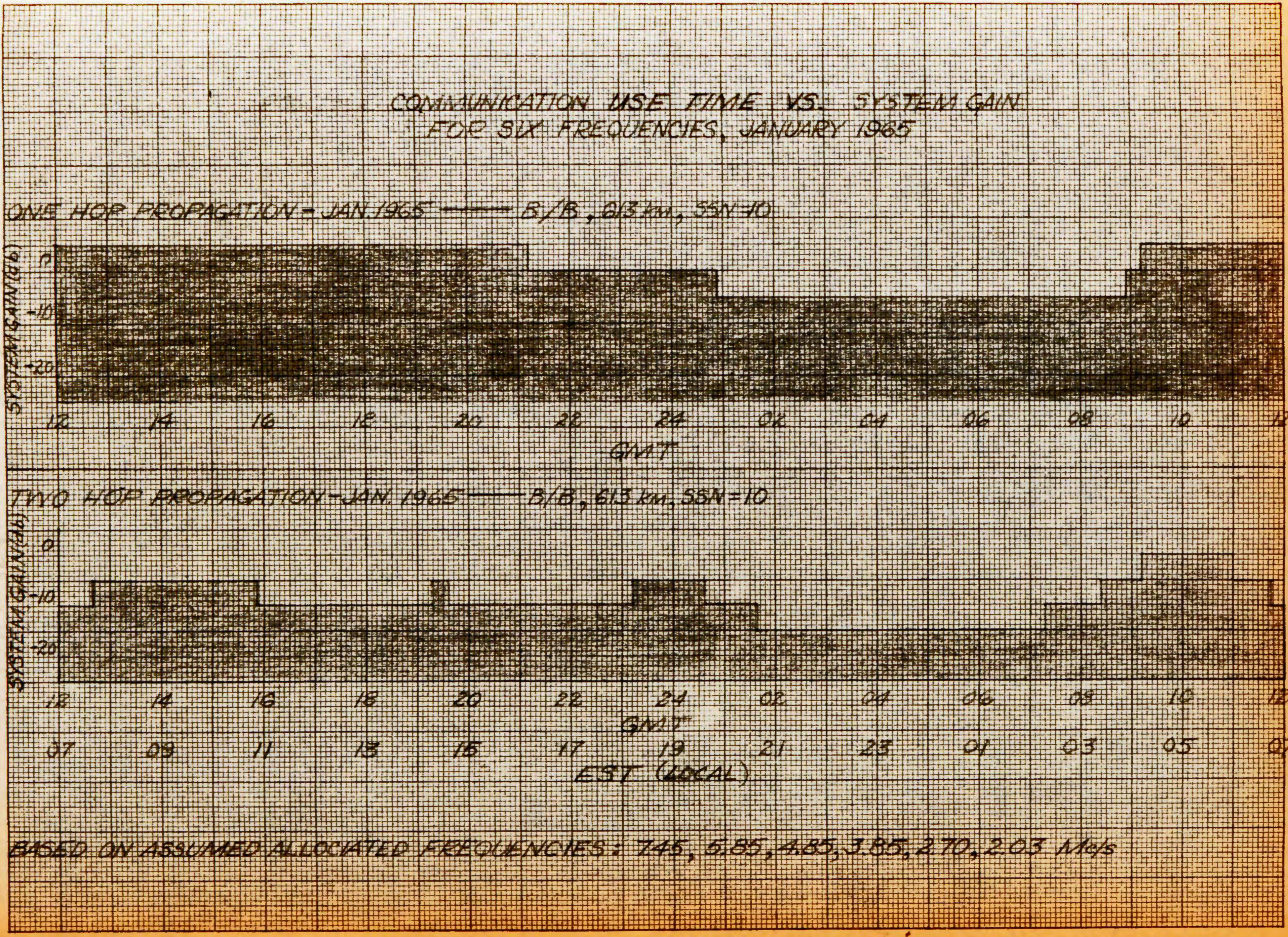
COMMUNICATION USE TIME VS. SYSTEM GAIN
FOR SIX FREQUENCIES, JANUARY 1965
ONE HOP PROPAGATION - JAN. 1965 —— B/B, 613 km, SSN=10
SYSTEM GAIN (db)
0
-10
-20
12
14
16
18
20
22
24
02
04
06
08
10
12
GMT
TWO HOP PROPAGATION - JAN. 1965 —— B/B, 613 km, SSN=10
SYSTEM GAIN (db)
0
-10
-20
12
14
16
18
20
22
24
02
04
06
08
10
12
GMT
07
09
11
13
15
17
19
21
23
01
03
05
07
EST (LOCAL)
BASED ON ASSUMED ALLOCATED FREQUENCIES: 7.45, 5.85, 4.85, 3.85, 2.70, 2.03 Mc/s

FIGURE 3.4

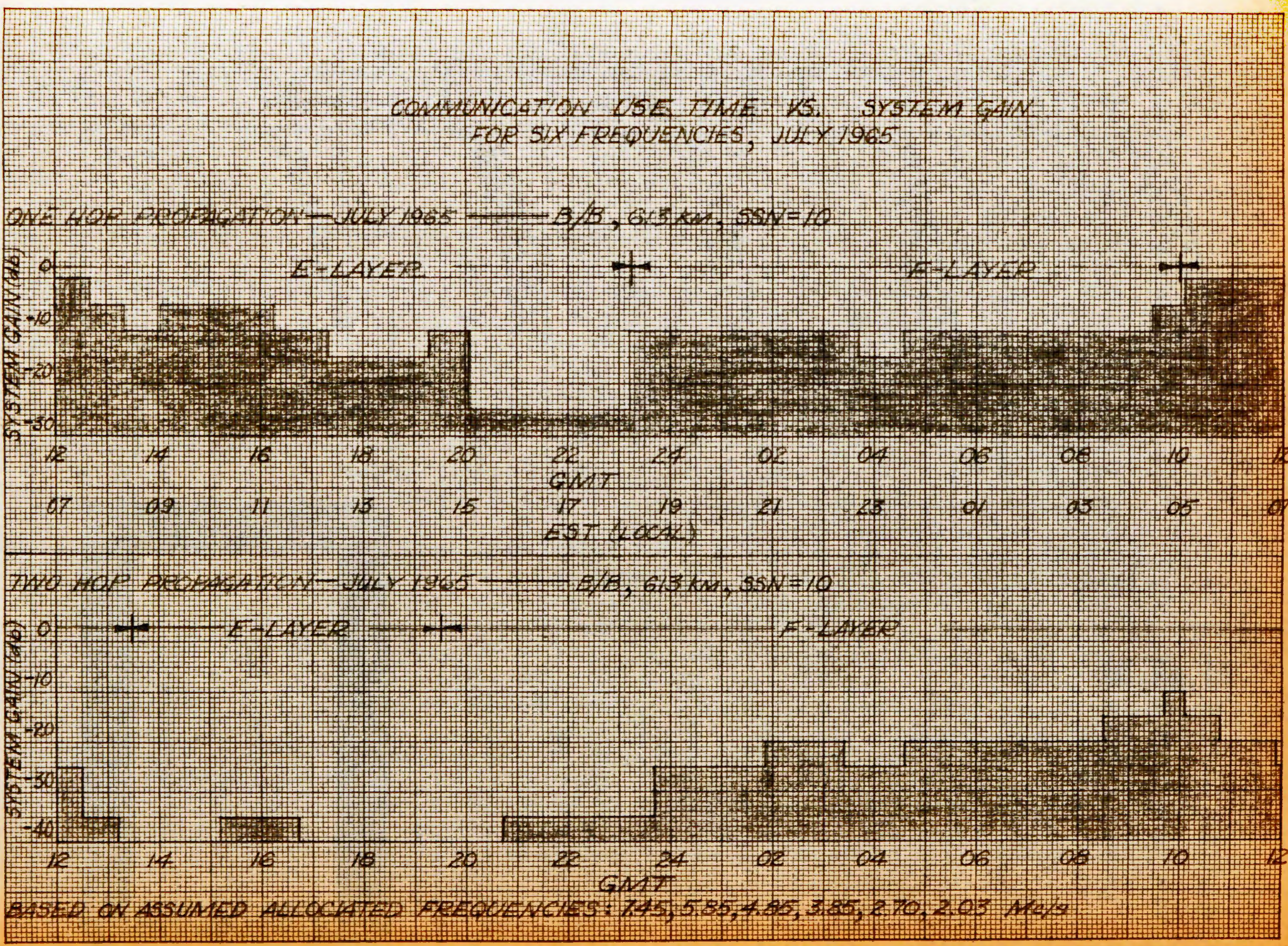
COMMUNICATION USE TIME VS. SYSTEM GAIN
FOR SIX FREQUENCIES, JULY 1965
ONE HOP PROPAGATION — JULY 1965 — B/B, 613 km, SSN=10
E-LAYER
F-LAYER
SYSTEM GAIN (db)
0
-10
-20
-30
12 14 16 18 20 22 24 02 04 06 08 10 12
GMT
07 09 11 13 15 17 19 21 23 01 03 05 07
EST (LOCAL)
TWO HOP PROPAGATION — JULY 1965 — B/B, 613 km, SSN=10
E-LAYER
F-LAYER
SYSTEM GAIN (db)
0
-10
-20
-30
-40
12 14 16 18 20 22 24 02 04 06 08 10 12
GMT
BASED ON ASSUMED ALLOCATED FREQUENCIES: 7.45, 5.85, 4.85, 3.85, 2.70, 2.03 Mc/s

FIGURE 3.5

FIGURE 3.6

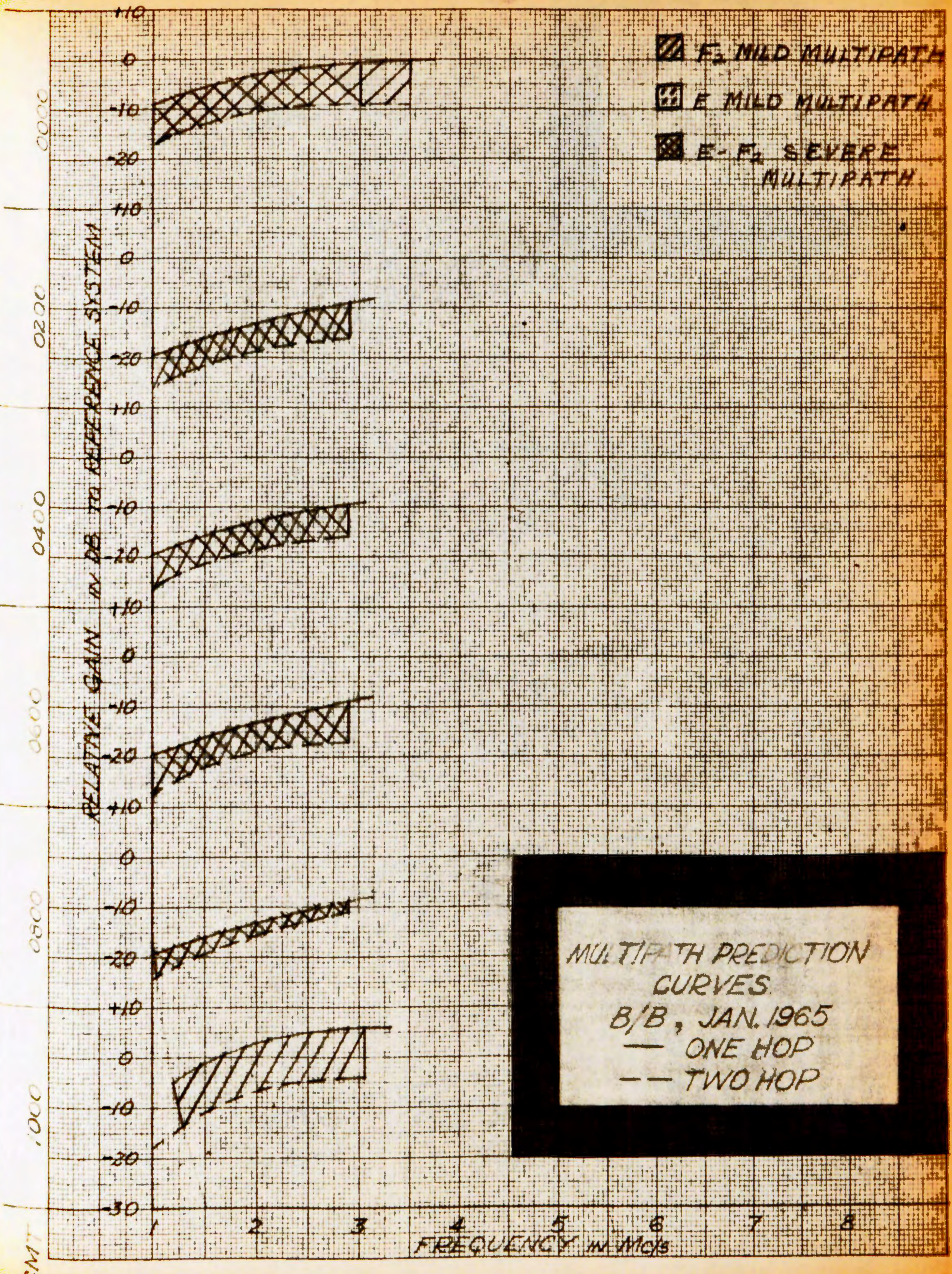
F2 MILD MULTIPATH
E MILD MULTIPATH
E-F2 SEVERE MULTIPATH
RELATIVE GAIN IN DB TO REFERENCE SYSTEM
FREQUENCY IN Mc/s
PREDICTION CURVES.
B/B, JAN. 1965
— ONE HOP
-- TWO HOP
0000
0200
0400
0600
0800
1000
GMT

FIGURE 3.7

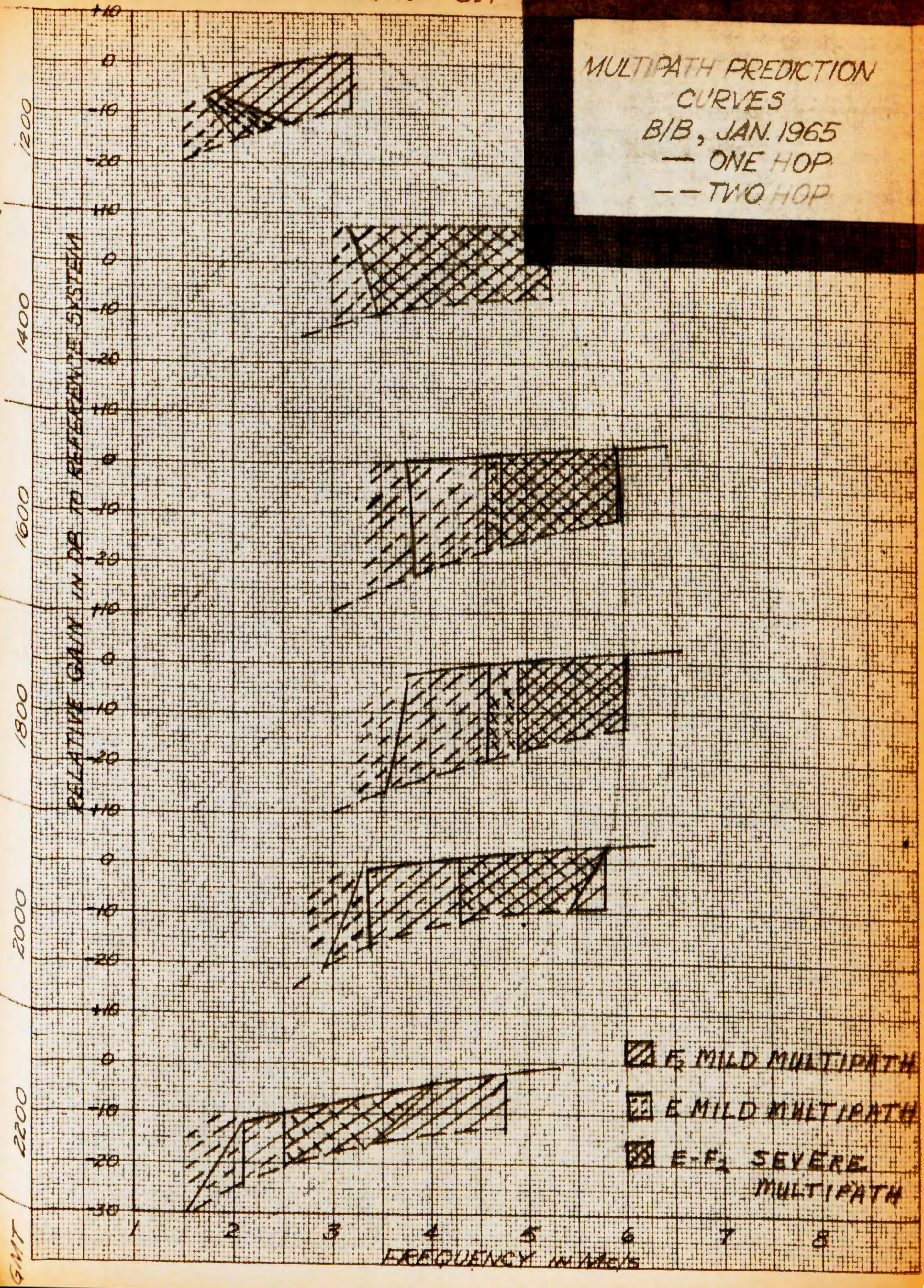
MULTIPATH PREDICTION
CURVES
B/B, JAN. 1965
— ONE HOP
- - TWO HOP
RELATIVE GAIN IN DB TO REFERENCE SYSTEM
+10
0
-10
-20
-30
1200
1400
1600
1800
2000
2200
GMT
1
2
3
4
5
6
7
8
FREQUENCY IN Mc/s
F_2 MILD MULTIPATH
E MILD MULTIPATH
E-F_2 SEVERE MULTIPATH

FIGURE 3.8

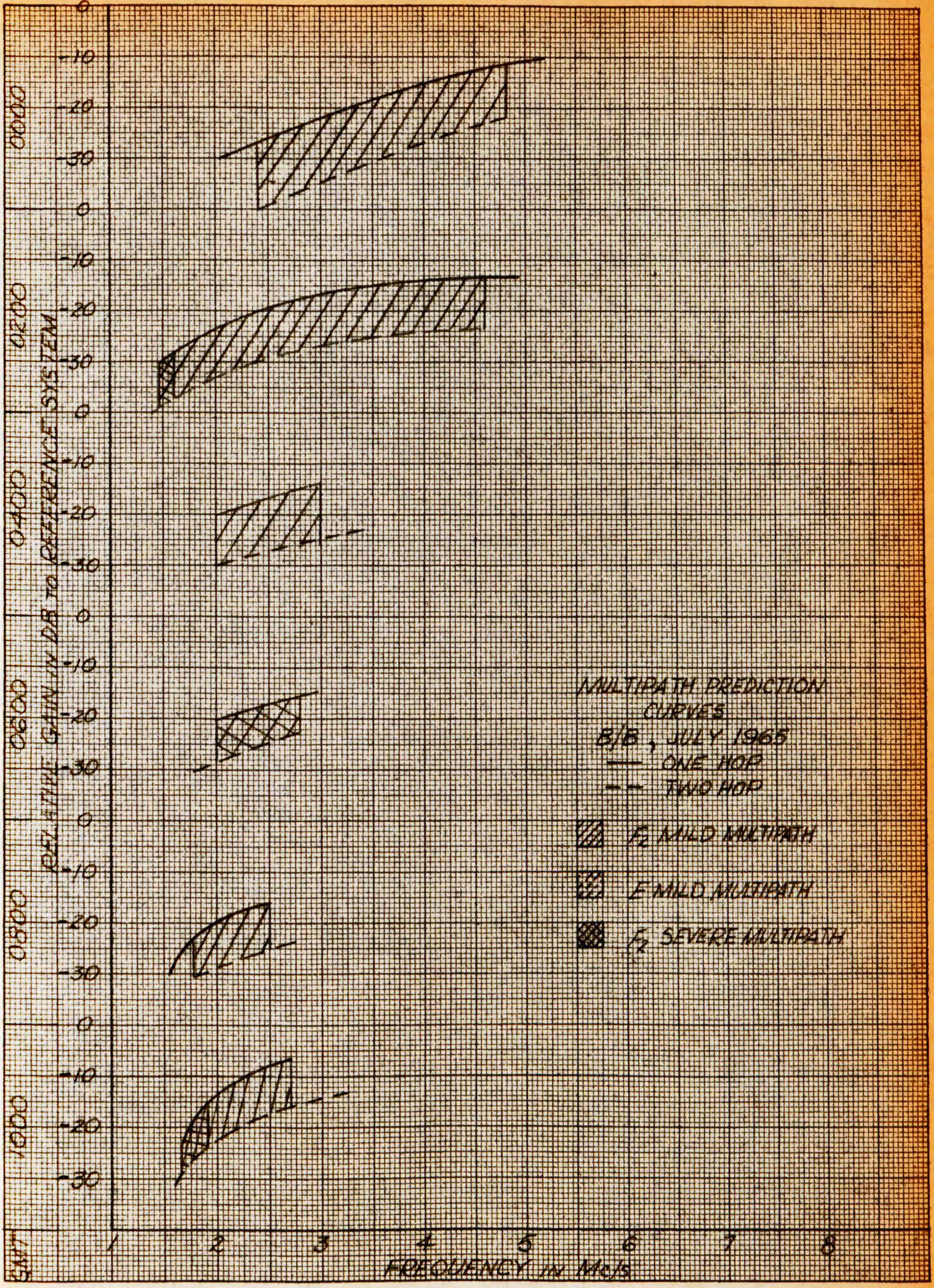
RELATIVE GAIN IN DB TO REFERENCE SYSTEM
GMT
0000
0200
0400
0600
0800
1000
0
-10
-20
-30
1
2
3
4
5
6
7
8
FREQUENCY IN Mc/s
MULTIPATH PREDICTION CURVES
B/B, JULY 1965
ONE HOP
TWO HOP
F_2 MILD MULTIPATH
E MILD MULTIPATH
F_2 SEVERE MULTIPATH

FIGURE 3.9

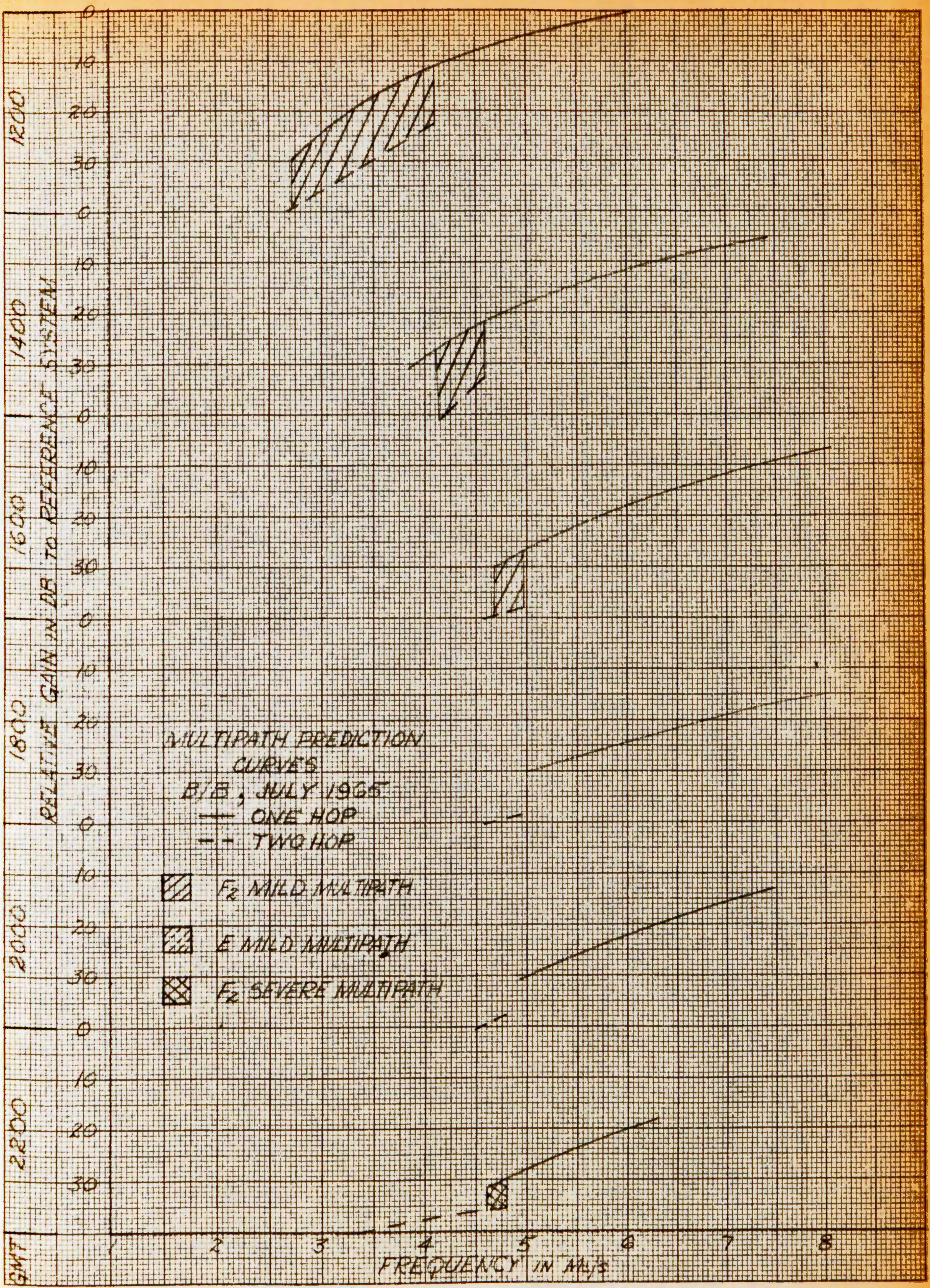
RELATIVE GAIN IN DB TO REFERENCE SYSTEM
1200
1400
1600
1800
2000
2200
GMT
FREQUENCY IN Mc/s
MULTIPATH PREDICTION CURVES
B/B, JULY 1965
ONE HOP
TWO HOP
F2 MILD MULTIPATH
E MILD MULTIPATH
F2 SEVERE MULTIPATH

FIGURE 3.10

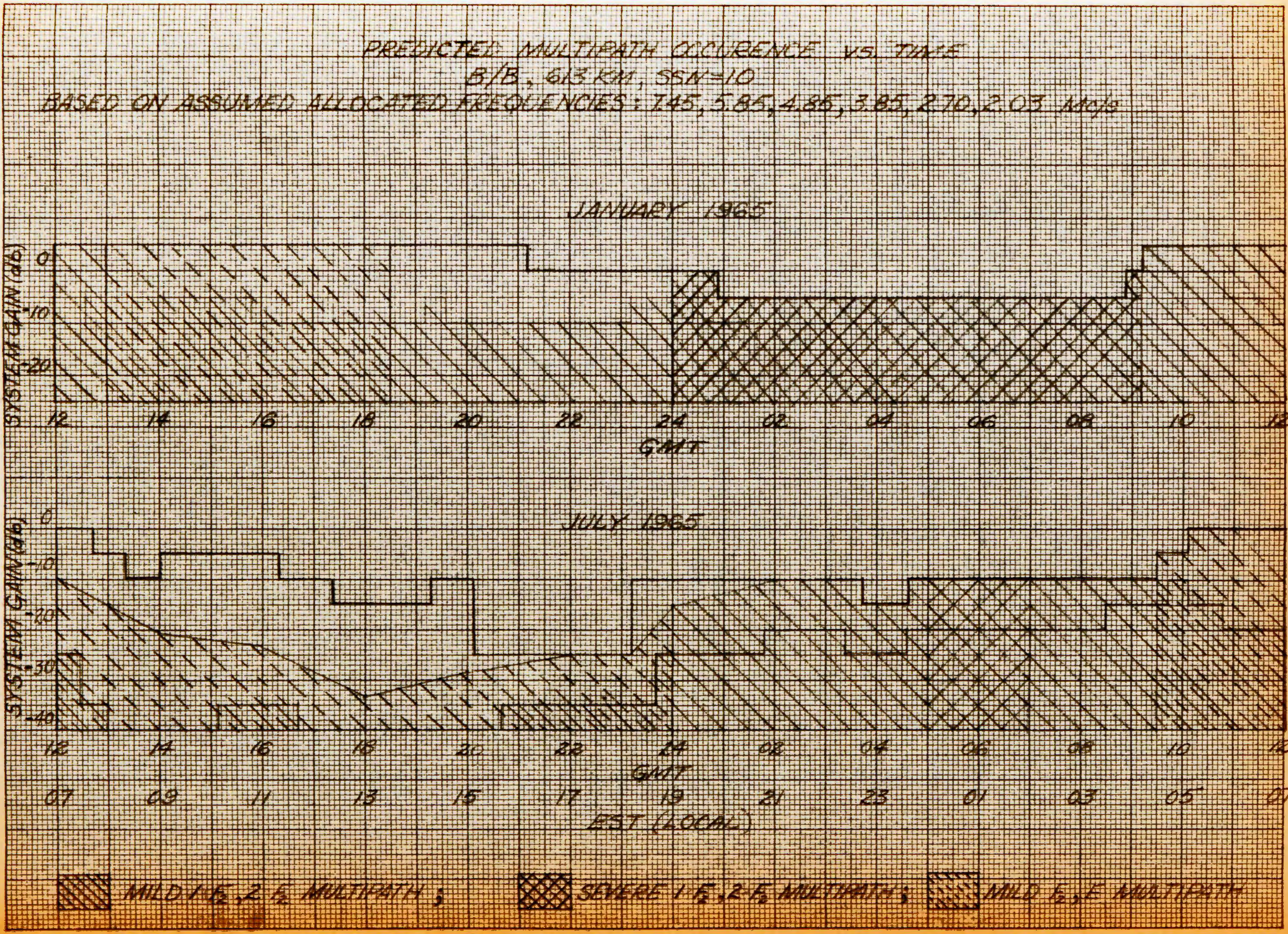
PREDICTED MULTIPATH OCCURENCE VS. TIME
B/B, 613 KM, SSN=10
BASED ON ASSUMED ALLOCATED FREQUENCIES: 7.45, 5.85, 4.85, 3.85, 2.70, 2.03 Mc/s
JANUARY 1965
SYSTEM GAIN (db)
0
-10
-20
12
14
16
18
20
22
24
02
04
06
08
10
12
GMT
JULY 1965
SYSTEM GAIN (db)
0
-10
-20
-30
-40
12
14
16
18
20
22
24
02
04
06
08
10
12
GMT
07
09
11
13
15
17
19
21
23
01
03
05
07
EST (LOCAL)
MILD 1-F2, 2-F2 MULTIPATH ;
SEVERE 1-F2, 2-F2 MULTIPATH ;
MILD Es, E MULTIPATH

FIGURE 3.11

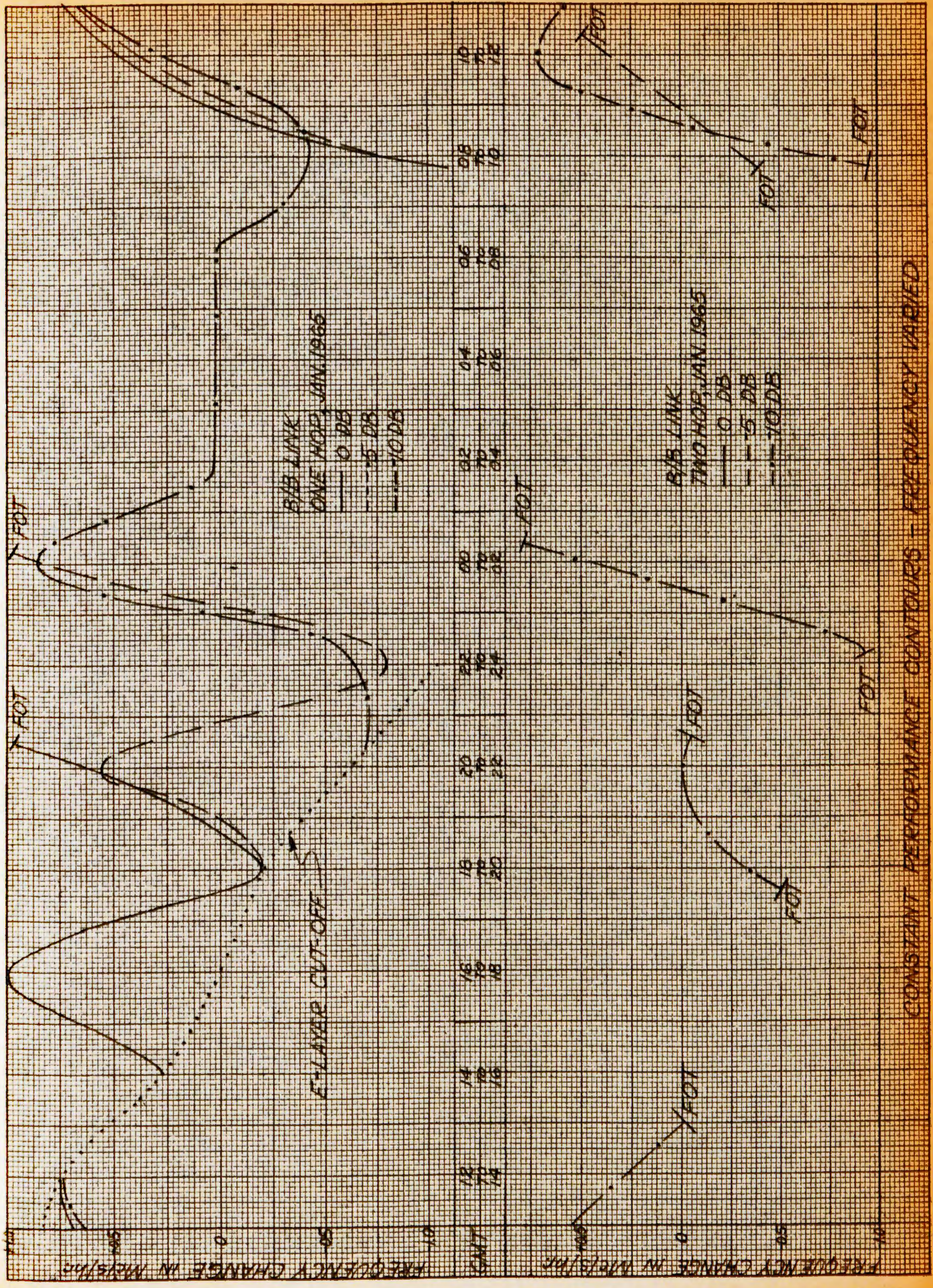
CONSTANT PERFORMANCE CONTOURS - FREQUENCY VARIED
R/B LINK
ONE HOP, JAN.1965
0 DB
-5 DB
-10 DB
R/B LINK
TWO HOP, JAN.1965
0 DB
-5 DB
-10 DB
E-LAYER CUT-OFF
FOT
GMT
FREQUENCY CHANGE IN MC/S/MC

FIGURE 3.12

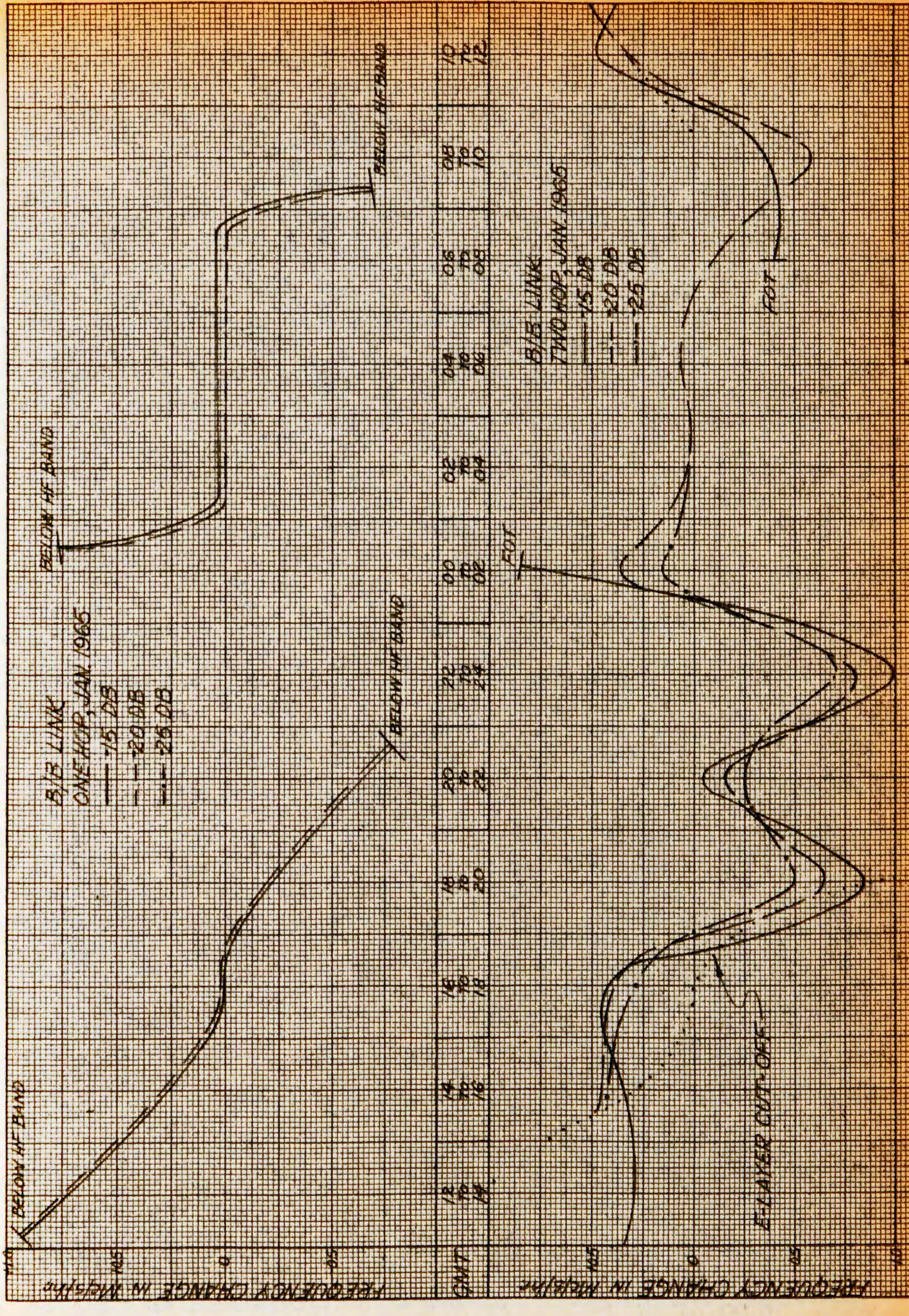

CONSTANT PERFORMANCE CONTOURS – FREQUENCY VARIED

FIGURE 3.13

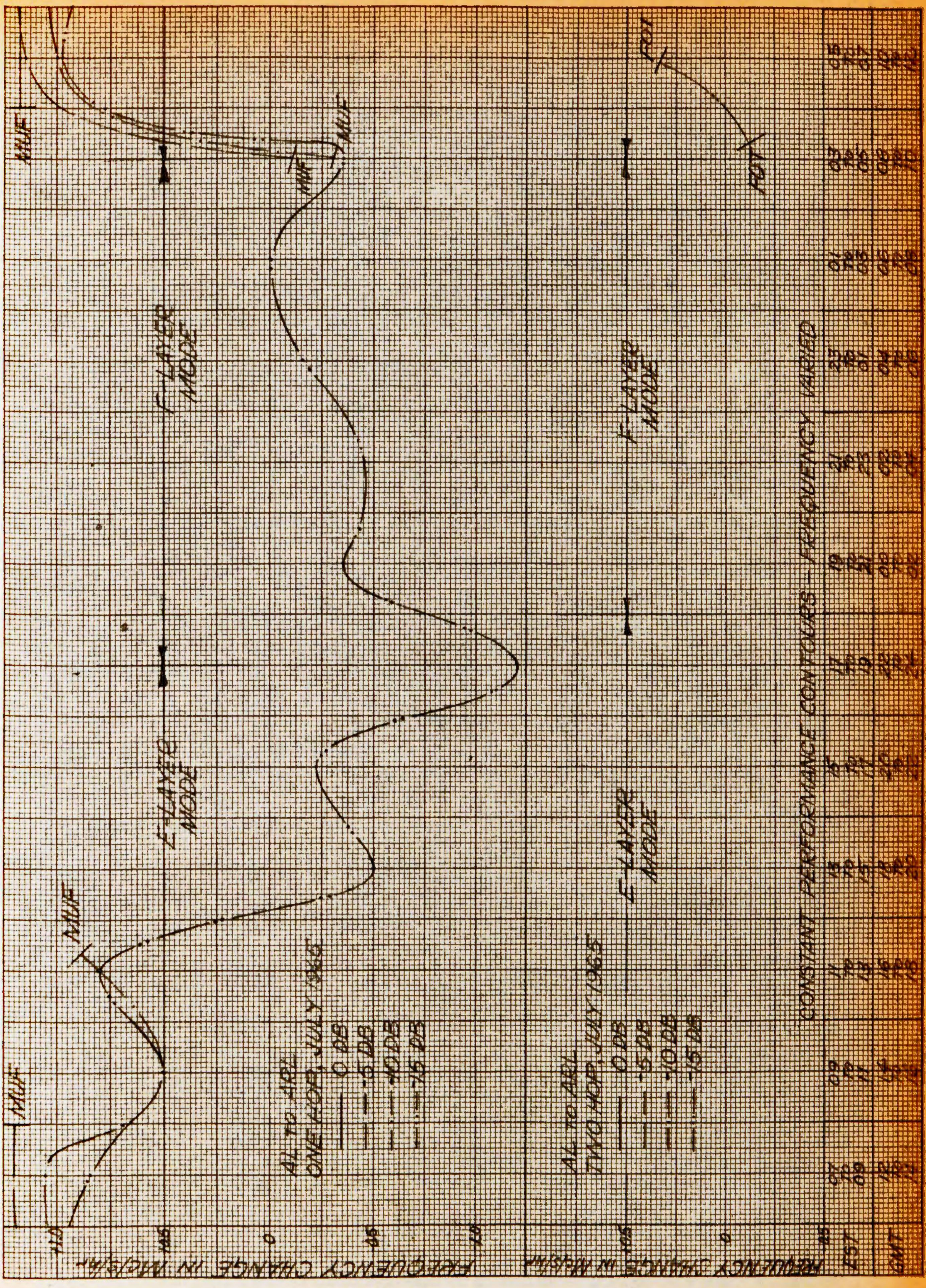
CONSTANT PERFORMANCE CONTOURS - FREQUENCY VARIED
FREQUENCY CHANGE IN MC/S/HR.
AL TO ARL
ONE HOP, JULY 1965
0 DB
-5 DB
-10 DB
-15 DB
AL TO ARL
TWO HOP, JULY 1965
0 DB
-5 DB
-10 DB
-15 DB
MUF
E LAYER MODE
F LAYER MODE
FOT
EST
GMT

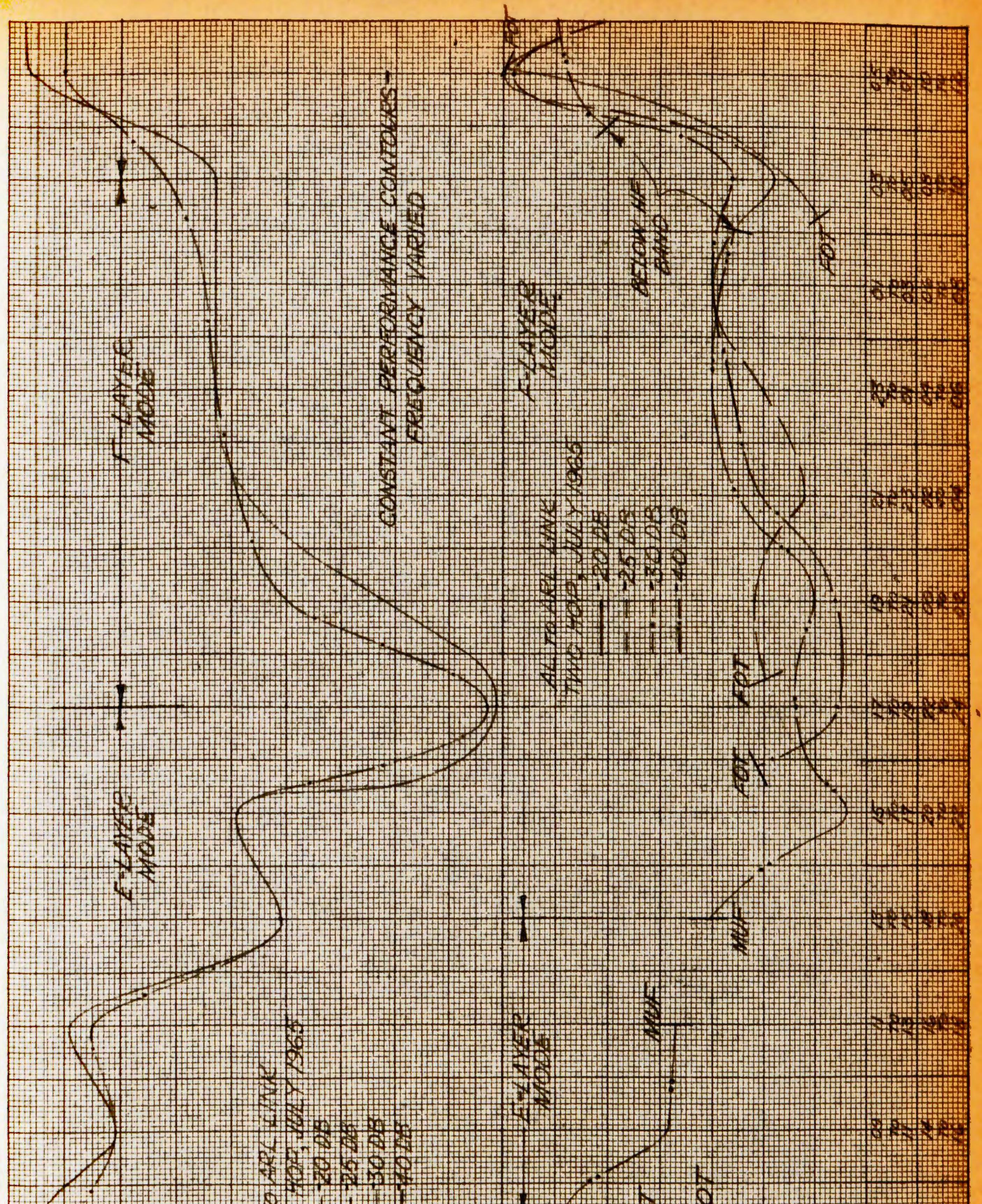
CONSTANT PERFORMANCE CONTOURS - FREQUENCY VARIED
AL TO ARL LINK
ONE HOP, JULY 1965
-20 DB
-25 DB
-30 DB
-40 DB
AL TO ARL LINK
TWO HOP, JULY 1965
-20 DB
-25 DB
-30 DB
-40 DB
E-LAYER MODE
F-LAYER MODE
E-LAYER MODE
F-LAYER MODE
BELOW HF BAND
FOT
MUF
FREQUENCY CHANGE IN MC/S/HR
FREQUENCY CHANGE IN MC/S/HR
+.5
0
-.5
-1.0

FIGURE 3.15

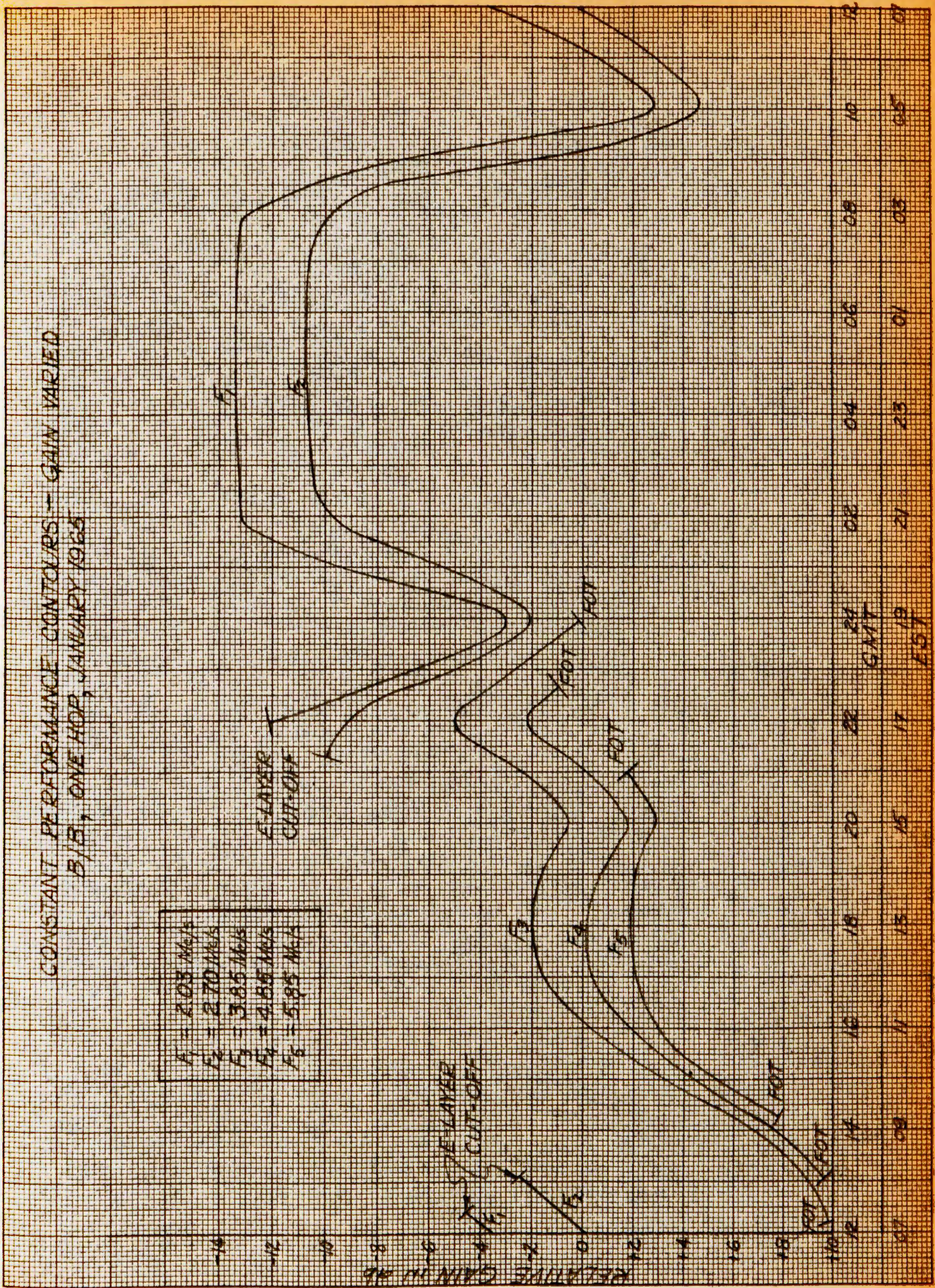
CONSTANT PERFORMANCE CONTOURS — GAIN VARIED
B/B, ONE HOP, JANUARY 1965
F1 = 2.03 Mc/s
F2 = 2.70 Mc/s
F3 = 3.85 Mc/s
F4 = 4.88 Mc/s
F5 = 5.85 Mc/s
E-LAYER CUT-OFF
E-LAYER CUT-OFF
FOT
RELATIVE GAIN in db
GMT
EST

FIGURE 3.16

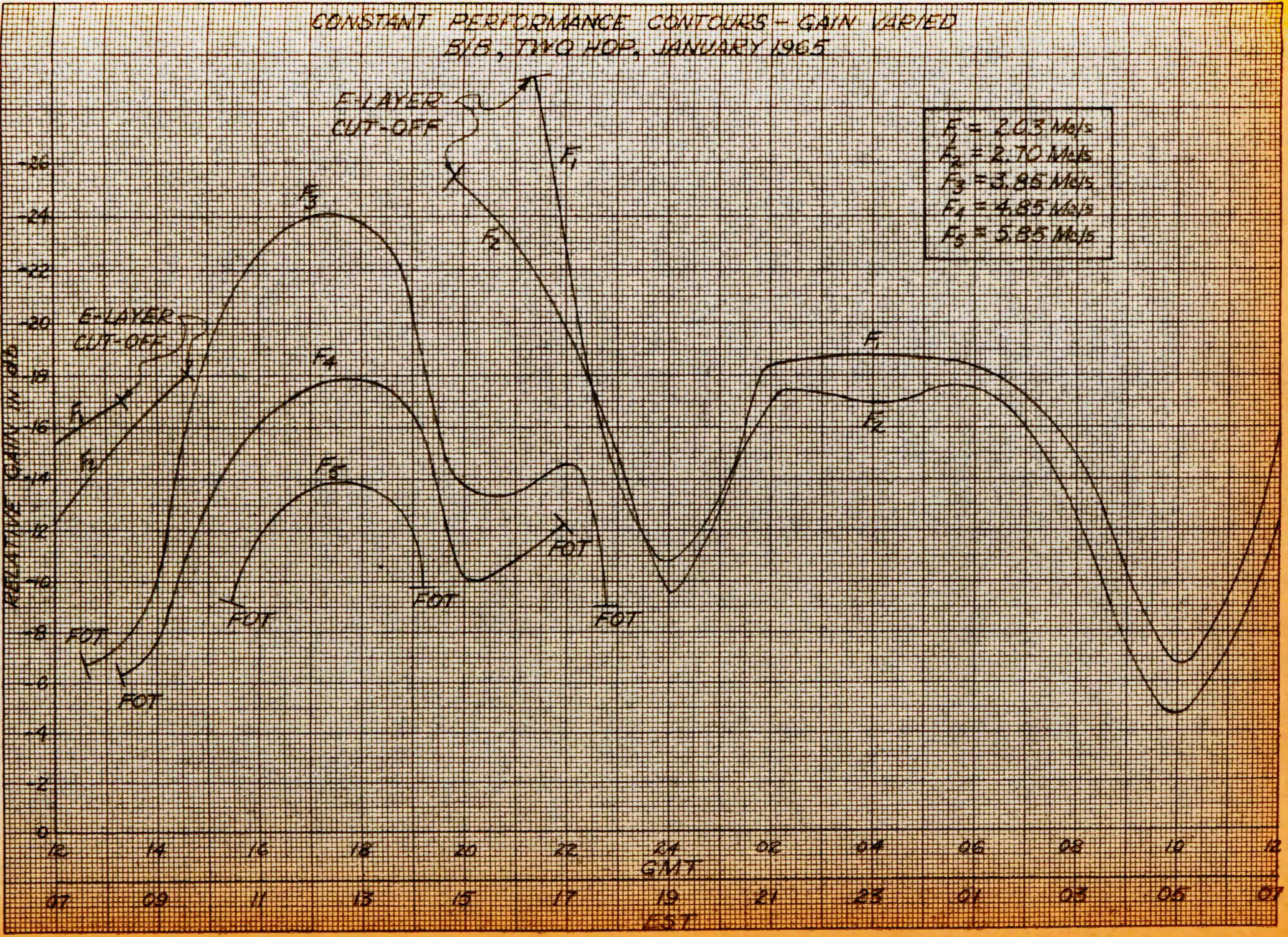
CONSTANT PERFORMANCE CONTOURS - GAIN VARIED
B/B, TWO HOP, JANUARY 1965
F_1 = 2.03 Mc/s
F_2 = 2.70 Mc/s
F_3 = 3.85 Mc/s
F_4 = 4.85 Mc/s
F_5 = 5.85 Mc/s
E-LAYER CUT-OFF
E-LAYER CUT-OFF
F_1
F_2
F_3
F_4
F_5
FOT
RELATIVE GAIN IN dB
-26
-24
-22
-20
-18
-16
-14
-12
-10
-8
-6
-4
-2
0
12
14
16
18
20
22
24
02
04
06
08
10
12
GMT
07
09
11
13
15
17
19
21
23
01
03
05
07
EST

FIGURE 3.17

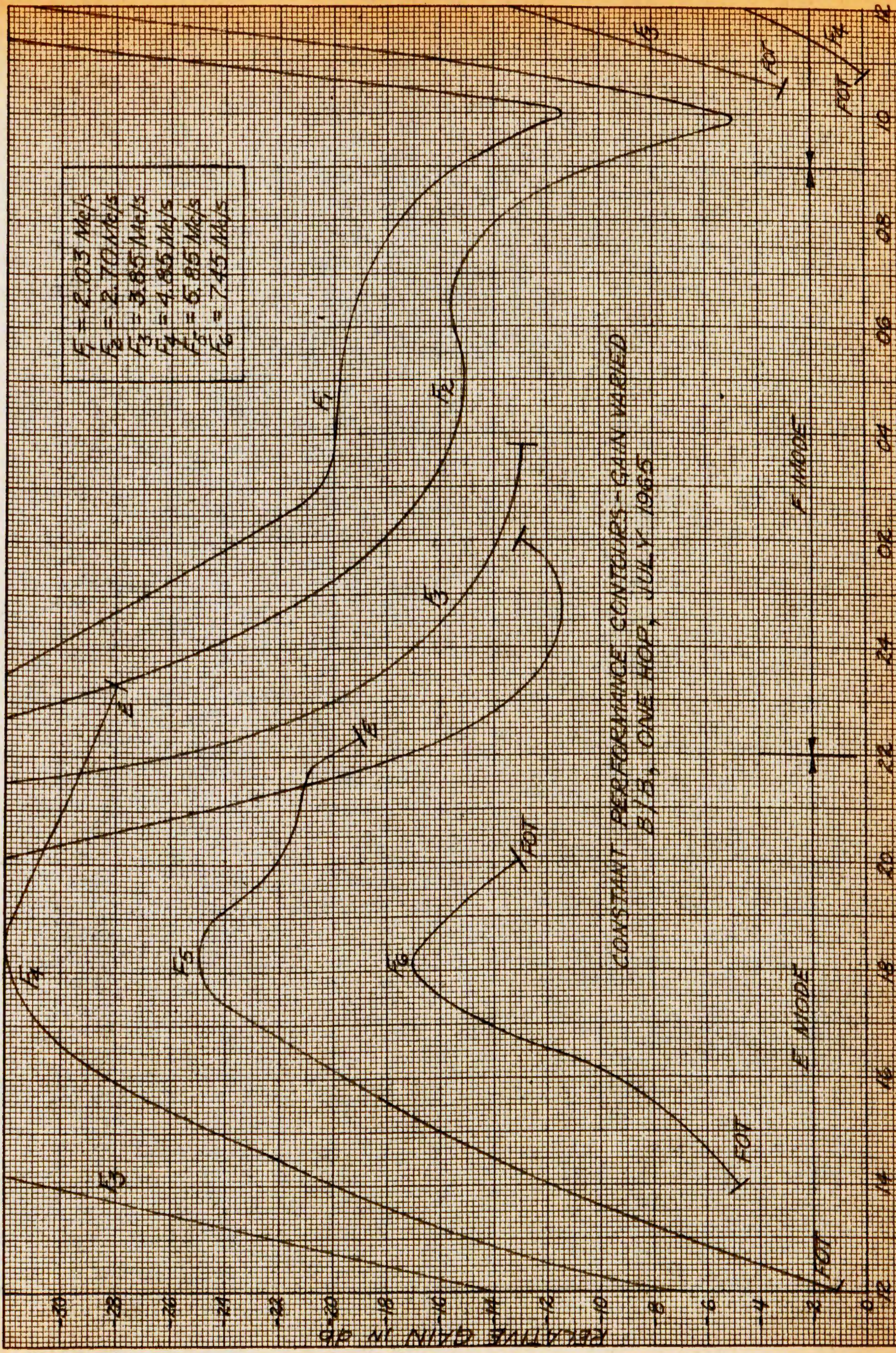

$F_1 = 2.03$ Mc/s
$F_2 = 2.70$ Mc/s
$F_3 = 3.85$ Mc/s
$F_4 = 4.85$ Mc/s
$F_5 = 6.85$ Mc/s
$F_6 = 7.45$ Mc/s
CONSTANT PERFORMANCE CONTOURS - GAIN VARIED
B/B, ONE HOP, JULY 1965
RELATIVE GAIN IN db
GMT
EST
E MODE
F MODE
FOT

FIGURE 3.18

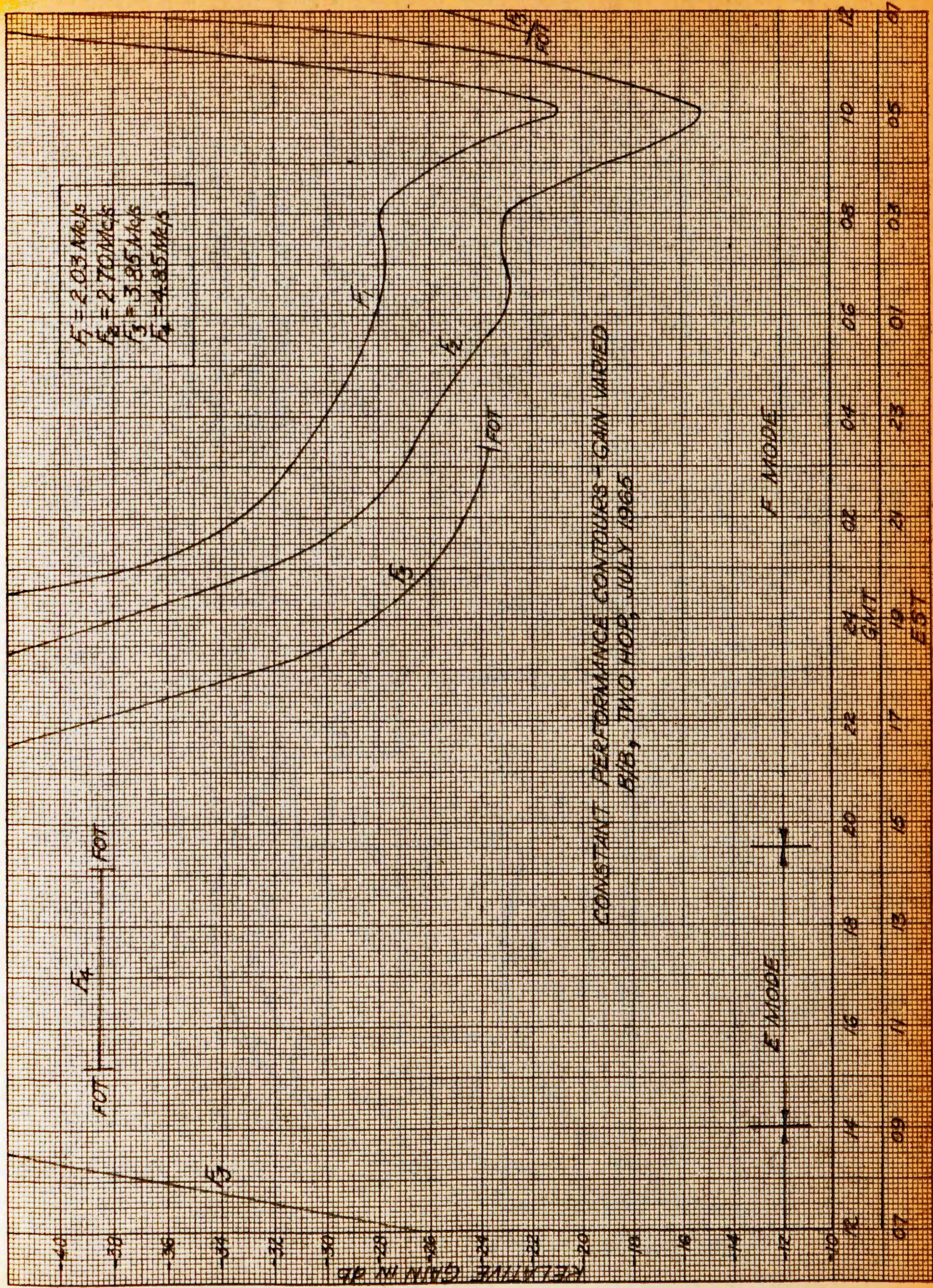
CONSTANT PERFORMANCE CONTOURS - GAIN VARIED
B/B, TWO HOP, JULY 1965
F_1 = 2.03 Mc/s
F_2 = 2.70 Mc/s
F_3 = 3.85 Mc/s
F_4 = 4.85 Mc/s
E MODE
F MODE
FOT
RELATIVE GAIN IN db
GMT
EST

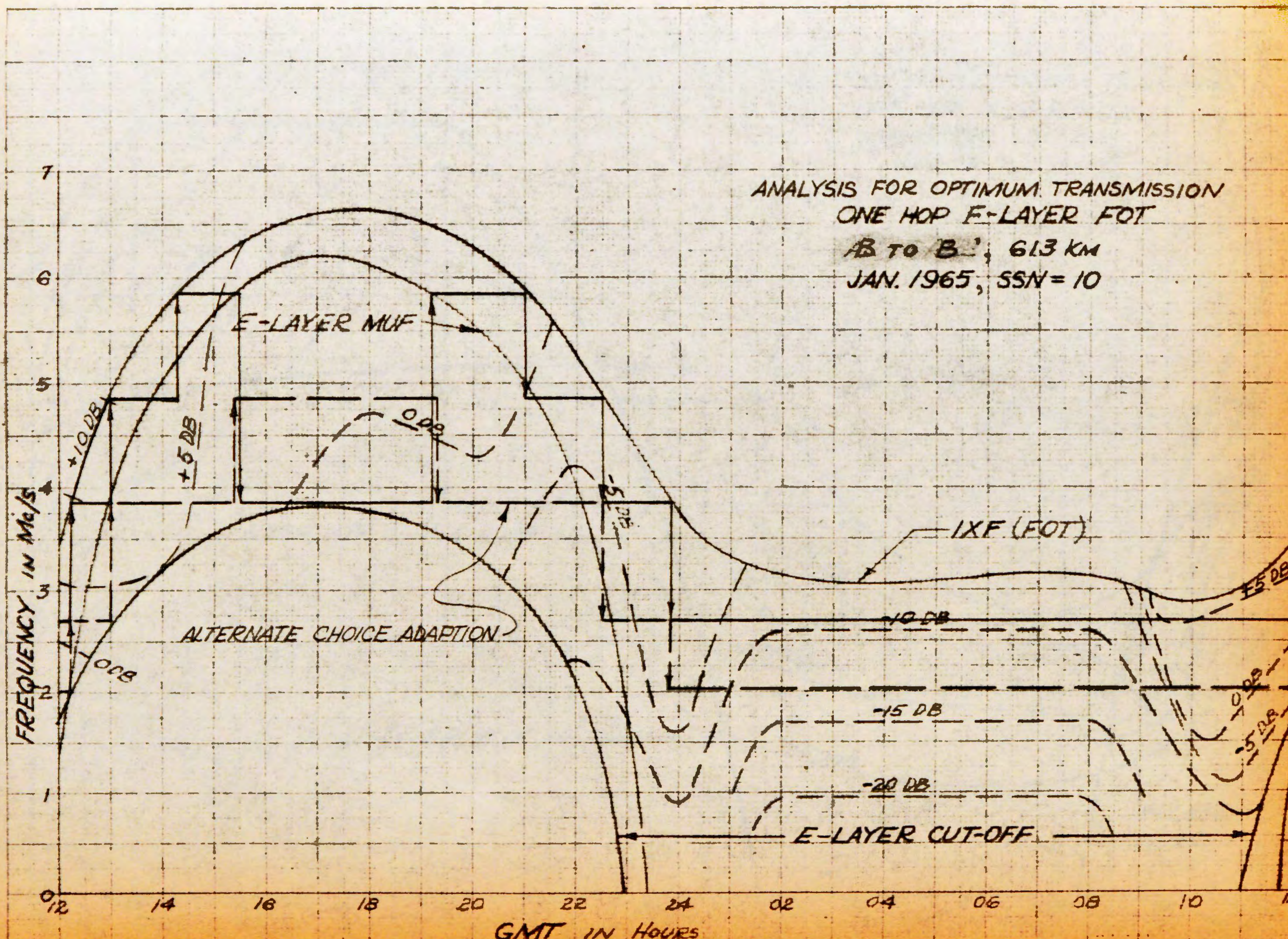

ANALYSIS FOR OPTIMUM TRANSMISSION
ONE HOP E-LAYER FOT
B TO B', 613 KM
JAN. 1965, SSN = 10
E-LAYER MUF
1XF (FOT)
ALTERNATE CHOICE ADAPTION
E-LAYER CUT-OFF
+10 DB
+5 DB
0 DB
-5 DB
-10 DB
-15 DB
-20 DB
FREQUENCY IN Mc/S
GMT IN HOURS
0
1
2
3
4
5
6
7
12
14
16
18
20
22
24
02
04
06
08
10
12

FIGURE 3.19

FIGURE 3.20

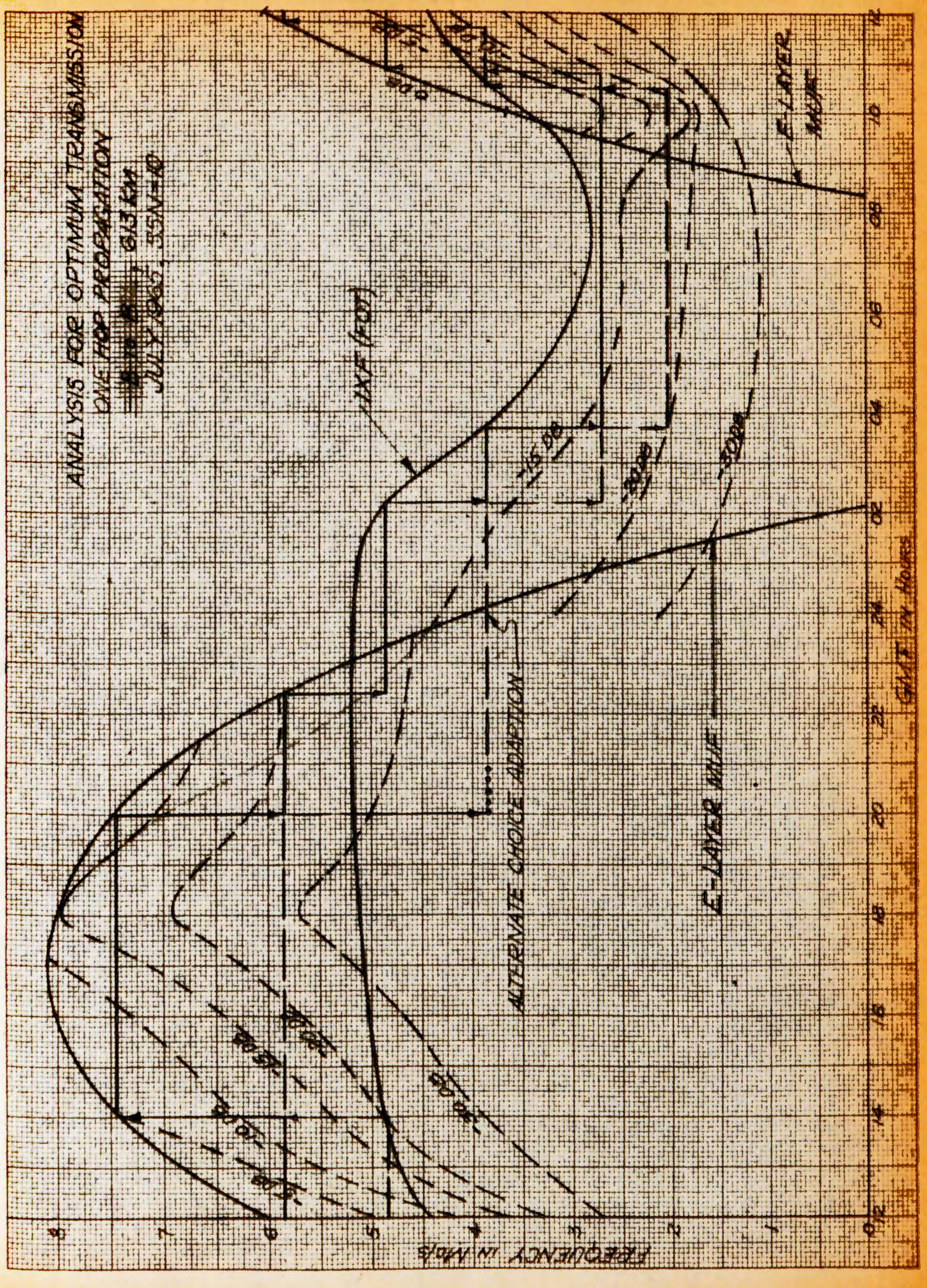
ANALYSIS FOR OPTIMUM TRANSMISSION
ONE HOP PROPAGATION
JULY 1960, SSN=10
1XF (FOT)
-15 DB
-30 DB
ALTERNATE CHOICE ADAPTION
E-LAYER MUF
E-LAYER MUF
FREQUENCY IN Mc/s
GMT IN HOURS

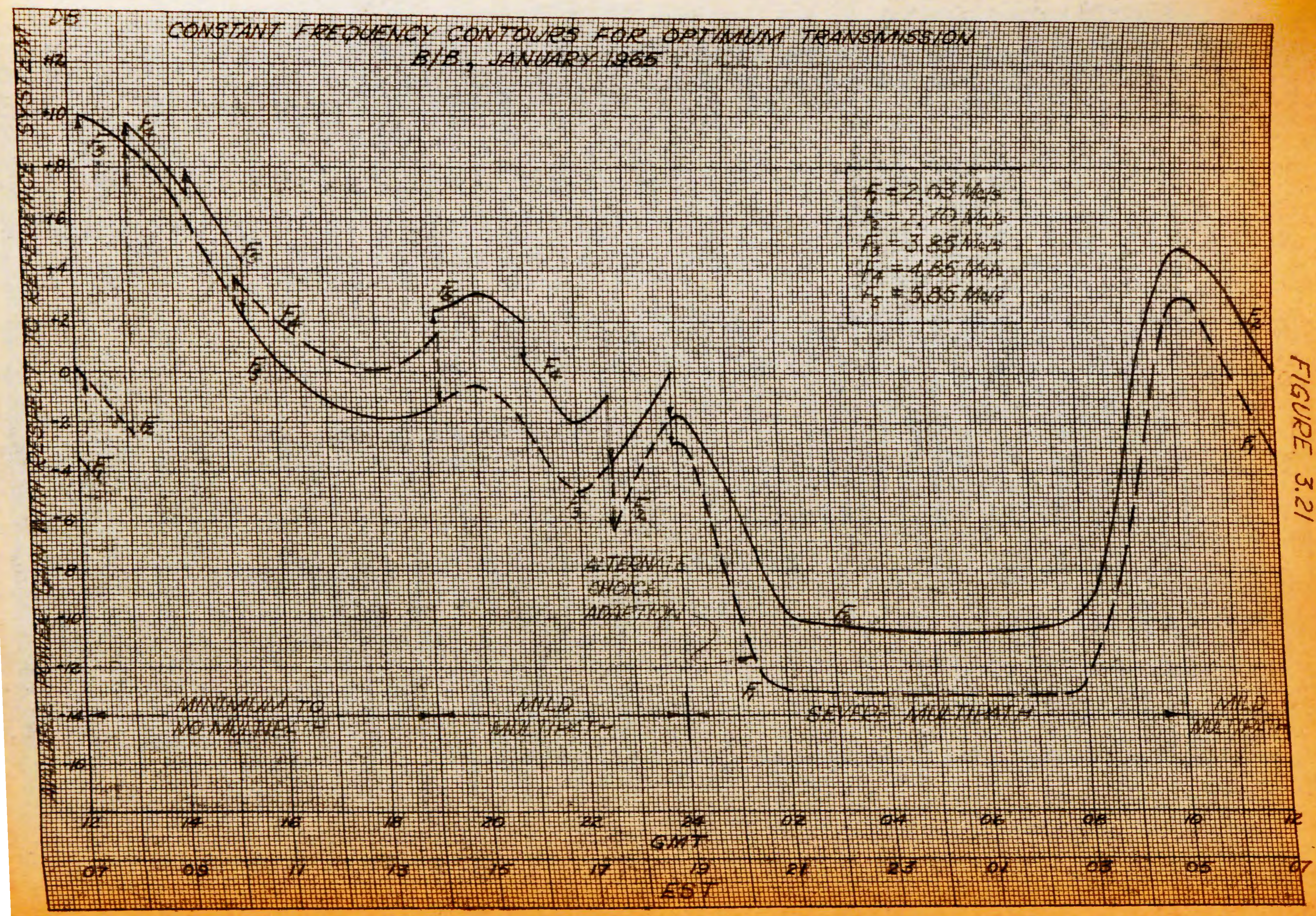

CONSTANT FREQUENCY CONTOURS FOR OPTIMUM TRANSMISSION
B/B, JANUARY 1965
DB
AVAILABLE POWER GAIN WITH RESPECT TO REFERENCE SYSTEM
F1 = 2.03 Mc/s
F2 = 2.70 Mc/s
F3 = 3.85 Mc/s
F4 = 4.85 Mc/s
F5 = 5.85 Mc/s
ALTERNATE CHOICE ADAPTION
MINIMUM TO NO MULTIPATH
MILD MULTIPATH
SEVERE MULTIPATH
MILD MULTIPATH
GMT
EST

FIGURE 3.21

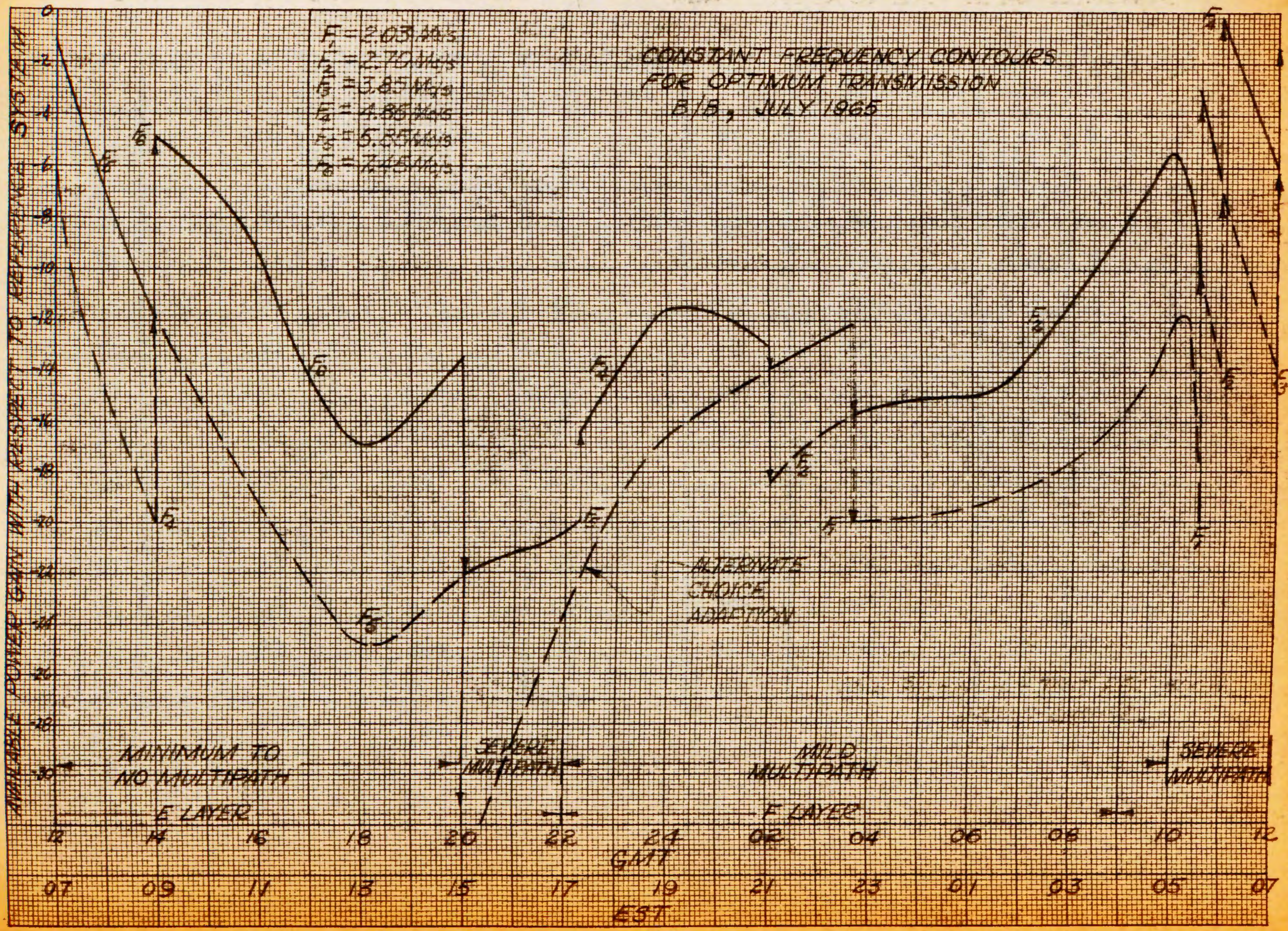

$F_1 = 2.03$ Mc/s
$F_2 = 2.70$ Mc/s
$F_3 = 3.85$ Mc/s
$F_4 = 4.86$ Mc/s
$F_5 = 5.85$ Mc/s
$F_6 = 7.48$ Mc/s
CONSTANT FREQUENCY CONTOURS
FOR OPTIMUM TRANSMISSION
B/B, JULY 1965
AVAILABLE POWER GAIN WITH RESPECT TO REFERENCE SYSTEM
0
-2
-4
-6
-8
-10
-12
-14
-16
-18
-20
-22
-24
-26
-28
-30
ALTERNATE CHOICE ADAPTION
MINIMUM TO NO MULTIPATH
SEVERE MULTIPATH
MILD MULTIPATH
SEVERE MULTIPATH
E LAYER
F LAYER
12
14
16
18
20
22
24
02
04
06
08
10
12
GMT
07
09
11
13
15
17
19
21
23
01
03
05
07
EST

FIGURE 3.22

TABLE 1
1 Hop, Jan. 1965
SSN = 10, 613 Km.
B/B

GMT	EST	MUF	FOT	MODE	Radiation Angle (ϕ)	Absorption Loss (L_A)	L_{rp}	Median System Loss	Atm. Noise	S/N at FOT
-	-	Mc/s	Mc/s	-	Degrees	db	db	db	1 cps BW DBW	DB 1 cps BW
00	19	-	3.74	IF	35.6	0	103	102	-158	83
02	21	-	3.14	IF	39.7	0	102	101	-150	76
04	23	-	3.06	IF	41.8	0	102	101	-149	75
06	01	-	3.14	IF	42.5	0	102	101	-150	76
08	03	-	3.14	IF	41.3	0	102	101	-150	76
10	05	-	3.31	IF	40.3	0	101	100	-162	89
12	07	-	3.48	IF	39.2	3.0	102	104	-162	85
14	09	-	5.7	IF	38.0	5.7	106	111	-175	91
16	11	-	6.46	IF	37.4	7.2	107	113	-173	87
18	13	-	6.63	IF	36.8	7.0	107	113	-172	86
20	15	-	6.29	IF	36.3	5.7	107	112	-172	87
22	17	-	5.27	IF	35.0	2.3	105	106	-161	82

TABLE 2
2 Hop, Jan. 1965
SSN = 10, 613 Km.
B/B

GMT	EST	MUF	FOT	MODE	Radiation Angle (ϕ)	Absorption Loss (L_A)	L_{rp}	Median System Loss	Atm. Noise	S/N at FOT
-	-	Mc/s	Mc/s	-	Degrees	db	db	db	1 cps BW DBW	DB 1 cps BW
00	19	-	3.48	2F	55.0	6.0	105	110	-157	74
02	21	-	2.89	2F	58.8	5.8	104	109	-149	67
04	23	-	2.89	2F	60.7	5.9	104	109	-149	67
06	01	-	2.89	2F	61.1	5.9	105	110	-149	66
08	03	-	2.89	2F	60.2	5.9	104	109	-154	72
10	05	-	3.06	2F	59.3	5.9	105	110	-162	79
12	07	-	3.23	2F	58.3	11.1	105	115	-162	74
14	09	-	5.27	2F	57.3	16.8	108	126	-175	76
16	11	-	5.95	2F	56.7	19.9	110	129	-174	72
18	13	-	6.04	2F	56.2	20.0	110	129	-172	70
20	15	-	5.78	2F	55.6	16.9	109	125	-172	74
22	17	-	4.76	2F	54.5	10.4	107	116	-159	70

TABLE 3
1 Hop, July 1965
SSN = 10, 613 Km.
B/B

GMT	EST	MUF	FOT	MODE	Radiation Angle (ϕ)	Absorption Loss (L_A)	L_{rp}	Median System Loss	Atm. Noise	S/N at FOT
-	-	Mc/s	Mc/s	-	Degrees	db	db	db	1 cps BW DBW	db 1 cps BW
00	19	-	5.2	1F	42.0	3.8	107	110	-156	73
02	21	-	4.93	1F	41.0	0	105	104	-147	70
04	23	-	3.71	1F	43.0	0	105	103	-146	70
06	01	-	2.98	1F	43.0	0	102	101	-143	69
08	03	-	2.82	1F	43.0	0	101	100	-143	70
10	05	3.67	-	1E	19.3	10.3	101	110	-166	83
12	07	6.05	-	1E	19.3	13.3	105	117	-167	77
14	09	7.41	-	1E	19.3	16.0	107	122	-173	78
16	11	8.02	-	1E	19.3	17.2	108	124	-173	76
18	13	8.02	-	1E	19.3	17.[illegible]	108	124	-166	69
20	15	7.48	-	1E	19.3	16.0	107	122	-165	70
22	17	6.23	-	1E	19.3	13.5	106	119	-157	65

TABLE 4

2 Hop, July 1965

SSN = 10, 613 Km.

B/B

GMT	EST	MUF	FOT	MODE	Radiation Angle (ϕ)	Absorption Loss L_A	L_{rp}	Median System Loss	Atm. Noise	S/N at FOT
-	-	Mc/s	Mc/s	-	Degrees	db	db	db	1 cps BW DBW	DB 1 cps BW
00	19	-	4.80	2F	60.7	13.6	108	121	-155	61
02	21	-	4.60	2F	59.8	6.6	108	114	-147	60
04	23	-	3.48	2F	61.1	6.0	106	111	-144	60
06	01	-	2.83	2F	61.6	5.5	104	109	-143	61
08	03	-	2.72	2F	61.6	5.5	104	109	-142	60
10	05	-	3.23	2F	62.0	17.2	106	122	-166	71
12	07	-	4.08	2F	64.0	27.8	108	135	-166	58
14	09	4.59	-	2E	35.0	47.8	104	151	-174	50
16	11	4.95	-	2E	35.0	51.4	105	155	-173	45
18	13	4.97	-	2E	35.0	51.4	105	155	-163	35
20	15	-	4.77	2F	67.5	35.2	111	144	-163	46
22	17	-	4.80	2F	67.5	24.5	111	134	-155	48

SELECTED BIBLIOGRAPHY

1. Laitinen, P. O., and Haydon, G. W., "Analysis and Prediction of Sky-Wave Field Intensities in the High-Frequency Band", Technical Report No. 9, RPU 203, U. S. Army Signal Radio Propagation Agency, Fort Monmouth, N. J., Oct. 1962.

2. NBS Circular No. 462, "Ionospheric Radio Propagation", June 1948.

3. NBS Handbook 90, "Ionospheric Predictions Based on Numerical Methods of Mapping", Dec. 1962.

4. Central Radio Propagation Lab, "D Series".

5. Zacharisen, D. H., "World Maps of F2 Critical Frequencies and Maximum Useable Frequency Factors", NBS Technical Note 2, 1960.

6. CCIR, "Radio Noise Data", Revised Report 65, Vol. III, 223, ITU, Los Angeles, 1959.

7. Jacobs, George, "Sunspots, and the Solar Influence Upon High-Frequency Radio Communications", Univ. of Maryland Master's Thesis, 1960.

8. Kift, F., "The Propagation of High-Frequency Radio Waves to Long Distances", Proc. IEE, vol. 107, Pt. B, No. 32, March 1960, pp. 127-140.

9. Piggott, W. R., "The Calculation of Median Sky-Wave Field Strength in Tropical Regions", Special Report No. 27, Dept. of Scientific and Industrial Research, Slough, England, 1959.

10. Rawer, K., "Calculation of Sky-Wave Field Strength", Wireless Engineer, Nov. 1952, pp. 287-301.

11. Reed, H. R., and Russell, M. S., Ultra High Frequency Propagation, 2nd Edition, Boston Technical Publishers, Lexington, Mass., 1964.